5-1-2023

Raspberry Polyphenols Target Molecular Pathways of Heart Failure

Rami Najjar

Recommended Citation
Najjar, Rami, "Raspberry Polyphenols Target Molecular Pathways of Heart Failure." Dissertation, Georgia State University, 2023.
doi: https://doi.org/10.57709/35063691

Raspberry Polyphenols Target Molecular Pathways of Heart Failure

by

Rami Salim Najjar

Under the Direction of Rafaela G. Feresin, PhD

A Dissertation Submitted in Partial Fulfillment of the Requirements for the Degree of

Doctor of Philosophy

in the College of Arts and Sciences

Georgia State University

2023

ABSTRACT

Approximately 650,000 new cases of heart failure (HF) are diagnosed annually with a 50% five-year mortality rate. HF is characterized by reduced left ventricular ejection fraction (EF) and hypertrophy of the left ventricular wall. The pathophysiological remodeling of the heart is mediated by increased oxidative stress and inflammation. Reactive oxygen species (ROS) derived from NADPH-oxidases (NOX), xanthine oxidase (XO), and mitochondria are the primary drivers of oxidative stress. In addition, damage associate molecular patterns (DAMPs) released from apoptotic cells can trigger toll-like receptor (TLR)4 activation, leading to an inflammatory response. Raspberries are rich in polyphenols which may favorably impact enzymes involved in redox homeostasis while also targeting inflammatory signaling. To elucidate these effects, Sprague Dawley rats consumed a 10% raspberry diet for seven weeks. At week three, HF was surgically induced via coronary artery ligation. Hemodynamics and morphology of the heart were assessed, and cardiac tissue was harvested at sacrifice from the rats following treatments. Expression of cardiac proteins involved in oxidative stress, inflammation, apoptosis and remodeling were assessed, and histological analysis was conducted. Additionally, human cardiomyocytes were pretreated with isolated raspberry polyphenol extract followed by $CoCl_2$ treatment to chemically induce hypoxia. Redox status, apoptosis and mitochondrial dysfunction were assessed. Raspberries effectively preserve cardiac function and morphology, and this may be mediated by reduced TLR4 signaling. This coincided with reduced oxidative stress, apoptosis, and remodeling in vivo. In vitro, raspberry polyphenol extract attenuated $CoCl_2$-induced oxidative stress and apoptosis in human cardiomyocytes despite pronounced hypoxia-inducible factor (HIF)-1α expression. In conclusion, these data indicate that the consumption of raspberries can reduce the underlying molecular drivers of HF, thus, leading to the observed improvements in cardiac

functional capacity and morphology. This dietary strategy may be an effective alternative treatment in treating HF. However, further investigation in alternative models of HF are warranted.

INDEX WORDS: Polyphenols, Heart failure, Nutrition

Raspberry Polyphenols Target Molecular Pathways of Heart Failure

by

Rami Salim Najjar

Committee Chair: Rafaela G. Feresin

Committee: Desiree Wanders

Hongyu Qiu

Binghe Wang

Electronic Version Approved:

Office of Graduate Services

College of Arts and Sciences

Georgia State University

May 2023

ACKNOWLEDGEMENTS

I would like to acknowledge and thank my major professor, Dr. Rafaela Feresin, for supporting me during my academic career. I would not be where I am today without her mentorship. I would also like to thank my committee members, Dr. Desiree Wanders, Dr. Hongyu Qiu, Dr. Binghe Wang and my committee chair and major professor, Dr. Rafaela Feresin, in their assistance in developing this dissertation project and final document. I would like to also acknowledge and thank Dr. Ranjan Roy, a postdoctoral associate, in providing training in the technique of coronary artery ligation, a critical surgical procedure for which my project was dependent upon. I would also like to thank Maureen Meister, Kendahl Heckstall, and Rita Zorh in their assistance in carrying out the animal study.

TABLE OF CONTENTS

LIST OF TABLES

LIST OF FIGURES

production from xanthine oxidase (XO) and mitochondria which raspberries reduce. C) excessive ROS can cause DNA breaks which triggers p53 phosphorylation. Additionally, ROS can modify reactive cysteine residues on p53 creating disulfide bonds. TLR4 also acts on p53 indirectly by inhibiting sirtuin (SIRT)2, a deacetylase, resulting in accumulation of acetylated p53. These post-translational modifications all result in p53 cytosolic accumulation and eventual nuclear translocation binding to the region of DNA encoding B-cell lymphoma (BCL)-2-associated X protein (BAX) synthesis. However, raspberry polyphenols reduce p53 cytosolic accumulation likely due to a combination of these mechanisms. D) BCL-extra-large (BCL-xL) can inhibit BAX activity and prevent mitochondrial pore opening, which raspberries appeared to preserve the expression of. Mitochondrial depolarization and pore opening results in the downstream cleavage of caspase-9 followed by capase-3 leading to cellular apoptosis, all of which was attenuated by raspberry polyphenols. E) TLR4 signaling leads to the downstream phosphorylation of stress-activated protein kinases (SAPK)/Jun amino-terminal kinases (JNK) and activation of transcription factor c-Jun and activator protein (AP)-1 in parallel to the phosphorylation of the transcription factor nuclear factor-κB (NF-κB). This leads to nuclear translocation, DNA transcriptional activity and an inflammatory response. Raspberry polyphenols reduced activity of SAPK/JNK and NF-κB, likely due to initial reduction of TLR4, overall reducing the inflammatory response. F) TLR4 activation also leads to the phosphorylation of extracellular signal-regulated kinase (ERK)1/2, which activates nuclear factor of activated T-cells (NF-AT) which then forms a complex with NF-κB to bind to the region of DNA encoding fetal gene protein synthesis resulting in hypertrophy. Raspberry polyphenols inhibited the phosphorylation of ERK1/2 attenuating

1 INTRODUCTION

Heart failure (HF) affects approximately 5.1 million people in the United States (US), and diagnoses have remained consistent with more than 650,000 new cases every year (1). The five-year survival rate after diagnosis is approximately 50%. While HF primarily affects the elderly, considering the growing age of the population, 1 in 33 individuals in the US will have HF by the year 2030, leading to a near doubling in healthcare costs (2). HF is characterized by reduced EF and increased left ventricular wall thickening due to structural and functional defects of the heart (3). This can be initiated by ischemia or increased ventricular pressure due to hypertension. This modified cardiac load increases stress of the ventricular wall, leading to structural remodeling due to cardiomyocyte hypertrophy and apoptosis (3).

Inflammation and oxidative stress play integral roles in the development of HF (4). Hypoxia alone can induce inflammation and cell death (5), causing release of damage associate molecular patterns (DAMPs) which bind to toll-like receptor (TLR)4 in neighboring cells (6), potentiating an inflammatory response. Reactive oxygen species (ROS) derived from NADPH-oxidases (NOX), xanthine oxidase (XO) and mitochondria are the primary sources of ROS (7-9). Both inflammation and ROS can promote cardiomyocyte apoptosis, fibrosis and cardiac dysfunction (10, 11). TLR4 signaling activates inflammatory signaling pathways including mitogen-activated protein kinases (MAPKs): p38MAPK, extracellular signal-regulated protein kinase (ERK1/2) and stress-activated protein kinases (SAPK)/Jun amino-terminal kinases (JNK) (12-15). This leads to phosphorylation and translocation of nuclear factor kappa-light-chain-enhancer of activated B cells (NF-κB) (16) into the cell nucleus, leading to the transcription of inflammatory cytokines including interleukin (IL)-6, IL-1β and tumor necrosis factor (TNF)-α (17, 18). Inflammation facilitates macrophage recruitment into the myocardium via chemoattractants

and also leads to differentiation of fibroblasts intro myofibroblasts, promoting fibrosis (19). Thus, these inflammatory and redox pathways play key regulatory roles in the pathogenesis of HF and their regulation is of clinical significance.

Plant-based diets, which are comprised of phytonutrient-rich foods, may reduce the risk of HF by decreasing oxidative stress and inflammation (20, 21) in part due to their phytochemical content. Indeed, raspberries are a rich source of polyphenols, and these secondary metabolites produced by plants may target numerous molecular pathways involved in HF (22). Our preliminary data suggest that raspberry consumption leads to the increased enzymatic antioxidant expression in the hearts of mice treated with angiotensin (Ang) II. This corresponded with decreased IL-6 expression and cardiac fibrosis. Nonetheless, the ability of raspberry to modulate cardiac function, inflammation and oxidative stress in a model of HF is not known. Thus, the **main goal of this proposed study is to determine whether raspberries can be used as a nutritional therapy in the treatment of HF**. *The **central hypothesis** of this proposed study is that raspberries attenuate the pathological characteristics of HF by reducing inflammation and oxidative stress, thus, improving cardiac function.*

Specific Aim 1. Determine whether raspberry consumption can improve functional parameters and morphological characteristics of the heart in rats with HF. Raspberry polyphenols in isolation have been shown to improve functional and morphological parameters in acute HF models; however, whole raspberries have a diverse polyphenol profile and may be more efficacious due to synergistic and/or additive effects. Rats will be fed a control diet or a 10% raspberry diet for 7 weeks. At week 3, HF will be surgically induced via coronary artery ligation (CAL). Hemodynamics and morphology of the heart will be assessed via echocardiography at week 7. Cardiac tissue will be harvested at sacrifice to assess fibrosis and hypertrophy using

histological techniques. We hypothesize that raspberry consumption will improve cardiac function and morphology in mice with HF.

Specific Aim 2. Determine whether raspberry polyphenols modulate molecular pathways involved in HF. Raspberry polyphenols can attenuate inflammation and oxidative stress based on preliminary data in a neurohumoral model of cardiac stress; however, it is not known whether these effects translate to overt HF induced by ischemia. Cardiac tissue will be analyzed for key proteins involved in inflammation, oxidative stress, apoptosis and remodeling using western blot. Protein localization and cardiomyocyte apoptosis will be visualized with immunohistochemistry. Additionally, human cardiomyocytes will be pretreated with raspberry polyphenol extracts followed by chemically-induced hypoxia and analysis.

The proposed investigation will elucidate the ability of raspberry to mitigate cardiac dysfunction both physiologically and at the cellular level. Raspberries may act in a targeted approach and mitigate the mechanisms underlying the development and progression of HF. These findings may lead to further investigation in alternative models of HF with potential introduction of the intervention into clinical practice.

2 BACKGROUND

2.1 HF pathophysiology

In the clinical setting, HF is categorized as either HF with preserved EF (HFpEF) or HF with reduced EF (HFrEF) (3). EF refers to the percent of blood by volume ejected by the left ventricle (LV) of the heart during contraction. Both forms of HF are characterized by the inability of the heart to adequately pump blood. In HFpEF, EF is normal; however, the walls of the LV are thickened and thus, stiffer, leading to overall decreased functional capacity of the heart due to reduced stroke volume (total volume measured in mL ejected from the ventricles of the heart) leading to reduced cardiac output (amount of blood pumped through circulation per minute). Approximately, half of patients diagnosed with HF have HFpEF (23). Causes for HFpEF and HFrEF are very similar; however, how these underlying pathologies impact the heart is different. Rather than being directly caused by underlying pathologies, HFpEF can be indirectly caused by obesity, hypertension, diabetes, renal disease and other chronic conditions (24). These conditions increase systemic inflammation and oxidative stress, which progressively damage the heart, leading to hypertrophy of the LV and HF.

In contrast, HFrEF refers to an EF $\leq$ 40% and is typically directly caused by coronary artery disease (CAD; direct damage to the heart due to hypoxia causing significant scaring) or hypertension (LV enlarges to compensate increased blood pressure, leading to scarring) (25). These causes are not exhaustive, as neurohormonal regulators, such as Ang II, can directly act on the heart, and chronic Ang II signaling can independently promote HFrEF by promoting cardiomyocyte ROS, apoptosis and scarring (26). Unlike HFpEF, patients who have HFrEF respond favorably to pharmacological treatments (3). Moving forward, discussion of HF will refer to HFrEF unless stated otherwise.

2.2 HF in clinical practice

The primary goal of pharmacological interventions to treat HF is to improve cardiac output by reducing stress on the heart walls as well as modifying contractile signaling. A target for pharmacological treatment includes the β-adrenergic receptor (β1AR) which is overstimulated by epinephrine and norepinephrine during times of decreased cardiac output, a compensatory mechanism to increase cardiomyocyte excitation and contraction (27). Overstimulation can cause cardiomyocyte toxicity, and transgenic animal models in which β1AR is increased 15-fold causes a progressive decline in heart function, reducing EF to 20% causing overt HF (28). β1AR blockers, such as carvedilol, can improve EF, reduce arrhythmias and reduce mortality from HF (27).

Another target in treating HF is the renin-angiotensin-aldosterone system (RAAS) which is involved in maintaining hemodynamics and fluid regulation via aldosterone and Ang II (29). Renin produced by the kidneys acts on angiotensinogen produced by the liver to produce Ang I, which is cleaved by angiotensin-converting enzyme (ACE) to yield the active Ang II peptide. Ang II is a ligand for Ang II type 1 (AT_1R) and type 2 receptor (AT_2R) which have differing effects on various tissue. AT_1R typically acts in a pathological manner while AT_2R mitigates these effects via negative feedback (30). AT_1R signaling in the proximal tubules of the kidneys increases Na-H ion exchange which increases the osmolarity of the blood, leading to increased blood volume (30). In vascular smooth muscle cells, AT_1R signaling promotes vasoconstriction, whereas in endothelial cell, this is potentiated by increased NOX expression, reducing nitric oxide (NO) bioavailability due to direct NO interaction with ROS forming peroxynitrite ($ONOO^-$), a reactive nitrogen species (RNS) (31). Combined, these effects increase blood pressure, attributable to excessive RAAS activation due to low-grade inflammation in the kidney and liver (32).

In addition to β1AR blockers, targeting Ang II with either ACE inhibitors or angiotensin receptor blocker (ARB) can improve vasodilation, reducing stress on the heart wall, and improving EF (3). ACE inhibitors prevent the conversion of Ang I to Ang II and ARB inhibits cellular Ang II signaling by competitively binding to AT_1R. ACE and ARB inhibitors also reduce aldosterone, as Ang II signaling in the adrenal cortex stimulates its release. Thus, these drugs prevent multiple outcomes: 1) reduced vasoconstriction which reduces blood pressure (33), 2) aldosterone increases sodium reabsorption, increasing blood volume leading to increased blood pressure (34) and 3) Ang II and aldosterone are directly involved in cardiomyocyte signaling leading to hypertrophy, apoptosis and fibrosis (35, 36). Other common pharmacological treatments include aldosterone antagonists as an adjunct, diuretics to reduce blood volume (reduce blood pressure) as well as digoxin which can improve cardiac output (3). Despite the efficacy of these treatments, HF still comes with a 50% five-year mortality rate irrespective of HF categorization (37). Thus, other therapeutic approaches are urgently needed to treat HF.

2.3 Animal models of HF

In pre-clinical models of HF, mice and rats are traditionally used. These HF models typically mimic either a myocardial infarction (MI), such as a heart attack, in which blood flow to the heart is restricted, or a hypertensive model in which the heart walls undergo chronic, excessive pressure. These models are typically representative of HFrEF, not HFpEF. One of the most popular models of HF is to induce MI in rats and mice by conducting a surgical procedure in which the left coronary artery is permanently ligated, or closed off (38). Within four weeks, HF has fully manifested. This model was initially used to test the efficacy of ACE inhibitors 35 years ago, bringing them from preclinical studies to human interventions and clinical practice; thus this model is highly translational (39). In the clinical setting however, when MI occurs due to atherosclerosis,

reperfusion of blood in the vessel is expected due to surgical intervention (angiogram) to open the artery. This reperfusion itself, although necessary to prevent death, is injurious and leads to significant cardiac injury independent of the prior hypoxic state of the heart, in part due to a surge of ROS, intracellular Ca^{2+} flux, inflammation and aberrant changes in pH (40). Mixed models exist utilizing ischemia and reperfusion (I/R), in which the left anterior descending artery is briefly ligated (30 to 60 min) and then perfused (41), although the surgeries are more complex and lengthy.

To induce pressure overload of the heart, a common procedure in rats is to restrict blood flow of the ascending aorta known as ascending aortic banding (38). Blood is restricted from leaving the heart, creating significant stress on the LV wall as observed in hypertension. Within eight weeks significant left ventricular hypertrophy occurs and after 18 weeks, overt HF has manifested (38). Thus, this procedure is typically conducted in younger animals (3-4 weeks old). In mice, a similar procedure known as transverse aortic constriction (TAC) produces a far more rapid response than the counterpart procedure in rats. Left ventricular mass increases 50% within two weeks of banding, although there is less clinical relevance considering the acute nature of this procedure (38). These are the most common modalities for inducing HF in pre-clinical models, although numerous others exists, including drug induced cardiotoxicity (e.g., doxorubicin and isoproterenol), Ang II infusion, diabetes, and transgenic lines, such as spontaneously hypertensive rats (42).

2.4 Major molecular pathways involved in HF pathology

2.4.1 HIF-1α

Due to the high oxygen demands of the heart to facilitate metabolism, hypoxic conditions can be detrimental, and ischemia is caused by prolonged hypoxia leading to tissue injury. One of the main proteins involved in mediating the hypoxic response is hypoxia-inducible factor (HIF)-

1α. Under normoxic conditions, HIF-1α is continually synthesized, hydroxylated by oxygen-dependent prolyl hydroxylase, a domain on HIF-1α, allowing polyubiquitination to occur (43, 44). This then leads to proteasomal degradation preventing its transcriptional activity. Indeed, HIF-1α has a <5 min half-life due to this constant cycle (45). However, under hypoxic conditions, hydroxylation does not occur due to lack of substrate (oxygen), leading to HIF-1α accumulation, nuclear translocation and transcriptional activity at the hypoxia-response element (HRE) DNA binding site (46). HRE transcriptional activity is an adaptive pathway and leads to survival mechanisms (47), such as greater reliance on the glycolytic pathway. Indeed, HIF-1α knockout is detrimental in animal models of HF and exacerbates the disease (48, 49). However, prolonged HIF-1α stabilization is also detrimental and can independently exacerbate HF (50), increasing apoptosis and inflammation (50).

To mimic hypoxia in cell culture systems, the requirement of Fe^{2+} in prolyl hydroxylase is taken advantage of (51). $CoCl_2$ causes stabilization of HIF-1α by replacing Fe^{2+} of prolyl hydroxylase preventing oxygen transfer to proline (52, 53). Thus, $CoCl_2$ mimics a hypoxic response without the need for an oxygen-depleted environment. In cardiomyocytes, HIF-1α stabilization via $CoCl_2$ results in significantly increased ROS and apoptosis (54, 55) as well as inflammation (56).

2.4.2 TLR4

TLR4 is a major receptor involved in innate immunity and is classically activated due to exogenous factors, such as in response to lipopolysaccharides (LPS), a perceived bacterial threat. However, TLR4 has numerous endogenous ligands as well, including DAMPs which are released from necrotic cells (57). It is worth noting that TLR4 is found in greatest abundance in the human heart compared with other TLR isoforms (58). TLR4 activation requires cytosolic adaptor proteins,

toll/interleukin-1 receptor (TIR)-domain-containing adaptor (TIRAP) and TIR domain-containing adaptor inducing interferon (IFN)-β-related adaptor molecule (TRAM). Upon binding, downstream signaling occurs in a myeloid differentiation primary response 88 (MYD88)-dependent and independent manner with the same end result, that is activation of MAPK and NF-κB signaling as well as inflammatory cytokine release. TLR4 is upregulated in humans with reduced LV function and ischemic heart disease and TLR4 was reduced following coronary bypass or stent placement (59). Under cardiac stress, blockade of TLR4 attenuates disease progression (60, 61) while upregulated TLR4 exacerbates it (6). Thus, it is clear that TLR4 is critically involved in mediating HF pathogenesis.

2.4.3 NOX

The NOX family of enzymes under normal physiological conditions produce low levels of superoxide (O_2^-), which undergoes subsequent enzymatic or spontaneous dismutation to hydrogen peroxide (H_2O_2). These ROS molecules are involved in a variety of cellular processes (e.g., sulfide bridge formation, cysteine oxidation, activation of transcription factors, etc.) vital for cell survival and function (14, 62). However, insult to the heart results in excessive ROS via NOX, which initiates a cascade of events, eliciting cardiomyocyte apoptosis and subsequent fibrosis at the organ level, severely inhibiting the functional capacity of the heart leading to HF (63-65). Furthermore, it is likely that ROS generation is increased in the failing heart rather than a detriment in the antioxidant response (66); thus, increased ROS tends to overwhelm the antioxidant system.

A variety of NOX isoforms exists (Nox1-5) with various tissue distributions (7). In cardiomyocytes, NOX2, NOX4 and NOX5 are the predominant isoforms, although NOX1 is also found in lesser concentrations (10). In cardiomyocytes, NOX are likely localized on the plasma membrane, endoplasmic reticulum, and the nuclear envelope (67, 68). A variety of stimuli can lead

to NOX transcription and overexpression, including shear stress (69), Ang II (70), endothelin-1 (71), TNF-α (72) as well as α-adrenergic receptor agonists (73). Regardless of isoform, the role of NOX is to abstract electrons from NADPH in the cytoplasm and reduce molecular oxygen to O_2^-, which is either released into the lumen of organelles or extracellularly. NOX is bound to lipid bilayers of organelles or the outer plasma membrane via 6 transmembrane α-helices. While O_2^- cannot freely pass between lipid bilayers, H_2O_2 can (74). The micro-environments within the lumen of organelles are under reducing conditions resulting in the spontaneous conversion of O_2^- to H_2O_2. Thus, cellular localization of each NOX determines whether O_2^- or H_2O_2 will be the predominant end-product, although some controversy exists as discussed later regarding NOX4.

NOX2 is highly expressed in cardiomyocytes and unlike in phagocytes, is constitutively active and does not require cytosolic translocation or subunit assembly. All four of the NOX isoforms in cardiomyocytes appear to have this constitutive feature, as under basal conditions, NOX are likely highly involved in regulating cell-to-cell signaling (75), whereas in phagocytes, OX is utilized as a defense mechanism in the presence of pathogens. In conjunction with a membrane bound subunit critical to its function ($p22^{phox}$), a unique feature of NOX2 is the $p67^{phox}$, $p47^{phox}$ and $p40^{phox}$ cytosolic subunit complex which is required for its function (76). It has been documented that in both humans (67) and animals (77), NOX2 expression is upregulated in the heart after MI. Deletion of NOX2 in mice attenuates cardiac dysfunction, fibrosis and thickening of the LV in mice with HF induced by CAL (77, 78).

NOX1 is 60% identical to NOX2 and also requires cytosolic subunits to form a complex to function. These subunits include NOX organizer 1 (NoxO1) and NOX activator 1 (NOXA1) which are homologous to $p47^{phox}$ and $p67^{phox}$ in NOX2, respectively (79). Interestingly, due to the high similarity between NOX1 and NOX2, $p47^{phox}$ and $p67^{phox}$ can also bind to NOX1 leading to

functional differences. For example, $p47^{phox}$ has an auto-inhibitory domain preventing assembly of the complex due to conformational shifts in its structure reducing its affinity for binding (79). However, NOXO1 lacks this auto-inhibitory domain leading to constitutive activity of NOX1. This varies by cell-type, but based on published data (80) and data generated in our lab using human cardiomyocytes obtained from the LV of the adult human heart, it is suggestive that NOXO1 is the predominant subunit that interacts with NOX1 in cardiomyocytes, as constitutive expression of NOX1 is present regardless of treatment conditions. This is somewhat controversial however, as NOXO1 binding reduces the affinity of NOX1 to $p22^{phox}$, although unlike NOX2, NOX1 is not dependent upon $p22^{phox}$ for its function (81). Very few investigations exist which have examined the role of NOX1 in cardiac tissue in the context of HF. In mice treated with high-dose doxorubicin, a chemotherapy drug which is known to be cardio-toxic in 11% of subjects taking it as prescribed (82), cardiac injury and fibrosis was attenuated in NOX1 knockout mice compared to wild-type mice (83). Additionally, survival was significantly improved in knockout animals.

NOX4 is unique among the other NOX isoforms, as no cytosolic subunits are required for its function, however, the trans-membrane bound $p22^{phox}$ is requisite for its function similar to NOX2 (7). Controversy exists regarding the type of ROS produced from NOX4. Unlike the other NOX isoforms, NOX4 is thought to be H_2O_2-producing rather than O_2^- producing (84). It has been suggested that NOX4 is actually O_2^--producing but much of the O_2^- would be produced within the lumen of organelles (7). This reducing environment results in spontaneous dismutation to H_2O_2, which can now pass through the lipid bilayer and be detected. However, compelling evidence suggests that NOX4 may indeed produce H_2O_2 preferentially (85). In a catalytic cell-free system, 90% of all oxygen uptake was converted to H_2O_2 by NOX4 due to differing kinetics compared with other NOX isoforms. This lends to its constitutive activity not just in cardiomyocytes, but

ubiquitously in other tissue (86). Due to its high Km, (18% in NOX4 vs 2-3% in NOX2), it has a lower binding affinity to oxygen, making it an oxygen sensor to respond to fluctuations within the cell, such as during changes in altitude. Similar to the other NOX isoforms however, over-expression can occur in vivo during HF (87) and due to inflammatory signaling in vitro (88). Indeed, NOX4 knockout mice who underwent TAC to induce HF (pressure overload model) demonstrated preserved cardiac function and reduced fibrosis compared to wild-type mice (87). Interestingly, NOX2 knockout mice who underwent Ang II infusion did not develop cardiac hypertrophy compared to wild-type mice, while in a pressure overload model using TAC, both NOX2 knockout mice and wild-type mice developed hypertrophy (89). This was due to NOX4 being predominantly expressed in this pressure overload model rather than in Ang II-induced HF. However, despite no effect on hypertrophy in NOX2 knockout mice during pressure overload, cardiac function is preserved (90). Thus, these studies illustrate that these NOX isoforms have independent effects within the same disease processes.

NOX5 is the most recently discovered NOX isoform and appears in humans, but not rodents (7). NOX5 is unique to any other isoform in that no cytosolic subunits are required for its function, and it is the only NOX that does not utilize $p22^{phox}$. NOX5 is a Ca^{2+} sensitive enzyme, and responds to intracellular increases in Ca^{2+} (91). In the context of HF, NOX5 may be of significant importance, since Ca^{2+} leak from the sarcoplasmic reticulum (SR) due to SR stress in cardiomyocytes is a common feature in the infarcted heart (92). In humans who have had a MI, NOX5 is highly expressed in cardiomyocytes, endothelial and vascular smooth muscle cells (93). Disease stage and progression in diseased coronary arteries in humans also positively correlates with NOX5 mRNA (94). Neurohormonal signaling, such as Ang II, can elicit intracellular increases in Ca^{2+} which leads to the activation of NOX5 (95). Because NOX5 does not appear in

rodents, it is more difficult to study its role in the pathogenesis of HF and other cardiac pathologies. However, in mice that have NOX5 genetically knocked-in in endothelial cells demonstrate that increased NOX5 expression results in hypertension (96). Nonetheless, it is clear that NOX5, among the other NOX isoforms are significant sources of ROS which are of detrimental to normal cardiac physiology.

2.4.4 Mitochondrial ROS

Mitochondria comprise 30% of total cardiomyocyte volume (97) and at the organ level, energy demands of the heart are so high that 30 kg of ATP are consumed daily by the heart in humans (98). ROS leak occurs in the mitochondria under normal physiological conditions due to metabolism (99) which the antioxidant system is capable of neutralizing. Mitochondria undergo regular fission and fusion and in healthy cardiomyocytes, this dynamic is at equilibrium (100). In HF, this equilibrium is disrupted, and mitochondria undergo excessive fission, leading to fragmented, dysfunctional mitochondria. This may be in part due to downregulation of fusion promoting protein, optic atrophy (Opa)1 and upregulation of fission proteins dynamin-related protein (DRP)1 under conditions of HF (101). Fragmented mitochondria due to excessive fission produce excessive ROS (100). Indeed, targeting mitochondrial ROS with mitochondrial antioxidants, such as MitoQ, significantly attenuates the detriments of HF in a variety of preclinical models by improving cardiac function, reducing cardiomyocyte apoptosis (102) reducing cardiac hypertrophy and reducing fibrosis (103). In healthy older adults, supplementation with six weeks of MitoQ (20 mg/d) significantly improved endothelium dependent vascular relaxation and arterial stiffness (104). Thus, in the context of HF, mitochondria are a significant source of ROS which is of clinical relevance.

2.4.5 Xanthine oxidase

In urea metabolism, purines derived from nucleotides are converted to hypoxanthine (derived from adenosine), which is then oxidized by XO to xanthine (derived from guanosine) (105). Xanthine undergoes oxidation by XO to form uric acid. XO catalysis involves the reduction of molecular oxygen followed by release of ROS in the form of either O_2^- or H_2O_2. In the context of HF, upregulation of XO can occur due to hypoxia as well as inflammatory signaling (106). Despite these observations, randomized trials have demonstrated weak evidence in reducing HF-associated mortality with allopurinol, a XO inhibitor (107). However, there was a trend for reduced hospitalizations and improved EF. Additionally, the trials were not long term, which may yield alternative findings.

2.4.6 Apoptosis

A key feature of HF, especially from ischemic injury, is the induction of cardiomyocyte apoptosis which results in a diminished capacity for cardiac contraction (108). Since cardiomyocytes do not multiply and share the same lifespan as their host (109), apoptosis ultimately drives diminished EF and remodeling observed in HF. In ischemia, cardiac tissue undergoes various pathological stimuli, including hypoxia, excessive cytokine release and oxidative stress, this can trigger the intrinsic apoptotic pathway which is mostly mediated by the mitochondria (110). The activation of the transcription factor p53 due to these pathological stimuli can lead to synthesis of B-cell lymphoma (BCL)-2-associated X protein (BAX) (111) which causes mitochondrial transition pore opening. This leads to release of cytochrome c and downstream activation of caspase-9 and caspase-3 (110). Once these caspases are activated, cell death then occurs; thus, targeting its upstream effectors are important to prevent this cascade. To that end, BCL-extra-large (BCL-xL) can inhibit BAX activity and prevent mitochondrial pore opening.

2.4.7 Inflammation and ROS in cardiac remodeling

Excessive activation of ROS-producing enzymes and mitochondrial ROS generation can overload endogenous antioxidant defense leading to pathological changes of the heart at the cellular and organ level. ROS can modify amino acid residues, such as cysteine, of kinases of MAPK (e.g., MAP3Ks) which act as regulatory proteins just upstream from the MAPK family (ERK1/2, p38MAPK and JNK) (112). Oxidative modification of these residues leads to their activation. Furthermore, regulators of negative feedback from MAPK phosphatases may also be modified, resulting in their inhibition preventing the de-phosphorylation of MAPKs. In adult rat ventricular myocytes, MAPK phosphorylation is dose-dependent upon H_2O_2 concentrations; 100 μM of H_2O_2 significantly increased the phosphorylation of ERK1/2, p38MAPK and JNK compared to control and 10 μM of H_2O_2, whereas μM um only increased ERK1/2 compared to control (113). The phosphorylation of the three aforementioned MAPKs can have differing effects. For example, ERK1/2 appears responsible for hypertrophic signaling via the nuclear translocation of the transcription factor calcineurin–nuclear factor of activated T cells (NF-AT) (114). NF-AT is required for cardiomyocyte hypertrophy to occur (115) and forms a complex with NF-κB to potentiate hypertrophic signaling (116). Consequently, transcription of fetal genes occurs, resulting in the synthesis of β-myosin heavy chain, α-skeletal muscle and α-smooth muscle actin which increase cardiomyocyte cross-sectional area (117). On the other hand, p38MAPK activation can lead to diminished cardiac functional performance and fibrosis of the heart, in part due to apoptotic signaling via transforming growth factor (TGF)β-activated kinase (TAK1) independent of hypertrophy (118, 119). Similarly, JNK may promote cardiomyocyte apoptosis (113) independent of hypertrophy (120).

Because the heart has limited healing capabilities, apoptotic cardiomyocytes are replaced with fibrotic materials (e.g., collagen) to maintain organ structure. Following excessive ROS production in cardiomyocytes due to pathologies leading to HF, NF-κB nuclear translocation occurs due to direct oxidative modifications just upstream from IκBα, leading to its ubiquitination, freeing the p65 and p50 dimer (121). Upon nuclear translocation and binding to anchoring protein, CREB-binding protein (CBP), binding to the κB regulatory region of DNA occurs leading to the synthesis of a variety of inflammatory cytokines (e.g., TNF-a, IL-1β, IL-6) as well as chemoattractants which guide leukocytes, such as monocytes and neutrophils, to infiltrate cardiac tissue (122, 123).

Monocytes differentiate into macrophages to ingest apoptotic and necrotic cells and release the cytokine TGFβ1 (124). Cardiomyocytes also harbor the inactive form of TGF-β which can be activated by ROS (125, 126) independent of ischemia, as is the case in stress overload due to hypertension (127). TGFβ is a key initiator of the fibrotic process by acting on fibroblasts which reside interstitially between cardiomyocytes, leading to their differentiation into myofibroblasts (127). Myofibroblasts disrupt the delicate architecture of the extracellular matrix between cardiomyocytes due to excessive collagen synthesis and deposition via matrix metalloproteinases (MMPs), disrupting coordinated contraction between cells, severely diminishing the functional capacity of the heart (128).

2.4.8 Endogenous antioxidant defense

To counteract the deleterious effects of excessive ROS, enzymatic antioxidants that catalyze the dismutation of O_2^- to H_2O_2 and further reduce H_2O_2 to H_2O. Superoxide dismutase (SOD)1 (a cytoplasmic enzyme) and SOD2 (a mitochondrial enzyme) convert O_2^- into H_2O_2 (129). Subsequently, catalase and GPx1 (found in both the mitochondria and cytosol) reduce H_2O_2 to

H_2O (130, 131). While SOD is involved in H_2O_2 signaling (132-134), it has a clear cytoprotective role despite H_2O_2 being a pro-oxidant, perhaps due to greater ROS availability towards catalase or GPx. For example, both SOD1 and SOD2 upregulation in transgenic mice appear to offer cardio-protective effects, including improved EF and reduced inflammatory cytokines compared to wild-type mice (135, 136). Further, knocking out SOD2 resulted in reduced EF, hypertrophy and fibrosis compared to wild-type mice (137). Similarly, GPx1 overexpression attenuates LV fibrosis, hypertrophy and cardiac function compared to wild-type after HF induced by ischemia due to coronary artery ligation (CAL) (138). Catalase overexpression was also beneficial, although less impactful in improving cardiac function (139).

In addition, nuclear factor erythroid 2-related factor 2 (NRF2) is a key regulator of glutathione synthesis and has involvement in transcriptional upregulation of heme oxygenase (HO)-1 expression as well as NADPH quinone dehydrogenase (NQO)1, both of which have antioxidant/cytoprotective functions (140). NRF2 is continually synthesized; however, it is sequestered in the cytosol by the enzyme kelch-like ECH-associated protein (KEAP)1 which undergoes continuous ubiquitination and degradation when the KEAP1-NRF2 complex is formed. However, under conditions of oxidative stress, such as excessive H_2O_2, reactive cysteine residues on KEAP1 undergo reduction, leading to conformational shifts in KEAP1, preventing NRF2 binding (141). As such, NRF2 is able to accumulate in the cytosol and translocate into the nucleus. As with NF-κB, NRF2 binds to anchoring protein CBP allowing it to bind to the transcriptional region of DNA encoding the antioxidant responsive element (ARE), leading to the transcription and synthesis of glutathione (142). Because CBP can bind to both NF-κB and NRF2, these proteins compete for binding (143). Under conditions of inflammation and oxidative stress however, NF-κB appears to bind 10-fold greater to CBP than NRF2 as observed in HepG2 cells treated with 12-

O-tetradecanoylphorbol-13-acetate, an inflammatory insult (144). Thus, under pathological conditions observed in HF, it can be assumed that NRF2 would be deprived of CBP binding, and under these circumstances, insufficient ARE transcription would occur in eliciting an overwhelming enough antioxidant response to counteract ROS. Targeting NRF2 upregulation is of major clinical importance as illustrated in a pressure-overload model of HF, cardio-specific NRF2 overexpression attenuated the decline in heart function and reduced fibrosis (145). Furthermore, knocking out NRF2 in this model led to a substantial decline in heart function compared to wild-type mice (146). An overview of the interplay between pro-oxidant enzymes and antioxidant enzymes is illustrated in Figure 2.1.

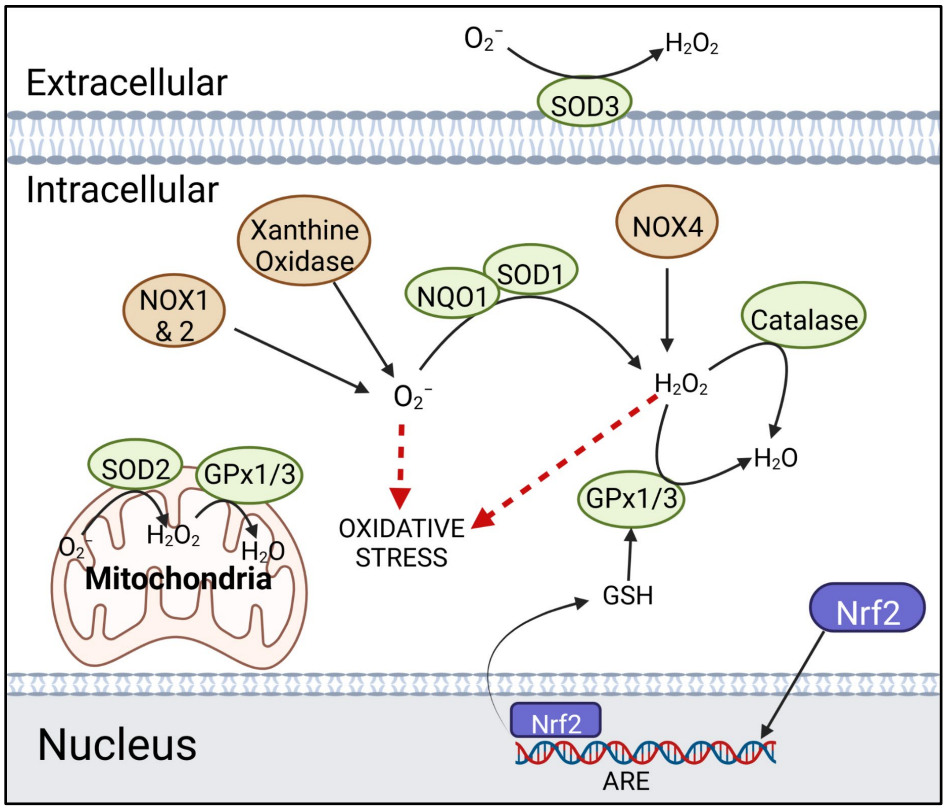

Figure 2.1 Interplay between redox enzymes.

2.5 Polyphenols in HF

Because inflammation and ROS are key pathological characteristics of HF and have significant crosstalk, attenuating inflammation, oxidative stress and increasing the antioxidant response is of significant therapeutic importance. Dietary phytonutrients may be able to modulate these factors. In particular, polyphenols have gained significant attention due to their therapeutic roles in a variety of cardiovascular-related disease states, including atherosclerosis (147) and hypertension (148). Polyphenols structurally vary, but a common feature is at least one aromatic ring with at least one hydroxyl group attached to it (149). Polyphenols are nearly ubiquitously found in plants, and they have differing medicinal properties as determined by their structure (149).

Figure 2.2 illustrates the four most common classes of polyphenols consumed in the human diet, which include flavonoids, phenolic acids, lignans, and stilbenes (150). Polymers and derivatives of these polyphenols comprise the structure of many commonly consumed polyphenols. Flavonoids, for example, are 15-carbon compounds with two benzene rings which are further divided into six different groups based on B-ring positioning in relation to C-ring, as well as the oxidative state of the C-ring. These include anthocyanins, flavanols, flavonols, flavanones, flavones, isoflavones (151). Polymers of flavonoids comprise hydrolysable tannins, which are hydrolysable by acids including those present during digestion, whereas condensed tannins, also known as proanthocyanidins, are not readily hydrolysable.

Phenolic acids contain single aromatic rings, however, differing hydroxyl group and extension of the carbon skeleton yielding differing classes of phenolic acids, including hydroxybenzoic and hydroxycinnamic acids (Figure 2.2). Flavonoids and phenolic acids are the dominant polyphenol classes found in berries.

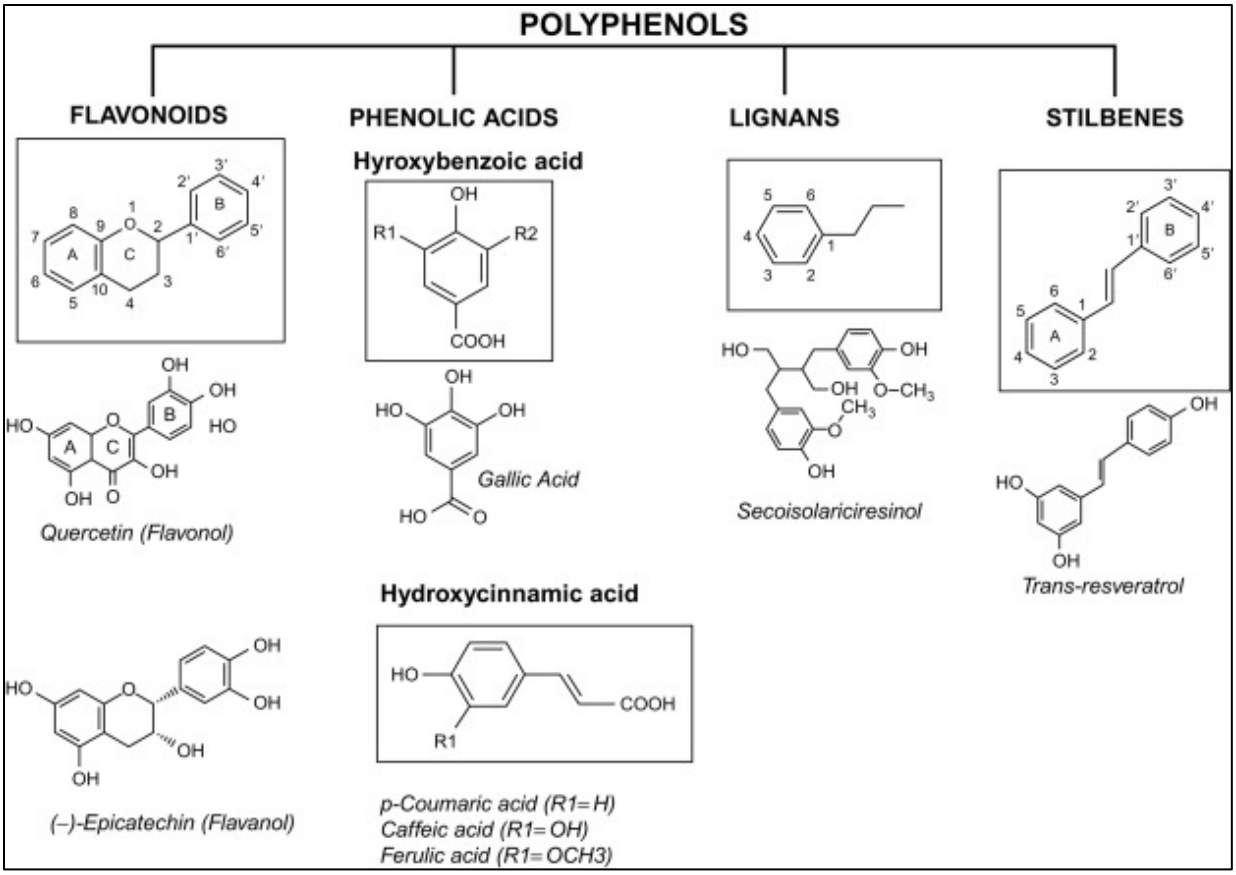

Figure 2.2 Common phenolic compounds found in consumable plant foods. Figure from Pathak et al. (150).

In the context of cardiac protection, polyphenols may reduce cardiac inflammation and oxidative stress, as well as improve cardiac morphological characteristics, and in some cases, improve functional capacity of the heart. For example, luteolin (3.5 g/10 kg chow), a flavone derived from green peppers, ameliorated Ang II-induced (0.7 μg/kg/min) increased NOX2, NOX4, and TGFβ in cardiac tissue of rats after three weeks of pre-treatment (152). While LV wall thickness was decreased from luteolin, functional parameters were not significantly different between groups. In TAC-induced HF, the stilbene resveratrol (320 mg/kg/day), a phenolic compound found in the skin of grapes, decreased collagen deposition in mice hearts and decreased expression of fibroblast derived MMPs (153). Reduced EF was not improved due to treatment; however, possibly due to resveratrol being used three weeks post-surgery (once HF was

established). In a type 1 diabetes model of cardiac dysfunction induced by streptozotocin (pancreatic β-cell toxin), a purple rice extract of anthocyanins (250 mg/kg/day), containing cyanidin-3-O-glucoside (a common berry anthocyanin), decreased cardiac fibrosis and hypertrophy, as well as expression of TGFβ and NF-κB after four weeks (154). Additionally, contractile function was improved. Rats consuming a diet enriched with 2% blueberry had decreased MI size following HF induction via CAL after three months (155). In a separate investigation, survival after MI was improved in rats consuming 2% blueberry diets after 12 months (156). These protective effects elicited by these phytonutrients likely stem from NRF2 upregulation. For example, in kaempferol-treated diabetic rats with isoproterenol-induced heart failure, kaempferol treatment dose-dependently (10 and 20 mg/kg/day) increased NRF2, SOD and GPx1 in addition to dose-dependently decreasing NF-κB and inflammatory cytokines including TNF-α, IL-1β and IL-6 after seven weeks (157).

2.6 Raspberry polyphenols: metabolism and vascular effects

While polyphenols are nearly ubiquitously found throughout the plant kingdom (149), raspberries have a particularly unique polyphenolic profile in which, unlike other berries, are the richest source of the hydrolysable tannin, ellagitannins (~3 mg/g) compared to strawberries (0.25 mg/g) and blackberries (~1.7 mg/g) (158). Ellagitannins in raspberries primarily include sanguiin H-6 and lambertianin C (Figure 2.3), which are essentially polymers of phenolic acids, ellagic and gallic acid, covalently bound to glucose molecules (159). Ellagitannins cannot be directly absorbed and are hydrolyzed to ellagic acid and gallic acid in the stomach and small intestine.

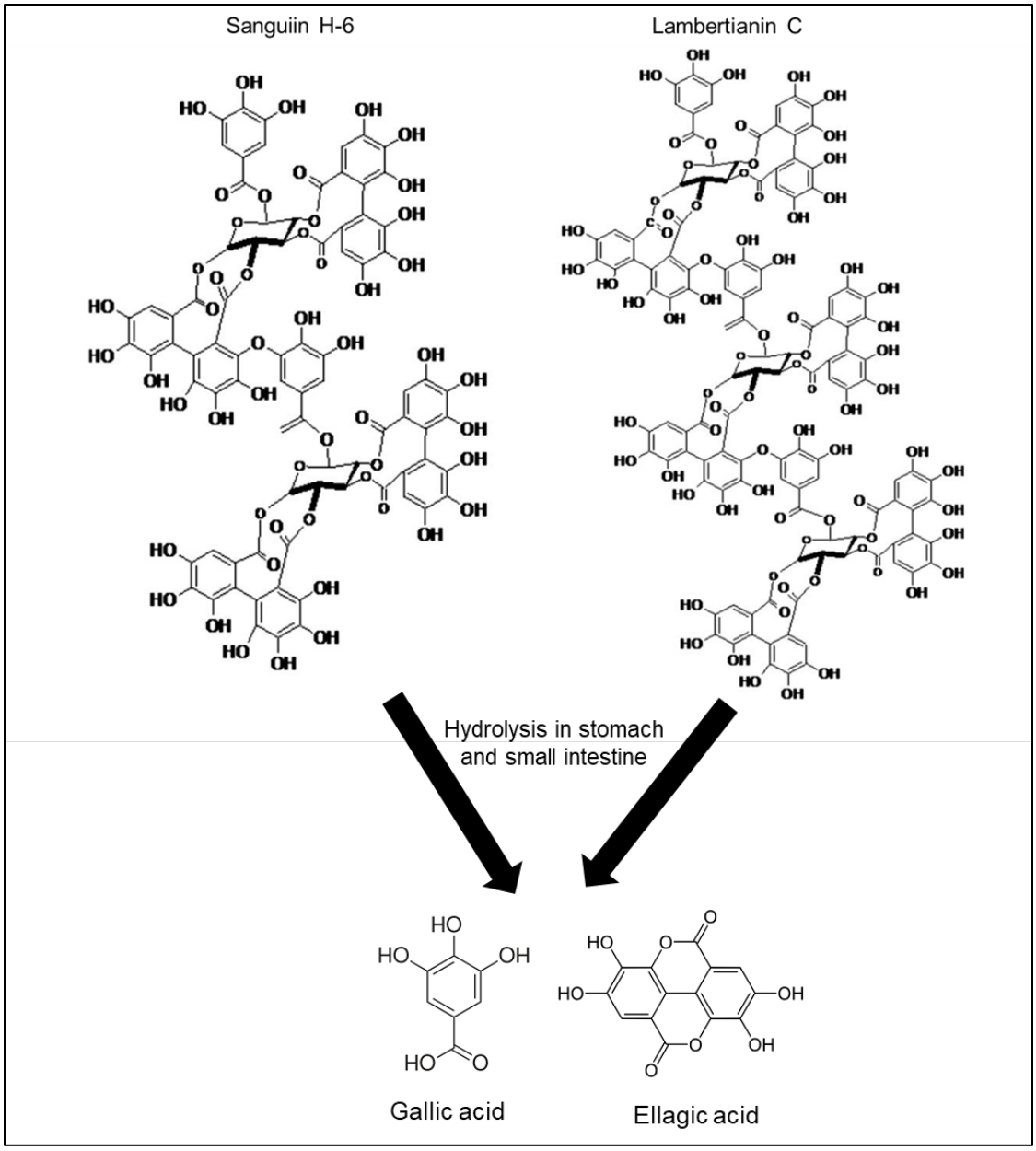

Figure 2.3 Ellagitannins found in red raspberry and their metabolites. Adapted and modified from Burton-Freeman et al. (159)

Polyphenols are poorly absorbed in the small intestine, with only 10-20% of polyphenols estimated to be absorbed (150). The small intestine lacks the enzymatic machinery to perform deglycosylation, dehydroxylation, and demethylation reactions needed to facilitate absorption. Gut microbiota, however, have these enzymatic capabilities. For example, ellagic acid metabolism yields urolithin A, urolithin B and other urolithin derivatives (158). In flavonoids, the C ring is

degraded whereas the A and B ring are hydroxylated and modified (Figure 2.2). Further, the liver can facilitate demethylation via cytochrome P450 and conjugation to glucuronic acid (a glycogenic glucose derivative) via UDP-glucuronosyl transferase (160).

Table 2.1 Polyphenol profile of fresh red raspberry. Adapted from phenol explorer (161).

Flavonoids	Polyphenols	Mean content
Anthocyanins	Cyanidin	0.53 mg/100 g FW
	Cyanidin 3-O-glucoside	14.89 mg/100 g FW
	Cyanidin 3-O-glucosyl-rutinoside	7.06 mg/100 g FW
	Cyanidin 3-O-rutinoside	5.20 mg/100 g FW
	Cyanidin 3-O-sophoroside	37.61 mg/100 g FW
	Delphinidin 3-O-glucoside	0.21 mg/100 g FW
	Malvidin 3-O-glucoside	0.62 mg/100 g FW
	Pelargonidin 3-O-glucoside	1.65 mg/100 g FW
	Pelargonidin 3-O-glucosyl-rutinoside	0.82 mg/100 g FW
	Pelargonidin 3-O-rutinoside	0.42 mg/100 g FW
	Pelargonidin 3-O-sophoroside	3.46 mg/100 g FW
Flavanols	(+)-Catechin	0.58 mg/100 g FW
	(-)-Epicatechin	5.05 mg/100 g FW
	Procyanidin dimer B2	0.10 mg/100 g FW
Flavonols	Kaempferol 3-O-glucoside	1.03 mg/100 g FW
	Quercetin	0.02 mg/100 g FW
	Quercetin 3-O-glucoside	3.58 mg/100 g FW
	Quercetin 3-O-glucuronide	0.63 mg/100 g FW
	Quercetin 3-O-rutinoside	11.00 mg/100 g FW
Phenolic acids		
Hydroxybenzoic acids	Ellagic acid	2.12 mg/100 g FW
	Ellagic acid acetyl-arabinoside	0.20 mg/100 g FW
	Ellagic acid acetyl-xyloside	0.36 mg/100 g FW
	Ellagic acid arabinoside	2.27 mg/100 g FW
	Lambertianin C	30.84 mg/100 g FW
	Sanguiin H-6	76.10 mg/100 g FW
Hydroxycinnamic acids	5-Caffeoylquinic acid	0.57 mg/100 g FW
	p-Coumaric acid	2.30e-04 mg/100 g FW
	p-Coumaric acid 4-O-glucoside	0.32 mg/100 g FW

Illustrating the effects of polyphenol metabolism, 29 different metabolites were identified in serum from healthy males following the consumption of 500 mg ^{13}C-labelled cyanidin-3-

glucoside (162), an anthocyanin found in high concentrations in blackberries (163). Major peaks were observed at 1, 6 and 24 h post-consumption with hippuric acid and vanillic acid as the primary metabolites found in serum. In healthy older adults, 24 g/day of freeze-dried strawberry for 90 days significantly increased the anthocyanin pelargonidin glucuronide, as well as the ellagic acid metabolites, urolithin A and B (164). In an exploratory study which comprehensively analyzed both raspberry polyphenol content and the metabolic fate of raspberry consumption from secondary analysis of two independent case studies (Case 1: n = 2, 125 g/day fresh raspberry for 4 weeks; Case 2: n = 1, lactating woman consumed 125 g/day fresh raspberries for 1 week), ellagitannins and ellagic acid comprised ~44% of all polyphenols found in red raspberry, followed by ~31% anthocyanins (particularly cyanidin 3-O-sophoroside) and ~20% flavan-3-ols (primarily procyanidin B) (165). In addition to Urolithin A and B being identified in human plasma samples, parent anthocyanins, such as cyanidin 3-O-sophoroside were also found intact in plasma.

As discussed, polyphenols are of major clinical relevance in the context of HF as they can attenuate oxidative stress and inflammation at the cellular level. This effect can be attributed to potential binding to KEAP1, causing conformational shifts preventing NRF2 from binding to KEAP1, thus leading to increased NRF2 cytosolic concentration and subsequent nuclear translocation (166). Computational studies revealed that kaempferol, found in negligible concentrations in red raspberry, may directly bind to KEAP1 in this fashion, preventing NRF2 binding (167). However, in both human and rat-specific proteins, it was revealed that gallic and ellagic acid were incapable of binding to KEAP1 in the domain associated with regulating binding of NRF2. Although direct interactions of polyphenols with KEAP1 may alter its binding affinity to NRF2, other interacting proteins which regulate KEAP1-NRF2 complex affinity are also of relevance (168).

For example, p62, a scaffolding protein involved in a variety of cellular processes such as autophagy, can directly bind to the binding pocket of KEAP1 which associates with NRF2, thus, preventing NRF2 from binding to KEAP1 (169). In an I/R model of HF in rats, urolithin B, a downstream microbiome derived metabolite of ellagic acid metabolism, was injected into the intraperitoneal cavity 0, 24 and 48 h prior to surgery in rats at a concentration of 0.7 mg/kg (170). Concentrations of p62 in cardiac tissue were significantly decreased in I/R rats who did not receive treatment however, urolithin B injection significantly abrogated reductions in p62 which was not different than p62 in sham control. This preservation of p62 corresponded with a significant reduction in MI size and improved cardiac hemodynamics compared to I/R controls. Further, although nuclear NRF2 was increased in I/R control compared to sham, urolithin B treatment elicited roughly 3-fold greater nuclear NRF2 compared to I/R control. Increased antioxidant enzyme expression was also observed. In a separate model of high-fat induced atherosclerosis, dietary ellagic acid (0.5 g/kg) in high-fat diet fed mice increased thoracic NRF2 and significantly reduced atherosclerotic lesion area (171).

These raspberry-derived polyphenols may also regulate NOX expression. In rats with spontaneous hypertension, gallic acid supplemented in the drinking water (1% concentration) from week 8 to week 24 led to significant reductions in cardiac NOX2 expression. Although NOX4 and NOX1 mRNA significantly decreased, this did not translate to reductions in their respective protein (172). Left ventricular mass thickening was also attenuated due to gallic acid supplementation. In a separate investigation, excised aortas of rats were treated in high glucose conditions to induce oxidative stress (173). NOX4 expression significantly increased due to treatment; however, ellagic acid inhibited the expression of NOX4. Lastly, ellagic and gallic acid supplementation in a variety of HF models appear to independently suppress cardiac inflammation,

including MAPK activation and NF-κB nuclear translocation, hypertrophy, dysfunction and fibrosis (174-178).

In addition to the phenolic acids discussed, the flavon-3-ol (−)-epicatechin is also found in high concentrations unbound in raspberries (Figure 2.2). In Sprague-Dawley (SD) rats that underwent I/R, a short-term and long-term (−)-epicatechin supplementation model (1 mg/kg/day) was used (179). Short-term supplementation consisted of 2 days prior to I/R surgery and 48 h post, whereas long-term supplementation consisted of 10 day prior to surgery and 3 weeks post. Infarct size was significantly reduced in the long-term model whereas no changes were observed in the short-term model in I/R control vs (−)-epicatechin. Collagen synthesis (MMP-9) and oxidative stress biomarker myeloperoxidase were also significantly reduced in the long-term supplementation group.

These data suggest that individual polyphenols may be of benefit; however, it is likely that polyphenols act in an additive or synergistic manner. For example, resveratrol, quercetin, ethyl gallate, and (+)-catechin were more effect in reducing vascular smooth muscle cell proliferation (a feature of atherosclerosis) in combination rather than in isolation (180). In RAW 264.7 macrophages, the combination of lueteolin and chicoric acid were more effective in reducing lipopolysaccharide-induced inflammation and NF-κB activation than in isolation (181).

Utilizing whole raspberries which have a unique polyphenolic profile may be an efficacious strategy to reduce inflammation and oxidative stress in HF. Thus, the aim of the study proposed herein is to 1) determine whether raspberry consumption can improve functional parameters of the heart in rats with HF and improve morphological characteristics, and 2) determine whether raspberry polyphenols target molecular pathways involved in HF.

3 Preliminary data

3.1 *In vitro* data

Our research team has previously shown that raspberry polyphenol extract attenuates Ang II-induced O_2^-; (Figure. 3.1A) and H_2O_2 (Figure. 3.1B) in rat aortic vascular smooth muscle cells by upregulating the expression of detoxifying enzymes including SOD1, SOD2 and GPx1 (Figure. 3.1C-F) (182). Additionally, the expression of p38MAPK and ERK1/2, was attenuated by raspberry treatment (Figure. 3.2A-C) in VSMCs.

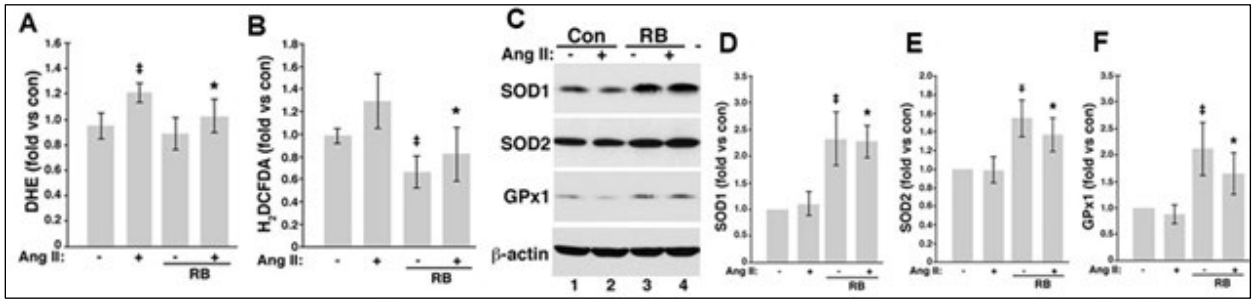

*Figure 3.1 Raspberry polyphenol extract decrease ROS by increasing the expression of antioxidant enzymes in Ang II-induced vascular smooth muscle cells. Cells were incubated in media containing 0.5% FBS with and without 200 µg/ml of raspberry polyphenol extract for 24 h prior to stimulation with Ang II for 72 h. ROS levels were determined after 30-min incubation with (A) DHE and (B) H2DCFDA; (C-D) SOD1, (C-E) SOD2, and (C-F) GPx1 protein expression was determined by western blot. Data are presented as means ± SD from three independent experiments. ‡P < 0.05 compared to control and *compared to Ang II.*

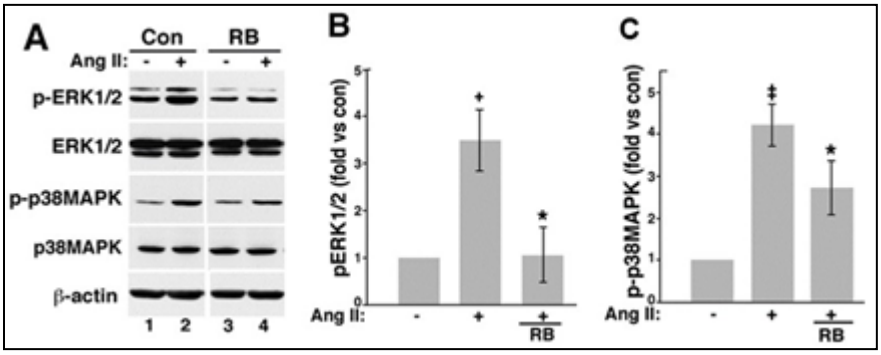

Figure 3.2 Raspberry polyphenol extract inhibits Ang II-induced MAPK signaling in vascular smooth muscle cells. Cells were incubated in media containing 0.5% FBS with and without 200 µg/ml of raspberry polyphenol extract for 24 h prior to stimulation with Ang II for 72 h. (A) Protein

*expression was determined by western blot and quantification of phospho-ERK1/2 and (A-C) phospho-p38MAPK was performed with Image J. Data are presented as means ± SD from three independent experiments. ‡P < 0.05 compared to control and *compared to Ang II.*

Human cardiomycytes were treated with 100 µM palmitate, a saturated fatty acid, for 1 h following pretreatment for 2 h with either 200 µg/mL raspberry polyphenol extract, 1 µM ML-090 and 1 µM VAS2870 (NOX inhibitors) or 100 µM MyD88 inhibitory peptide (Figure 3.3). Palmitate treatment alone significantly increased the release of O_2^- compared to control. While raspberry treatment did not significantly reduce O_2^- production compared to palmitate treatment alone, it was also not signficiantly different from control suggesting some attenuation. As expected, NOX inhibition reduced O_2^- compared to palmitate. However, MYD88 inhibitory peptide operated in a similar manner to raspberry treatment, suggesting that raspberry may be attenuating ROS via reducing inflammation since effects of both treatments were similair.

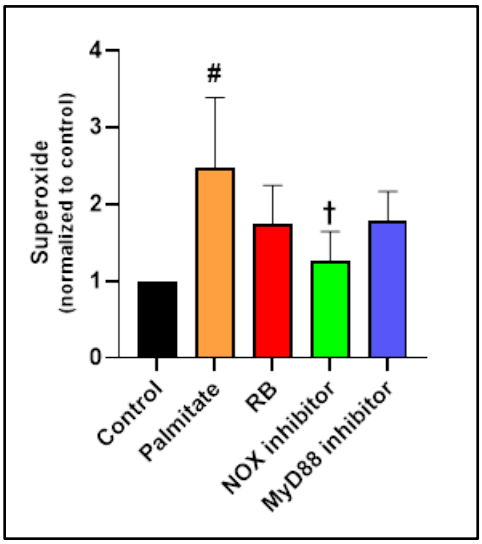

Figure 3.3 Raspberry attenuates cellular oxidative stress in human cardiomyocytes. Human cardiomyocytes grown in vitro were pretreated with 200 µg/ml of raspberry (RB) extract or 1 µM ML-090 + 1 µM VAS2870 for 2 h or 24 h with 100 µM MyD88 inhibitory peptide. Cells were then treated with 100 µM sodium palmitate (PA) for 1 h and probed with DHE for 30 min. Intracellular reactive oxygen species (ROS) was quantified using a fluorometric plate reader. Data are expressed as mean ± standard deviation. Significance (P ≤ 0.05) is denoted by # vs control and † vs palmitate.

3.2 *In vivo* data

Our *in vivo* preliminary data suggest that in Ang II-treated C57BL6/N male mice, a 10% raspberry diet decreases cardiac fibrosis (Figure 3.4). In Ang II-treated SD rats, trends towards decreased LV mass were observed in animals fed a 10% raspberry diet compared to Ang II. (Figure 3.5). Additionally, in mice fed a high-fat, high-sucrose diet, cardiac inflammation was reduced and antioxidant activity was increased as evidenced by decreased MYD88 protein expression and increased SOD2 protien expression. (Figure 3.6).

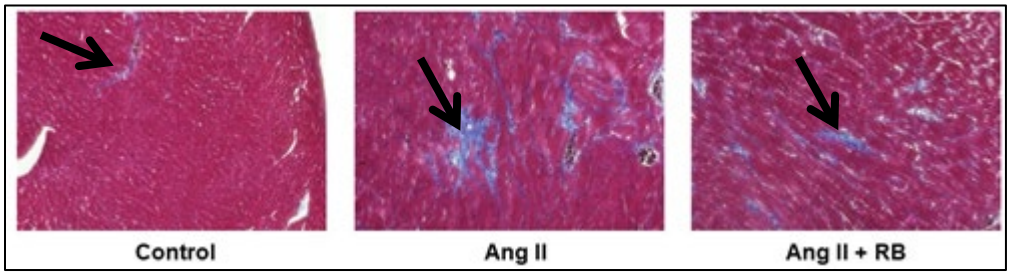

Figure 3.4 Raspberry consumption reduces fibrosis of the heart in Ang II-treated mice. Twelve-week-old C57BL/6N male mice were fed either AIN-93M diet or 10% raspberry supplemented diet for 8 weeks. At week 4, osmotic minipumps were implanted delivering 1,000 ng/kg body weight/day of Ang II or saline for control. Masson's trichrome staining was performed on paraffinized heart tissue. Arrows point to blue staining which indicates fibrosis. Images are 20x magnification.

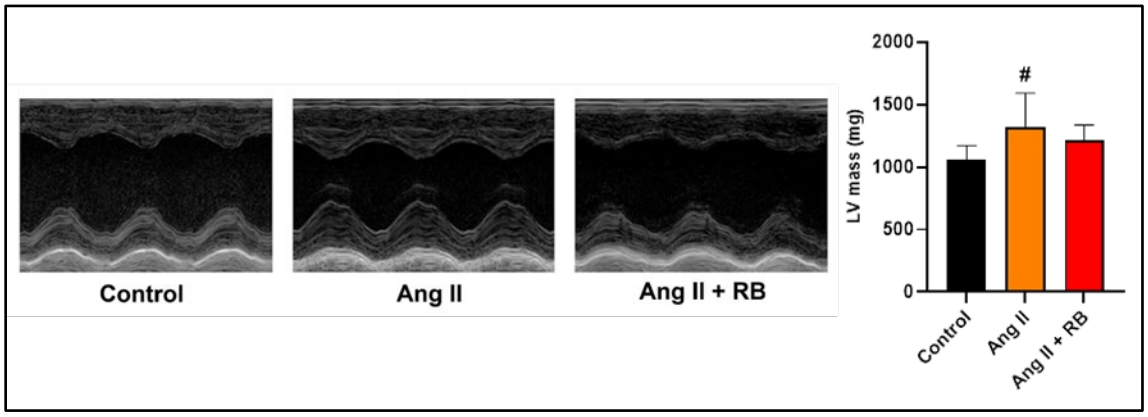

Figure 3.5 Raspberry consumption attenuates left ventricular hypertrophy in rat hearts. Sprague Dawley rats (age six weeks) consumed either AIN-93M control diet or a 10% raspberry supplemented diet for 8 weeks (n = 2/group). At week 4, osmotic minipumps were implanted delivering 270 ng/kg body weight/day of Ang II or saline for control. Echocardiograms were

performed at week 8 to measure left ventricular mass. Data are presented as means ± SD. Significance (P ≤ 0.05) is denoted by # vs control.

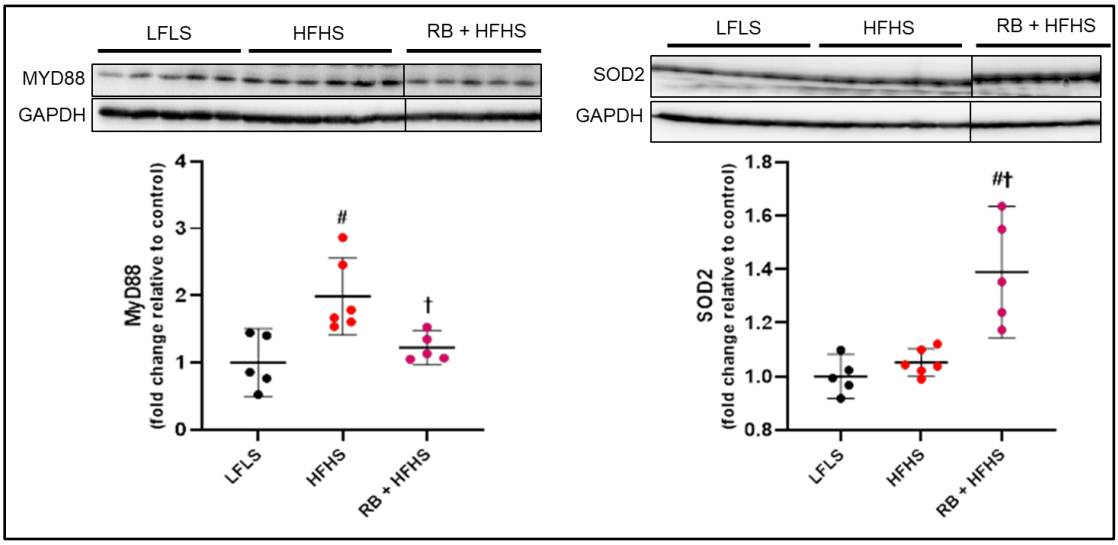

Figure 3.6 Raspberry reduces in MYD88 and increases SOD2 in high-fat, high-sucrose (HFHS)-induced cardiac stress. Animals were fed a low-fat, low-sucrose (LFLS) diet with or without 10% (RB) for four weeks. At week four, half of the animals consuming the LFLS diet without berry were switched to a high-fat, high-sucrose (HFHS) diet without berry, while all animals consuming the RB diet switched to a HFHS diet which was also supplemented with 10% RB. Data are expressed as mean ± 95% confidence interval (CI). Significance (P ≤ 0.05) is denoted by # vs LFLS and † vs HFHS alone.

4 Methods

Reagents: Accutase solution (Cat #: 25-058-CI). Corning, Glendale, AZ). Horseradish peroxidase (Cat #: 20-188) and radioimmunoprecipitation assay buffer (Cat #: 20-188) from EMD Millipore, Burlington, MA. Phosphatase inhibitor cocktails 2 (Cat #: P5726), 3 (Cat #: P0044), protease inhibitor cocktail (Cat #: P8340) and $CoCl_2$ (Cat #: C8661) from Sigma-Aldrich, St. Louis, MO. TAK242 (Cat #: 13871) and NRF2 transcription factor assay kit (Cat #:600590) from Cayman Chemical, Ann Arbor, MI). Dihydroethidium (Cat #: D11347) and NucBlue (Cat #: R37605) from Invitrogen, Waltham, MA. The following antibodies were utilized: α-tubulin (Cat #: 2144), β-actin, (Cat #: 3700), BAX (Cat #: 2772), BCL-xL (Cat #: 2762), caspase-3 (Cat #: 9662), caspase-9 (Cat #: 9508), catalase (Cat #: 14097), DRP1 (Cat #: 8570), HO-1 (Cat #: 82206), HIF-1α (Cat #: 36169), Lamin B1 (Cat #: 12586), MYD88 (Cat #: 4283), Mouse secondary (Cat #: 7076S), phospho-NF-κB (Cat #: 3033), NF-κB (Cat #: 4764), OPA1 (Cat #: 80471), phospho-p38MAPK (Cat #: 4511), p38MAPK (Cat #: 8690), phospho-ERK1/2 (Cat #: 9101), ERK1/2 (Cat #: 9102), p53 (Cat #: 2524), phospho-SAPK/JNK (Cat #: 4668), SAPK/JNK (Cat #: 9252), SOD2 (Cat #: 13141) and Rabbit secondary (Cat #: 7074) from Cell Signaling Technology (Danvers, MA); MMP-2 (Cat #: NB200-113), MMP-9 (Cat #: NBP2-13173), TLR4 (Cat #: NBP2-27149), NQO1 (Cat #: NB200-209) and SOD1 (Cat #: NBP2-24915) from Novus Biologicals (Centennial, CO); 4-hydroxynonenal (Cat #: MAB3249), GPX-1 (Cat #: AF3798), GPX-3 (Cat #: AF4199-SP) and GAPDH (Cat #: MAB5718) from R&D systems (Minneapolis, MN); 3-Nitrotyrosine (Cat #: ab7048), IL-1β (Cat #: ab254360), IL-6 (Cat #: ab9324), NOX1 (Cat #: ab131088), NOX2 (Cat #: ab180642), NOX4 (Cat #: ab133303), TGFβ1 (Cat #: ab215715) and TNF-α (Cat #: ab205587) from Abcam (Waltham, MA).

4.1 *In vivo* experiments

Experimental plan: Eight-week-old male SD rats were purchased from Envigo (Indianapolis, IN). Preliminary data from our previous work utilized male animals. Thus, male rats were used for continuity. Upon arrival, rats were singly housed in an environmentally controlled animal care facility and maintained on 12-hr light/dark cycles. Rats had free access to water and were maintained on a semi-purified casein-based diet (AIN-93M). After seven days of acclimation, rats were assigned one of three groups (n=8-16/group): 1) Control diet, sham surgery (Sham), 2) control diet + left anterior descending CAL surgery (CHF) and 3) raspberry supplemented diet + CHF surgery (RB-CHF) and started on their respective diets. Animals in Sham and CHF consumed the control diet while animals in RB-CHF consumed a diet supplemented with 10% raspberry freeze-dried powder for the entire duration of the study (seven weeks). The overall study design is depicted in Figure 4.1. The 10% raspberry diet is equivalent to approximately 2.5 of fresh raspberries per day for humans. This is based on body surface area and metabolic differences between rats and humans (183). The control diet and raspberry supplemented diet were isocaloric and matched for macronutrients, fiber, and micronutrients such as potassium and sodium. Food intake and body weight was monitored weekly throughout the study. Echocardiograms were conducted prior to sacrifice. Upon sacrifice, hearts were harvested from all rats for histological analysis and protein expression.

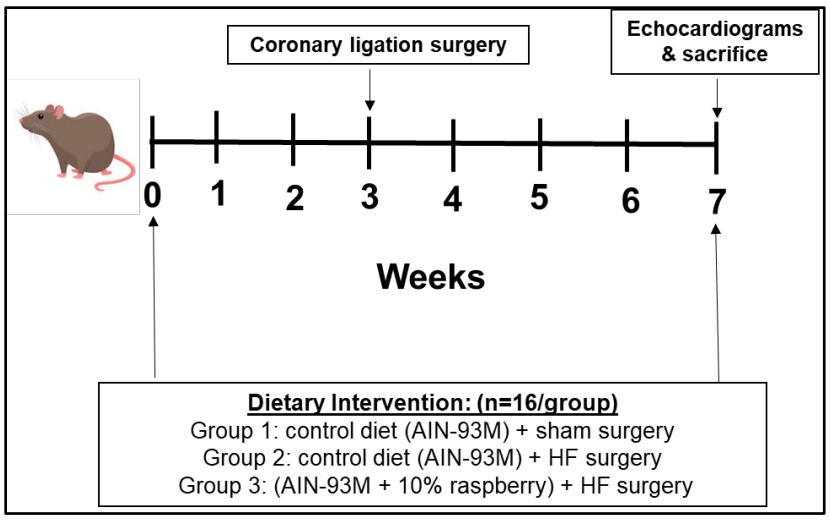

Figure 4.1 Overall study design. Sprague Dawley rats consumed their respective diets for 7 weeks. At week 3, coronary artery ligation surgery was conducted to induce left ventricle ischemia and HF. At week 7, echocardiograms were conducted, followed by tissue harvesting.

Coronary artery ligation: At week 3, animals were anaesthetized with isoflurane (1-5%) and intubated for mechanical ventilation. As described elsewhere, (184)**,** a left thoracotomy was performed, and the heart exteriorized. The ligation was placed on the main diagonal branch of the left anterior descending coronary artery. Buprenorphine SR (1 mg/kg) was given prior to surgery to minimize postsurgical pain. Sham animals underwent the same procedure; however, the coronary artery was not occluded.

Echocardiography: Vevo® 3100 Imaging Platform (Fujifilm Visual Sonics; Toronto, Canada) was used to measure functional and morphological parameters in M-mode with 4-wall LV measurements. These measurements were performed at week 7.

Histological analysis: Following sacrifice, hearts were stored in 10% neutral-buffered formalin for 24 h following sacrifice. Tissue samples were processed, embedded in paraffin, and used for histological analysis. Left ventricle infarct site was utilized for all assessments. Hematoxylin and eosin (H&E) staining was used to assess morphology. Trichrome staining was

used to assess the extent of fibrosis. Heart sections were separately stained with antibodies against 4-hydroxynonenal (4-HNE) and 3-nitrotyrosine (NT) followed by chromogenic horseradish peroxidase (HRP) staining to assess oxidative stress. Samples were counterstained with hematoxylin. TUNEL staining was also conducted utilizing a commercially available kit (Cat #: ab66110; Abcam, Waltham MA) to visualize apoptotic cardiomyocytes.

Protein expression analyses: Left ventricle cardiac tissue at the infarct site was homogenized in radioimmunoprecipitation assay buffer (RIPA) supplemented with protease and phosphatase inhibitor cocktail 2 and 3 by Dounce homogenization and lysates were then centrifuged at 16,000 x g for 20 min. Alternatively, nuclear extraction was performed utilizing a commercially available kit (Cat #: 10009277; Cayman Chemical Company, Ann Harbor MI). Protein concentration of lysates was determined using the DC protein assay kit (BioRad Laboratories, Hercules, CA). Next, lysates were separated in 8-15% SDS-PAGE gels and transferred to polyvinylidene difluoride (PVDF) membranes (Thermo Fisher Scientific, Rockford, IL) using Trans-Blot Turbo (BioRad Laboratories, Hercules, CA). Enhanced chemiluminescence (Immobilon Forte Western HRP Substrate; EMD Millipore, Billerica, MA) was used to determine protein expression of inflammation-associated proteins as well as redox enzymes, apoptotic enzymes and enzymes involved in remodeling using the ChemiDoc Imaging Systems (BioRad Laboratories, Hercules, CA). The density of protein bands was quantified using Image Lab 6.0 (BioRad Laboratories, Hercules, CA) which was normalized to total lane protein. Phosphorylated proteins were normalized to their respective total protein. If phosphorylated and total proteins were on different membranes, then each protein was first normalized to the total lane protein followed by normalization of phosphorylated protein to total protein from each respective membrane.

Total lane protein was utilized due to an inability to use common housekeeping proteins, such as GAPDH or α-tubulin (Figure 4.2A-C) as in this model of HF they were either substantially decreased or increased in CHF animals, respectively. Additionally, nuclear proteins, lamin B1 and histone-3 (Figure 4.2D, E) were also significantly increased in CHF animals. Total lane protein (Figure 4.2F) was not significantly different between groups however and was most appropriate to utilize as also evidenced by other CHF models (185, 186).

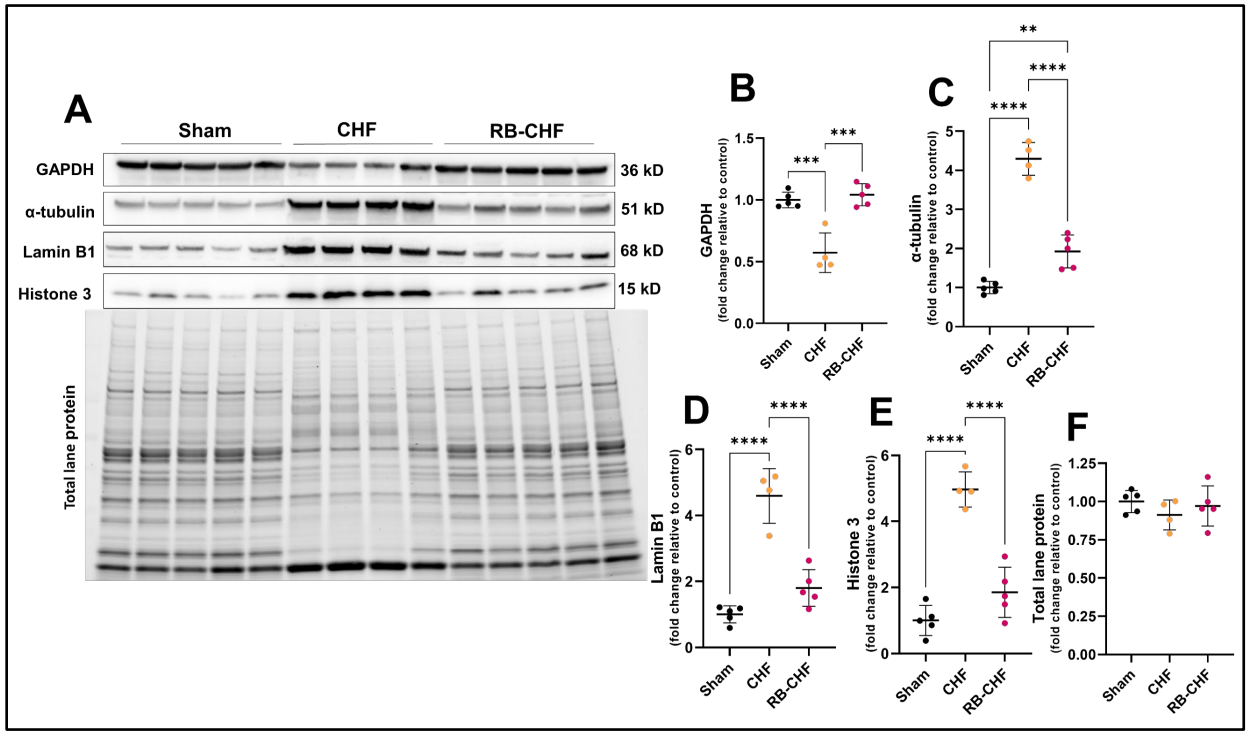

*Figure 4.2 Differences in the expression of housekeeping proteins between groups. Animals consumed a control diet (AIN-93M) or a raspberry supplemented diet for three weeks. Animals consuming the control diet underwent either a sham procedure or underwent coronary artery ligation (CHF), while animals consuming the raspberry supplemented diet only underwent coronary artery ligation (RB-CHF). After four additional weeks, animals were sacrificed. Hearts were excised and immediately frozen in -80 °C. Protein expression of GAPDH (A, B), α-tubulin (A, C), lamin B1 (A, D), histone 3 (A, E) and total lane protein (A, F) were assessed by western blot and converted to fold change vs sham for each respective protein. Data are expressed as means ± SD. *P ≤ 0.05, **P ≤ 0.01, ***P ≤ 0.001, **** P ≤ 0.0001.*

Serum antioxidant capacity: Blood was collected in 1.5 mL microcentrifuge tubes from animals following decapitation and allowed to clot for 30 min at room temperature. Blood was

then centrifuged at 5,000 RPM for 10 min at 4 °C. Serum was then aliquoted from the upper phase and stored at -80 °C until later use. To assess serum antioxidant capacity, the ferric reducing antioxidant power (FRAP) assay was conducted which measures the reductive ability of serum components to reduce ferric iron (Fe^{3+}) to the ferrous ion (Fe^{2+}) (187). Additionally, the oxygen radical absorbance capacity (ORAC) assay was conducted, which measures the ability of serum components to act as peroxyl radical scavengers (188).

For the FRAP assay, a master mix containing 300 mM acetate buffer (pH 3.6), 10 mM 2,3,5-triphenyltetrazolium chloride (TPTZ) in 40 mM HCl, and 20 mM FeCl $6H_2O$ at a final ratio of 10:1:1 was first prepared, and this master mix was combined with sample at a ratio of 9:1 in a 96-well plate. FRAP values were calculated against a $Fe^{2+}SO_4$-$7H_2O$ standard curve and absorbance was measured at 593 nm with a microplate reader (Synergy HT; BioTek, Winooski, VT). For the ORAC assay, serum samples were added to a 96-well black plate 5x diluted with PBS. A PBS solution containing disodium fluorescein (120 nM) was added to each well and allowed to incubate for 30 min at 37 °C. After which, a PBS solution containing 75 mM of 2′,2′- azobis (2-amidinopropane) dihydrochloride, the source of peroxyl radicals, was added to each well and allowed to react for 2 h at 37 °C, with measurements at baseline and final (Ex/Em = 485/528).

Protein carbonylation assay: A commercially available kit (Cat #: ab178020; Abcam, Waltham MA) was utilized to quantify protein carbonyl groups produced from protein oxidation of LVs, a measure of oxidative stress. Western blot was performed on processed samples and whole lanes were quantified on Image Lab.

ATP quantification: A commercially available kit (Cat #: ab113849; Abcam, Waltham, MA) was utilized to detect ATP content of isolated LVs with luminescent detection in a 96-well white plate with a microplate reader (Synergy HT; BioTek, Winooski, VT).

4.2 *In vitro* experiments

Experimental plan: Human cardiomyocytes (C-12810; PromoCell, Heidelberg, Germany) were cultured in Myocyte Growth Medium (C-22070; PromoCell, Heidelberg, Germany) containing 5% FCS, EGF (0.5 ng/ml), FGR (2 ng/ml), insulin (5µg/ml), and 1% antibiotics. These cells have a progenitor-like phenotype allowing proliferation unlike adult fully differentiated cardiomyocytes. Media was changed every two days. When cells reached approximately 70% confluency, they were detached with Accutase solution. Cells were then seeded in complete media with a density of 10,000 cells per cm^2 and allowed to adhere and reach 80-90% confluency in 6-well for protein analyses or 96-well plates for cell viability and fluorometric assays.

Polyphenol extraction: Polyphenol extraction and purification of red raspberry freeze-dried powder was performed as described by Feresin et al. (189). Briefly, freeze-dried raspberry powder was extracted with 80% ethanol in an ultrasonic bath under subdued light with nitrogen purging to avoid oxidation. Solution was filtered, evaporated, and freeze-dried prior of removal of organic molecules using chloroform. Samples were stored at −20 °C for later use.

Table 4.1 Polyphenol profile and quantification of raspberry extract. Adapted from Feresin et al. (182).

Phenolic acids		**Flavonoids**	
Gallic acid	74.6	*Flavonols*	
p-Coumaric acid	27.9	Quercetin	26.7
Ferulic acid	—	*Anthocyanins*	
Chlorogenic acids		Cyanidin-3-glucoside	33.8
3-*O*-Caffeoylquinic acid	114.4	Cyanidin-3-galactoside	3.6
4-*O*-Caffeoylquinic acid	10.4	Delphidin-3-*O*-glucoside	45
5-*O*-Caffeoylquinic acid	—	*Flavan-3-ols*	
		(−)-Epicatechin	478
		(−)-Epigallocatechin	199

Note: anylates measured in parts per million

Protein analysis: Following confluency in 6-well plates, cells were placed in starvation medium (0.5% FCS) and pretreated for 1 h with 400 μg/mL of raspberry polyphenol extract (RBE) or 1 μM TAK242 an inhibitor of downstream TLR4 signaling (190), followed by 24 h incubation with 400 μM of $CoCl_2$ to induce hypoxia. Protein expression of cleaved caspase-3 as well as HIF-1α was normalized to β-actin.

Cell viability: Following confluency in clear 96-well plates, cells were treated with either $CoCl_2$ (200-800 μM), raspberry extract (200-800 μg/mL), or TAK242 (1-4 μM) for 24 h. Following incubation, MTT reagent (Cat #: 10009365, Cayman Chemical, Ann Arbor, MI) was added to each well (10% of volume) and was incubated for 3-4 h, followed by addition of SDS-crystal dissolving solution for 24 h. Colorimetric absorbance was read at 570 on a Synergy HT microplate reader (BioTek, Winooski, VT).

Apoptosis assay: Following confluency in black, clear-bottom 96-well plates, cells were pretreated for 1 h with 400 μg/mL of raspberry polyphenol extract or 1 μM TAK242 followed by 24 h incubation with 400 μM of $CoCl_2$. Apoptosis was assessed fluorometrically with AnnexinV-

FITC Apoptosis Detection Kit (Cat #: V13242; ThermoFisher Scientific, Waltham, MA) per manufacturer instruction in a Synergy H1 microplate reader (BioTek, Winooski, VT).

Superoxide detection: In a black, clear-bottom 96-well plate following treatments as described above in starvation medium, dihydroethidium (DHE) was dissolved in dimethyl sulfoxide and added to wells (10 μM final concentration) followed by 30 min incubation (37 °C and 5% CO_2). Cells were then gently washed with warm phosphate-buffered saline (PBS) twice, and phenol red-free starvation medium supplemented with NucBlue™ (1 drop/mL) was added. Fluorescence was read using a Synergy H1 microplate reader at the following Ex/Em (nm): 518/606 (DHE; O_2^-) and 360/460 (Hoechst 33342 with NucBlue™). Additionally, cells were visualized qualitatively with fluorescent microscopy.

Mitochondrial membrane potential: In a black, clear-bottom 96-well plate following treatments as described above in starvation medium, mitochondrial membrane depolarization was assessed with JC-10 fluorometric probe using a commercially available kit (Cat #: MAK159; Sigma Aldrich, Saint Louis, MO) per manufactures instructions. JC-10 forms red-fluorescent aggregates (Ex/Em 540/590) in the mitochondria of cells with a polarized mitochondrial membrane. Cells were visualized qualitatively with fluorescent microscopy.

4.3 Statistical Analyses

Sample Size Calculation: The sample size calculations for these experiments are based on our preliminary data and were obtained using a priori analyses (G*Power 3). In a two-group comparison, considering $\alpha = 0.05$, power = 0.80 and d (effect size) = 2.5, we estimated that 8 animals per group would be necessary to detect a significant difference in means using two-sided

0.05-level hypothesis tests. To avoid compromising the data by random mortality, 16 rats per group were studied to account for a potential 40% mortality rate.

Data Analyses: GraphPad Prism (San Diego, CA) was used for all statistical analyses. All animal data were normalized to Sham, while cell culture data were normalized to control or $CoCl_2$ where indicated. Animal data were analyzed using one-way ANOVA followed by Tukey-Kramer post-hoc multiple comparison analysis. Cell data were compared either to control or to $CoCl_2$ alone using Dunnett's multiple comparisons analysis. Values are represented as mean ± standard deviation (SD). Data were deemed significant if $P \leq 0.05$.

5 RESULTS

Body weight (Figure 5.1A) and food intake (Figure 5.1B) were similar between treatment groups with no overall significant differences following area under the curve (AUC) analysis (data not shown). As expected, following surgeries, all groups experienced a significant decline in food intake and a slight, non-significant decline in body weight during week 4, both of which rebounded during weeks 5-7.

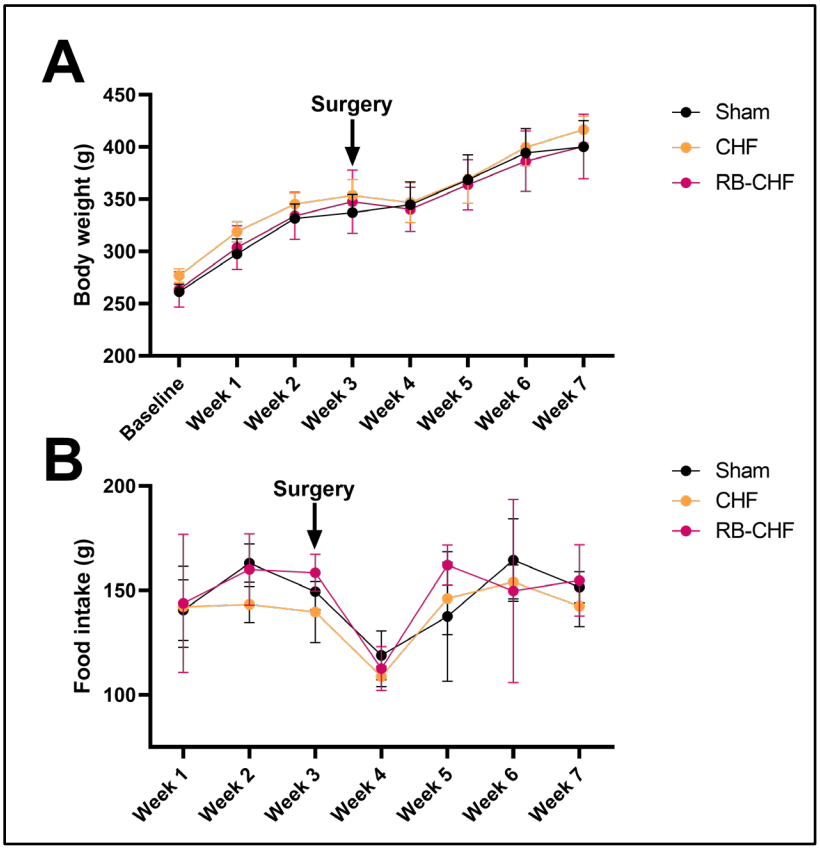

Figure 5.1 Body weight and food intake. Animals consumed a control diet (AIN-93M) or a raspberry supplemented diet for three weeks. Animals consuming the control diet underwent either a sham procedure or underwent coronary artery ligation (CHF), while animals consuming the raspberry supplemented diet only underwent coronary artery ligation (RB-CHF). After four additional weeks, animals were sacrificed. Body weight and food intake was monitored weekly.

5.1 Raspberry consumption attenuates cardiac dysfunction and remodeling in HF.

Qualitatively, echocardiograms of the LV in M-mode in CHF animals revealed significantly flattened LV contractions compared to Sham animals which had much greater anterior and posterior wall peaks (Figure 5.2). This flattening observed in CHF animals was attenuated in RB-CHF animals, with stronger contractions observed; however, not to the extent of Sham. Quantification of echocardiograms are provided in Table 5.1. With respect to functional parameters, a significant decline in EF and fractional shortening (FS) was observed in CHF animals (EF: 39 ± 6%; FS: 20 ± 3%) and RB-CHF animals (EF: 51 ± 3%; FS: 27 ± 2%) following CAL compared to sham (70 ± 5% and 41 ± 4%, $P < 0.0001$). Both EF and FS were significantly greater in RB-CHF compared to CHF ($P \leq 0.01$); however, demonstrating an attenuation in the decline of these parameters.

Cardiac output (CO) was significantly reduced in both CHF animals (70 ± 14 mL/min) and RB-CHF animals (69 ± 11 mL/min) compared to sham (86 ± 7 mL/min, $P \leq 0.05$); however, raspberry consumption did not attenuate these effects. Stroke volume (SV) was not significantly different across groups. With respect to morphological echocardiographic parameters (Table 1), LV mass was significantly increased in CHF animals (1670 ± 683 mg) compared to sham (1066 ± 140 mg, $P = 0.04$). However, LV mass in RB-CHF animals (1405 ± 285 mg) was not significantly different from either Sham or CHF. Left ventricular internal diameter at end systole (LVIDs) and at end diastole (LVIDd), a measure of the distance between the anterior and posterior wall of the LV, was significantly increased in CHF animals (LVIDs: 7.6 ± 0.5 mm; LVIDd 9.5 ± 0.5 mm) compared to sham animals (LVIDs: 4.6 ± 0.5 mm, $P <0.0001$; LVIDd 7.9 ± 0.4 mm, $P = 0.0005$). LVIDs in RB-CHF (6.1 ± 0.5 mm) was significantly lower than CHF ($P = 0.002$) and sham ($P =$

0.001), while LVIDd (8.4 ± 0.7) was significantly lower than CHF ($P = 0.02$) but was not different from sham.

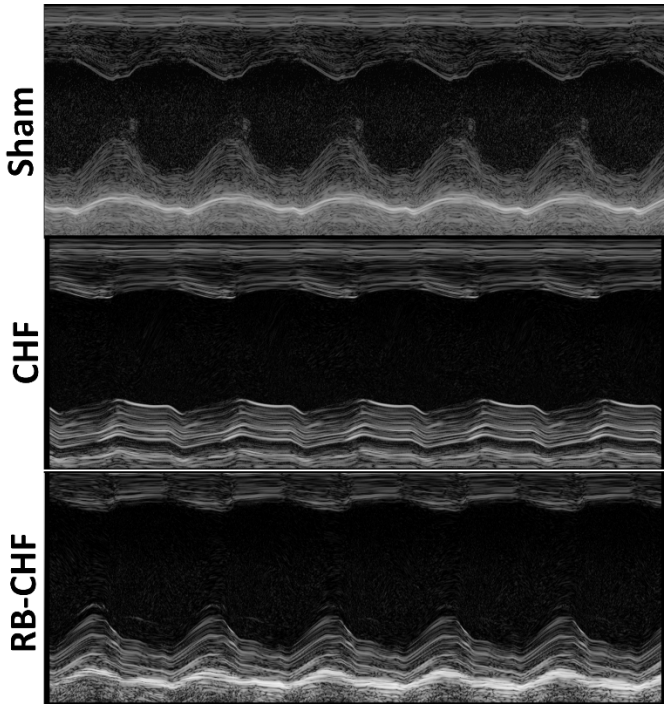

Figure 5.2 Qualitative assessment of echocardiogram images in M-mode. Visualized are the posterior and anterior walls of the cardiac left ventricle during systole and diastole as indicated by the observed peaks and troughs, respectively.

Table 5.1 Functional and morphological echocardiographic parameters. #symbol denotes significant vs sham, while †denotes significance vs CHF. Abbreviations: heart rate, HR; ejection fraction, EF; fractional shortening, FS; stroke volume, SV; cardiac output, CO; LV, left ventricular internal diameter end systole, LVIDs; Left ventricular internal diameter end diastole, LVIDd. Data are expressed as mean ± SD.

Parameters	**Sham**	**CHF**	**CHF + RB**
HR (BPM)	366 ± 26	347 ± 20	343 ± 21
EF (%)	70 ± 5	39 ± 6$^{\#}$	51 ± 3 $^{\#\dagger}$
FS (%)	41 ± 4	20 ± 3$^{\#}$	27 ± 2 $^{\#\dagger}$
SV (µL)	237 ± 20	201 ± 34	202 ± 38
CO (mL/min)	86 ± 7	70 ± 14$^{\#}$	69 ± 11$^{\#}$

LV mass (mg)	1066 ± 140	1670 ± 683 $^{\#}$	1405 ± 285
LVIDs (mm)	4.6 ± 0.5	7.6 ± 0.5 $^{\#}$	6.1 ± 0.5$^{\#\dagger}$
LVIDd (mm)	7.9 ± 0.4	9.5 ± 0.5 $^{\#}$	8.4 ± 0.7†

Qualitative histological assessments with H&E staining (Figure 5.3A) at the infarct site revealed disorganized cardiomyocytes with numerous sites of immune cell infiltration in CHF, whereas the disorganization and frequency of immune cell infiltration was reduced in RB-CHF. In the qualitative assessment of fibrosis at the infarct site utilizing trichrome staining, substantial fibrosis was identified in CHF whereas this was attenuated in RB-CHF. Protein analysis revealed that both the inactive and active (cleaved) form of TGFβ1 (Figure 5.3B-D) were significantly increased in CHF animals (12.2 ± 3.4-fold and 3.5 ± 0.9-fold, respectively) compared to Sham ($P < 0.0001$) and RB-CHF (1.7 ± 0.5-fold, $P < 0.0001$; 1.9 ± 0.3-fold, $P = 0.002$). While the increase in the active form of TGFβ1 was attenuated in RB-CHF animals, it was also significantly greater than sham ($P = 0.04$). In RB-CHF animals, MMP2 (2.1 ± 0.5-fold) & MMP9 (1.4 ± 0.3-fold) were significantly attenuated (Figure 5.3B, E, F) compared to CHF animals (MMP2: 12.2 ± 5.9-fold, $P = 0.001$; MMP9: 5.9 ± 0.8-fold, $P < 0.0001$). Phosphorylation of ERK1/2, a MAPK involved in hypertrophic signaling, was increased in both CHF (33.9 ± 6.6-fold) and RB-CHF (7.4 ± 5.0-fold) compared to Sham ($P \leq 0.04$) (Figure 5.3B, G). However, ERK1/2 phosphorylation in RB-CHF animals was significantly lower than CHF animals ($P < 0.0001$).

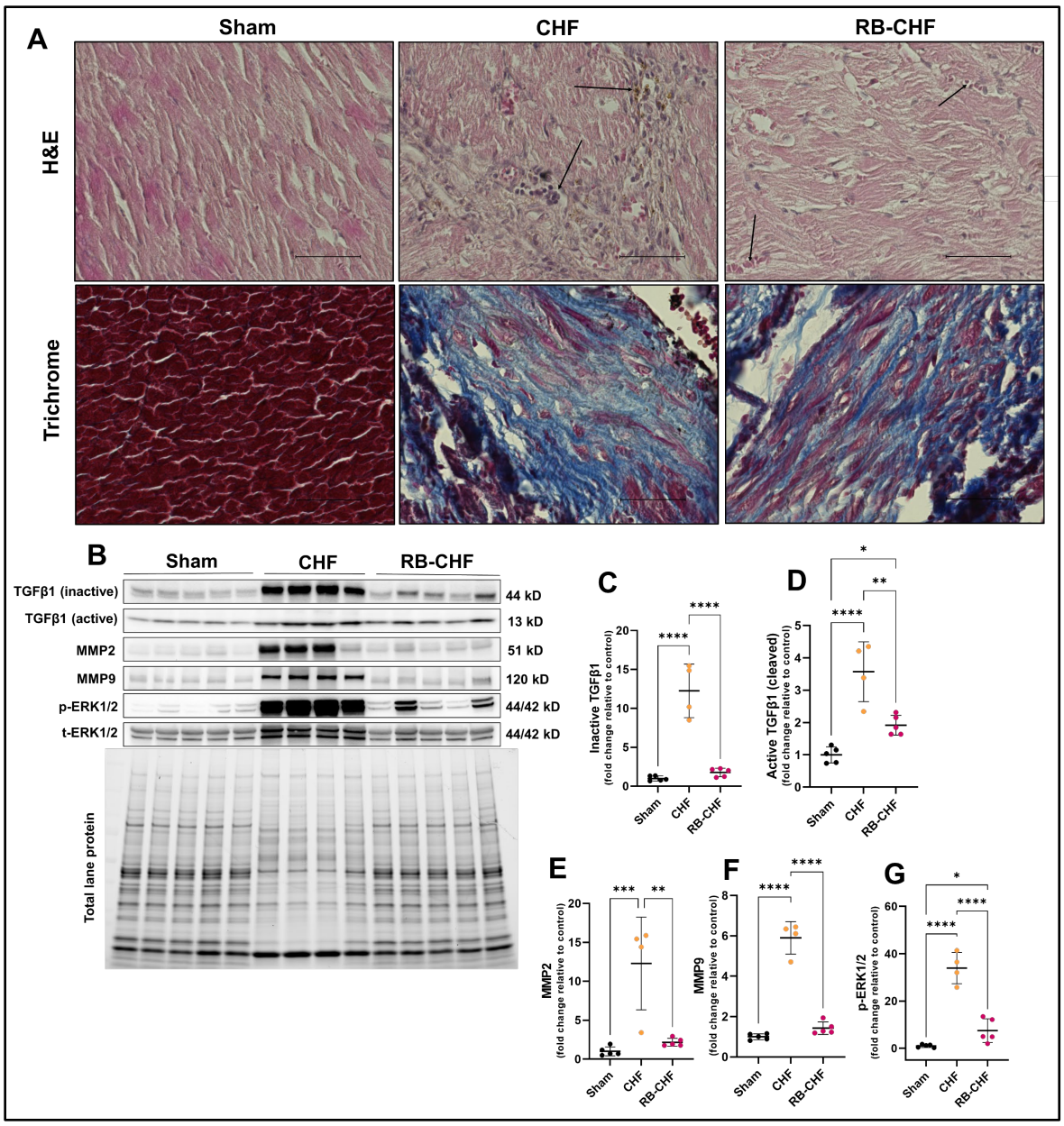

Figure 5.3 Effects of raspberry consumption on cardiac remodeling and associated molecular pathways in heart failure. Animals consumed a control diet (AIN-93M) or a raspberry supplemented diet for three weeks. Animals consuming the control diet underwent either a sham procedure or underwent coronary artery ligation (CHF), while animals consuming the raspberry supplemented diet only underwent coronary artery ligation (RB-CHF). After four additional weeks, animals were sacrificed. Hearts were excised and either stored in 10% formalin for histological analysis or immediately frozen in -80 °C for protein analysis. (A) Images of H&E and trichrome staining at 60x magnification (50 μM scale bar). Arrows in H&E stain are representative of sites of immune cell infiltration. The blue color in the trichrome staining is indicative of fibrosis. Protein expression of inactive or active TGFβ1 (B-D), MMP2 & 9 (B, E, F) and phosphorylation of ERK1/2 were assessed by western blot and normalized to total lane protein

*followed by fold change vs sham for each respective protein. Total lane protein blot is representative. Data are expressed as means ± SD. *P ≤ 0.05, **P ≤ 0.01, ***P ≤ 0.001, **** P ≤ 0.0001.*

5.2 Raspberry consumption attenuates TLR4-mediated inflammatory signaling in HF.

Due to the involvement of TLR4 in HF pathophysiology, the protein expression of TLR4 and its downstream targets were evaluated (Figure 5.4). A significant increase in TLR4 protein expression (Figure 5.4A, B) was observed in CHF animals (21.6 ± 10.5-fold) compared with RB-CHF and Sham ($P \leq 0.0005$). The TLR4 adaptor protein, MYD88, was also significantly increased (Figure 5.4A, C) in CHF animals (8.0 ± 1.3-fold) compared to RB-CHF and Sham ($P < 0.0001$). Consequently, the phosphorylation of NF-κB p65 subunit was significantly increased (Figure 5.4A, D) in CHF animals (3.4 ± 1.9-fold) compared to both RB-CHF and Sham ($P \leq 0.02$). To confirm the nuclear translocation of NF-κB, nuclear isolation of the LV was also performed. Purity was assessed by lack of α-tubulin, a cytosolic protein, in nuclear extracts. Indeed, nuclear extracts were mostly free of α-tubulin when compared with the cytosolic fraction following 10-second chemiluminescent exposure without any contrast modifications (Figure 5.4E, G). Cytosolic NF-κB p65 trended towards being significantly lower (Figure 5.4E, F) in CHF animals (0.6 ± 0.2-fold) compared to Sham ($P = 0.051$). However, NF-κB p65 expression in the cytosol of RB-CHF animals (0.7 ± 0.2-fold) was not significantly different from either Sham or CHF ($P \geq 0.2$). In the nuclear fraction, NF-κB p65 was significantly greater (Figure 5.4G, H) in CHF animals (17.2 ± 14.6-fold) compared to both Sham and RB-CHF ($P \leq 0.02$).

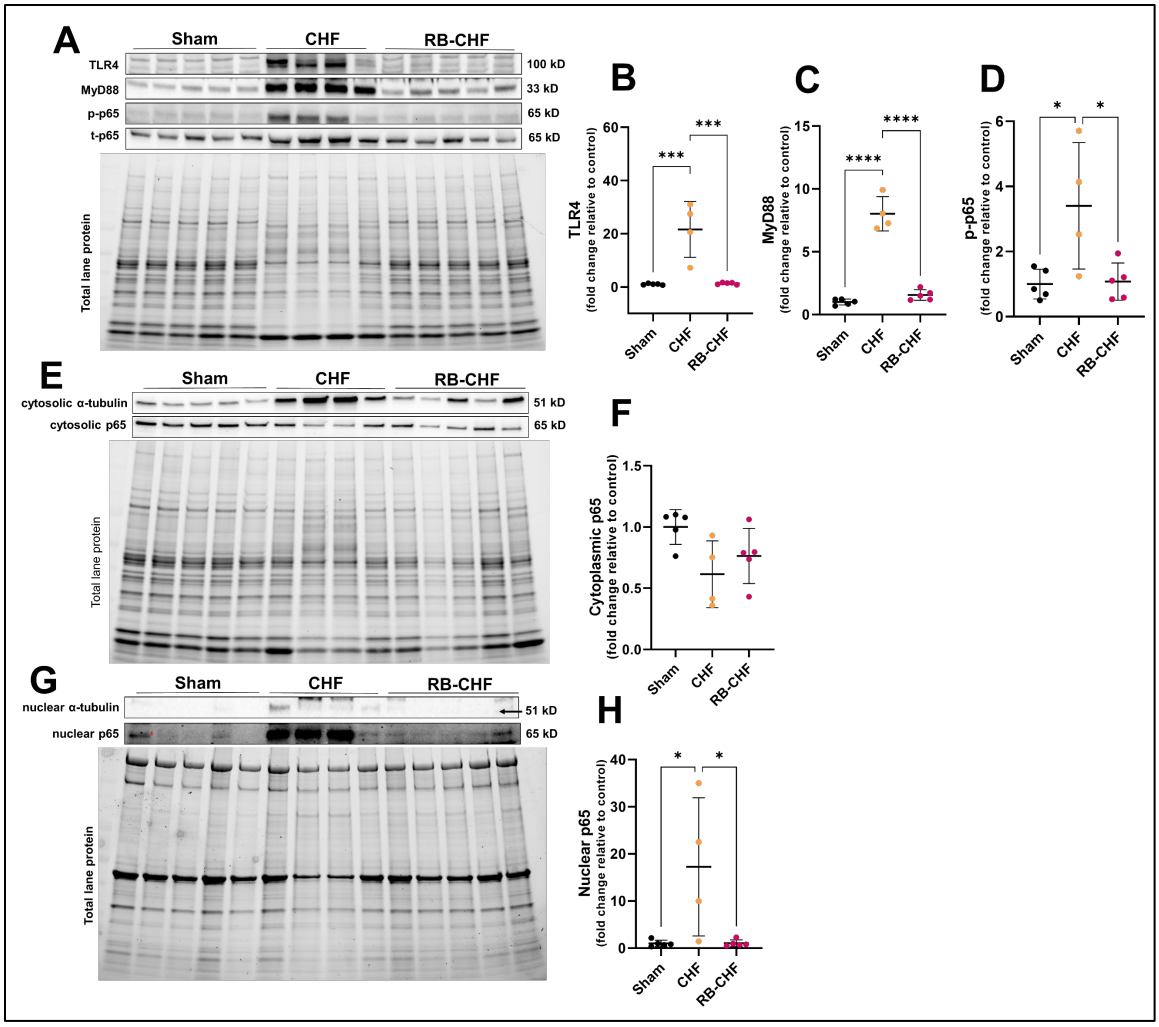

*Figure 5.4 Effects of raspberry consumption on cardiac TLR4 signaling and NF-κB nuclear localization in HF. Animals consumed a control diet (AIN-93M) or a raspberry supplemented diet for three weeks. Animals consuming the control diet underwent either a sham procedure or underwent coronary artery ligation (CHF), while animals consuming the raspberry supplemented diet only underwent coronary artery ligation (RB-CHF). After four additional weeks, animals were sacrificed. Hearts were excised and immediately frozen in -80°C. Protein expression of TLR4 (A, B), MYD88 (A, C), p-p65 (A, D) cytosolic p65 (E, F) and nuclear p65 (G, H) were assessed by western blot and normalized to total lane protein followed by fold change vs sham for each respective protein. The arrow in panel G points to the bands of interest. Total lane protein blot (A) is representative. Data are expressed as means ± SD. *P ≤ 0.05, **P ≤ 0.01, ***P ≤ 0.001, **** P ≤ 0.0001.*

In parallel to NF-κB, TLR4 signaling also mediates p38MAPK and SAPK/JNK phosphorylation. There were no significant differences in the phosphorylation of p38MAPK between groups (Figure 5.5A, B). However, SAPK/JNK phosphorylation was significantly

increased (Figure 5.5A, C) in CHF animals (3.7 ± 1.3-fold) compared to RB-CHF (1.6 ± 0.1-fold, $P = 0.002$) and Sham ($P = 0.0003$). SAPK/JNK and NF-κB are both involved in inflammatory cytokine expression; thus, IL-6, IL-1β and TNF-α were assessed. IL-6 and IL-1β were increased (Figure 5.5A, D, E) in CHF animals (IL-6: 3.1 ± 0.7-fold; IL-1β: 15.3 ± 7.8-fold) compared to RB-CHF (IL-6: 0.9 ± 0.4-fold, $P < 0.0001$; IL-1β: 3.3 ± 1.2-fold, $P = 0.003$) and Sham ($P \leq 0.0009$). However, TNF-α protein expression (Figure 5.5A, F) was not significantly different between groups.

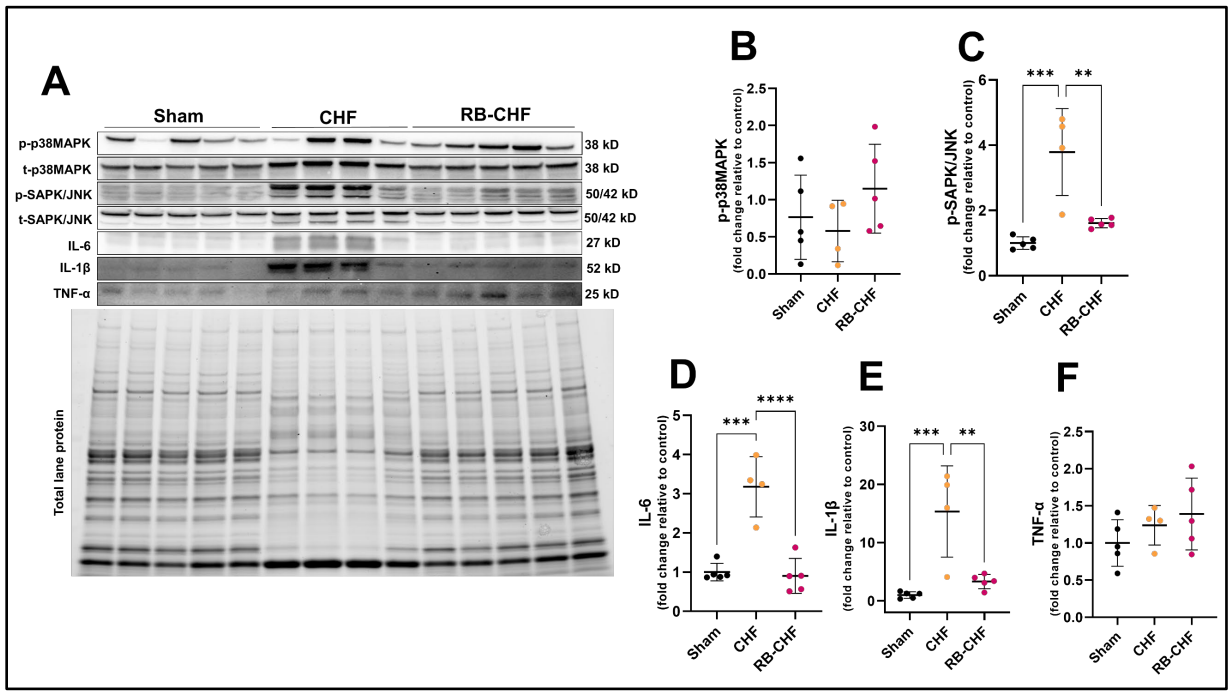

*Figure 5.5 Effects of raspberry consumption on cardiac MAPKs and inflammatory cytokine expression in HF. Animals consumed a control diet (AIN-93M) or a raspberry supplemented diet for three weeks. Animals consuming the control diet underwent either a sham procedure or underwent coronary artery ligation (CHF), while animals consuming the raspberry supplemented diet only underwent coronary artery ligation (RB-CHF). After four additional weeks, animals were sacrificed. Hearts were excised and immediately frozen in -80°C. Protein expression of p-p38MAPK (A, B), p-SAPK/JNK (A, C), IL-6 (A, D) IL-1β (A, E) and TNF-α (A, F) were assessed by western blot and normalized to total lane protein followed by fold change vs sham for each respective protein. Total lane protein blot is representative. Data are expressed as means ± SD. *P ≤ 0.05, **P ≤ 0.01, ***P ≤ 0.001, **** P ≤ 0.0001.*

5.3 Raspberry consumption favorably alters cardiac redox status in HF.

Due to the influence of oxidative stress in driving HF development, a thorough assessment of cardiac redox status was evaluated. Contrary to expectations, the expression of pro-oxidant NOX1 (Figure 5.6A, B) was significantly reduced in CHF animals (0.17 ± 0.09-fold) compared to RB-CHF (1.19 ± 0.27-fold, P < 0.0001) and Sham (P = 0.0003). No differences were observed in the protein expression of NOX2 (Figure 5.6A. C); however, NOX4 protein expression (Figure 5.6A, D) was also significantly reduced in CHF animals (0.6 ± 0.2) compared to RB-CHF (1.2 ± 0.1-fold, *P* = 0.008), but not compared to Sham (P = 0.10). Unlike NOX proteins, XO protein expression (Figure 5.6A, E) was significantly greater in CHF animals (131.6 ± 72.3-fold) compared to RB-CHF (8.2 ± 6.7-fold, *P* = 0.001) and Sham (*P* = 0.0009).

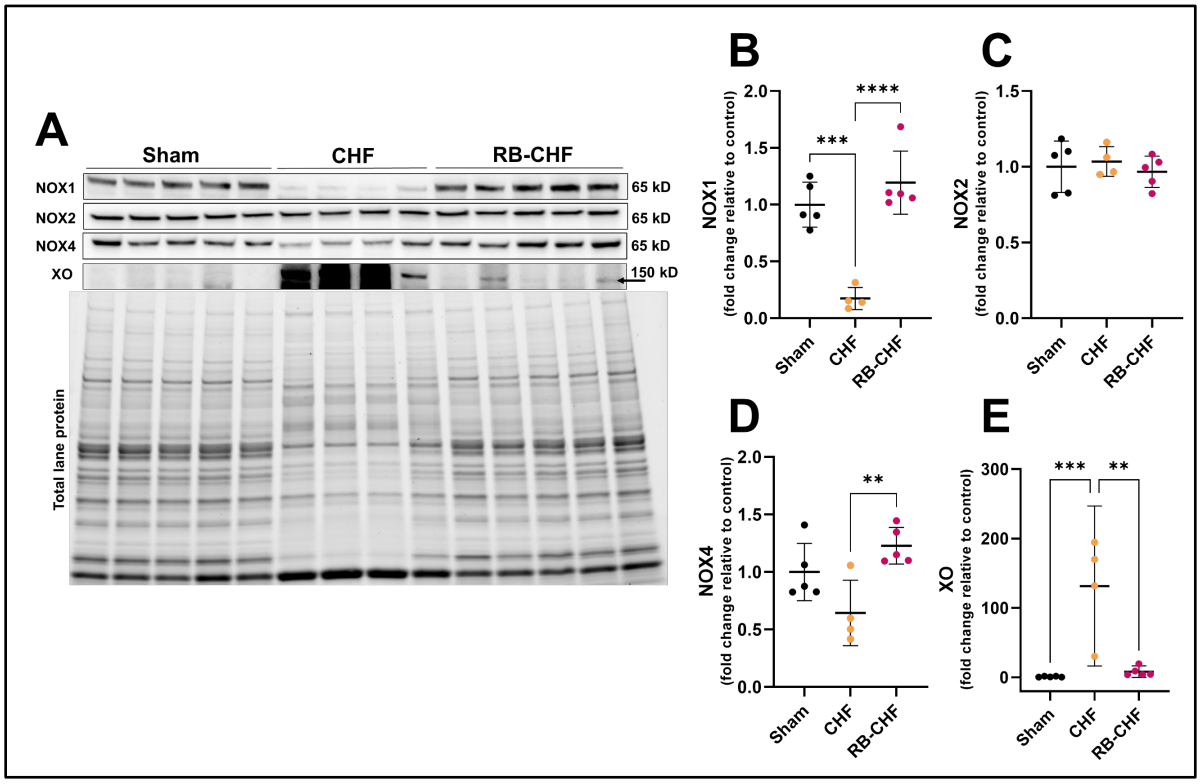

Figure 5.6. Effects of raspberry consumption on cardiac pro-oxidant enzymes in HF. Animals consumed a control diet (AIN-93M) or a raspberry supplemented diet for three weeks. Animals consuming the control diet underwent either a sham procedure or underwent coronary artery

*ligation (CHF), while animals consuming the raspberry supplemented diet only underwent coronary artery ligation (RB-CHF). After four additional weeks, animals were sacrificed. Hearts were excised and immediately frozen in -80°C. Protein expression of NOX1 (A, B), NOX2 (A, C), NOX4 (A, D) and XO (E, F) were assessed by western blot and normalized to total lane protein followed by fold change vs sham for each respective protein. The arrow in panel A points to the bands of interest. Total lane protein blot (A) is representative. Data are expressed as means ± SD. *P ≤ 0.05, **P ≤ 0.01, ***P ≤ 0.001, ****P ≤ 0.0001.*

With respect to LV antioxidant enzyme expression, cytosolic SOD1 (Figure 5.7A, B) was significantly increased in CHF animals (1.5 ± 0.1-fold) compared to both RB-CHF (1.1 ± 0.1-fold, $P = 0.01$) and Sham ($P = 0.003$). Mitochondrial SOD2 (Figure 5.7A, C) was significantly increased in RB-CHF animals (1.1 ± 0.1-fold) when compared to CHF (0.7 ± 0.2-fold, $P = 0.007$) but not Sham ($P = 0.27$). Extracellular SOD3 (Figure 5.7A, D) was significantly increased in CHF animals (60.5 ± 37.9-fold) compared to both RB-CHF (2.5 ± 2.1-fold, $P = 0.002$) and Sham ($P = 0.002$). NQO1 (Figure 5.7A, E), an enzyme also involved in O_2^- neutralization, was significantly reduced in CHF animals (0.5 ± 0.3-fold) compared to both RB-CHF (1.4 ± 0.1-fold, P = 0.0002) and Sham ($P = 0.02$). NQO1 was also significantly increased in RB-CHF compared to Sham ($P = 0.02$). The expression of the peroxidase, catalase (Figure 5.7A, F), was not significantly different between groups. In contrast, cellular GPx1 (Figure 5.7A, G) and excretory GPx3 (Figure 5.7A, H) were significantly increased in CHF animals (GPx1: 1.3 ± 0.1-fold; GPx3: 2.7 ± 0.2-fold) compared to both RB-CHF (GPx1: 0.9 ± 0.1-fold, P = 0.009; GPx3: 1.3 ± 0.3-fold, $P < 0.0001$) and Sham (P ≤0.02). HO-1 protein expression (Figure 6.7A, I) was significantly increased in CHF animals (3.6 ± 0.7-fold) compared to both RB-CHF (1.3 ± 0.2-fold, $P < 0.0001$) and Sham ($P < 0.0001$). To determine whether NRF2 played a role in mediating antioxidant defense, NRF2 transcriptional activity was assessed via ELISA (Figure 5.7A, J). NRF2-ARE binding activity was reduced in both CHF animals (0.5 ± 0.1-fold) and RB-CHF animals (0.4 ± 0.1-fold) compared to Sham ($P \leq 0.004$).

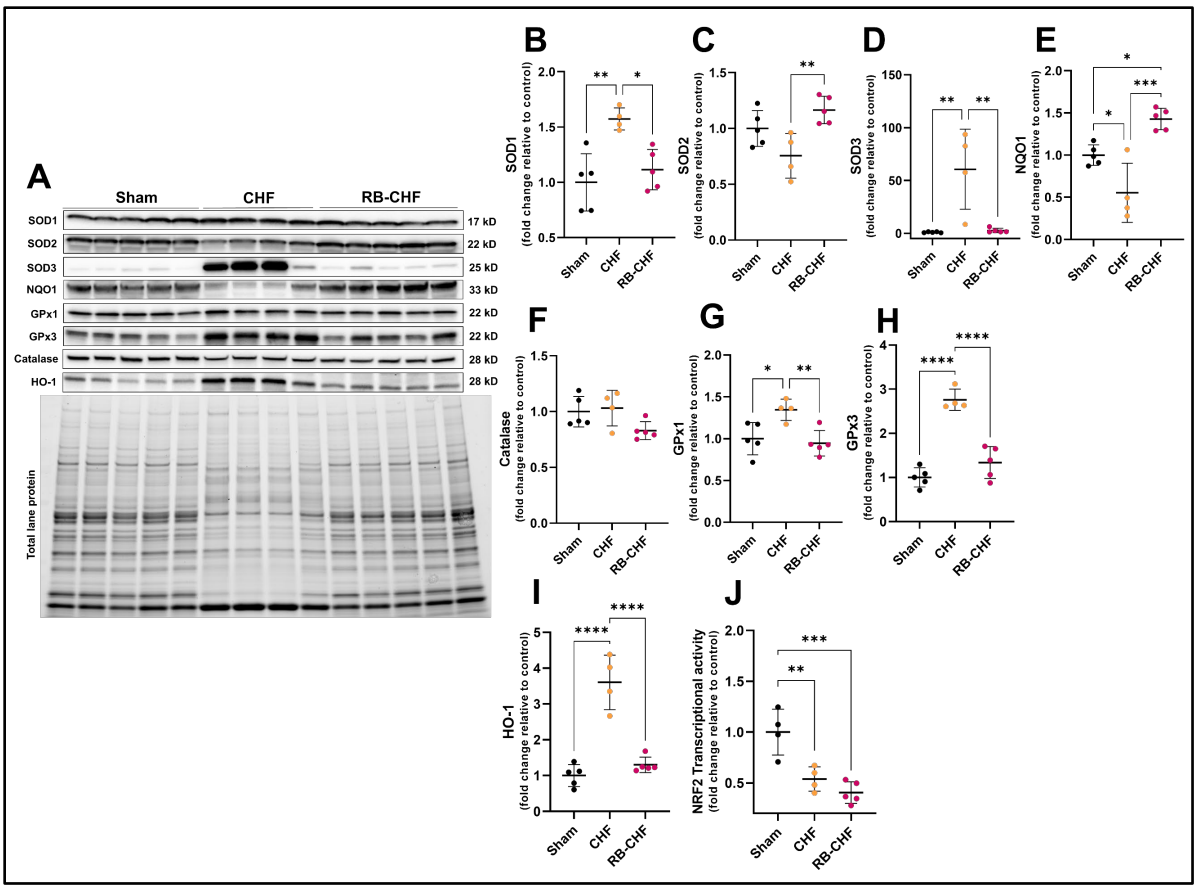

*Figure 5.7 Effects of raspberry consumption on cardiac antioxidant enzymes in HF. Animals consumed a control diet (AIN-93M) or a raspberry supplemented diet for three weeks. Animals consuming the control diet underwent either a sham procedure or underwent coronary artery ligation (CHF), while animals consuming the raspberry supplemented diet only underwent coronary artery ligation (RB-CHF). After four additional weeks, animals were sacrificed. Hearts were excised and immediately frozen in -80°C. Protein expression of SOD1 (A, B), SOD2 (A, C), SOD3 (A, D), NQO1 (E, F), Catalase (A, F), GPx1 (A, G), GPx3 (A, H) and HO-1 (A, I) were assessed by western blot and normalized to total lane protein followed by fold change vs sham for each respective protein. (J) Nuclear lysates of the LV were utilized for the assessment of NRF-ARE binding using an ELISA. Total lane protein blot (A) is representative. Data are expressed as means ± SD. *P ≤ 0.05, **P ≤ 0.01, ***P ≤ 0.001, ****P ≤ 0.0001.*

Due to the diverging effects of pro-oxidant and antioxidant enzymes observed (Figures 5.6 and 5.7), cumulative redox status was assessed. The antioxidant activity of serum was quantified by FRAP (Figure 5.8A) and ORAC (Figure 5.8B) which were significantly elevated in RB-CHF animals (FRAP: 1.09 ± 0.08-fold; ORAC: 1.11 ± 0.11-fold) compared to CHF (FRAP: 0.94 ± 0.10-fold, $P = 0.04$; ORAC: 0.86 ± 0.15-fold, $P = 0.02$) but not Sham ($P \geq 0.17$). In the LV itself, protein

carbonylation (Figure 5.8C) was significantly increased in CHF animals (2.9 ± 0.3-fold) compared to Sham (P = 0.01). However, this was not attenuated in RB-CHF animals (1.6 ± 1.2-fold, P = 0.11), nor was protein carbonylation significantly increased compared to Sham (P = 0.46). Additionally, qualitative assessment of 4-HNE and NT expression in the LV utilizing chromogenic immunohistochemistry revealed more brown staining in CHF compared to both Sham and RB-CHF (Figure 5.8D). Due to the ~21-fold increase in TLR4 protein expression observed in cardiac LV in CHF animals and the significant attenuation observed with raspberry consumption (Figure 5.4A & B), human cardiomyocytes were co-cultured with 400 μM of $CoCl_2$ as well as TAK242, an inhibitor of TLR4 signaling (190), to observe whether RBE could induce similar effects as TLR4 inhibition. Hypoxia was confirmed *in vitro* with significantly increased HIF-1α protein expression in $CoCl_2$-treated human cardiomyocytes irrespective of RBE and TAK242 treatment (Figure 5.8E). The detection of O_2^- *in vitro* with DHE (Figure 5.8F) revealed significantly increased fluorescence in $CoCl_2$-treated cells (1.5 ± 0.3-fold) compared to control (P = 0.006), RBE pretreatment (1.1 ± 0.2-fold, P = 0.04) and TAK242 pretreatment (1.0 ± 0.2-fold, P = 0.01). There were no significant differences compared to control and both RBE- and TAK242-pretreatment (P ≥0.66). Qualitative assessments of DHE staining (Figure 5.8G) provided confirmation of these findings under microscopy, with increased red fluorescence in cells treated with $CoCl_2$ alone compared to other groups.

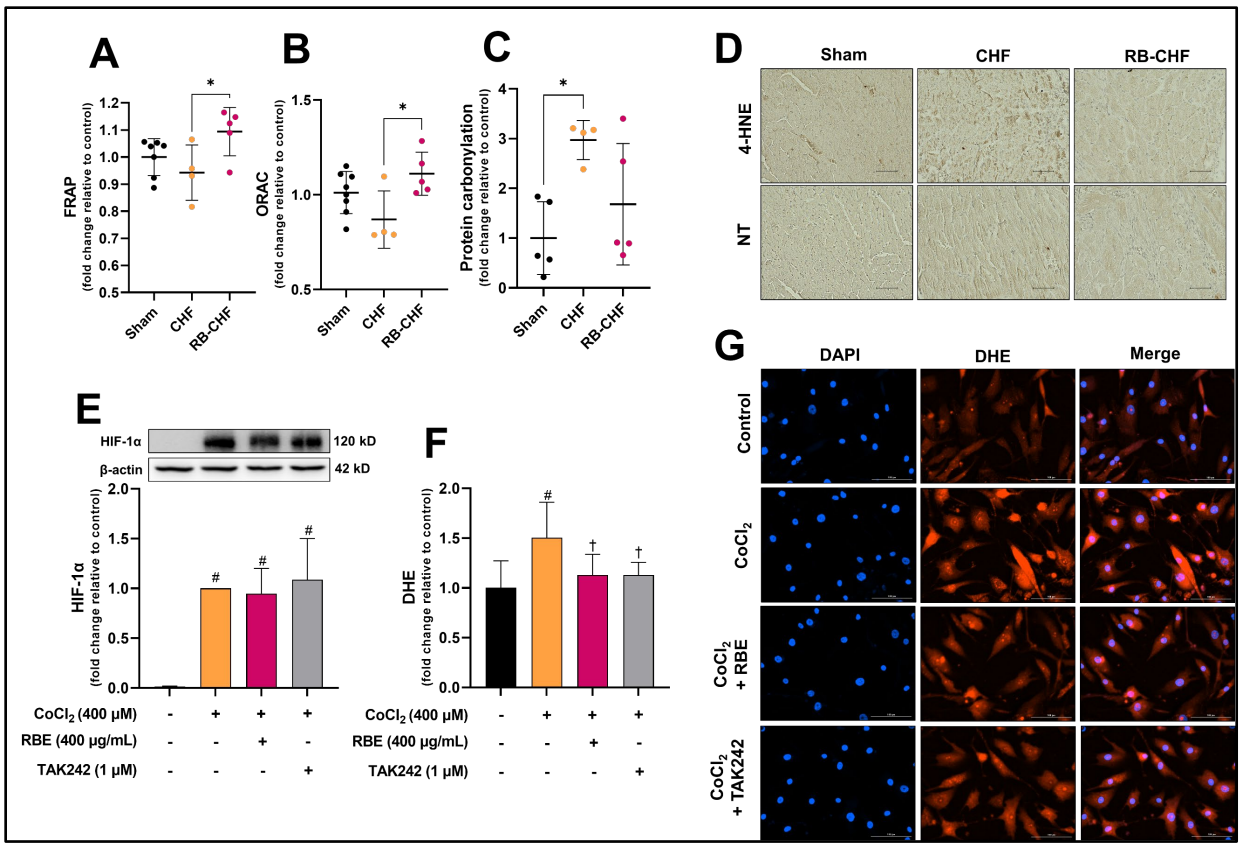

*Figure 5.8 Effects of raspberry consumption in HF in vivo and raspberry polyphenol treatment under hypoxia in vitro on overall redox status. Animals consumed a control diet (AIN-93M) or a raspberry supplemented diet for three weeks. Animals consuming the control diet underwent either a sham procedure or underwent coronary artery ligation (CHF), while animals consuming the raspberry supplemented diet only underwent coronary artery ligation (RB-CHF). After four additional weeks, animals were sacrificed. Serum was obtained from whole blood for antioxidant analysis via (A) FRAP or ORAC (B). Data are expressed as means ± CI. Hearts were excised and either immediately frozen in -80°C for (C) protein carbonylation analysis or (D) 10% formalin for immunohistological analysis of 4-HNE and NT. Histological images were taken at 20x magnification (50 μM scale bar). Brown staining is indicative of respective protein expression. (E-G) Additionally, human cardiomyocytes of the left ventricle were cultured in starvation medium at ~80% confluency and treated with or without $CoCl_2$ (400 μM) for 24 h with RBE (400 μg/mL) or TAK242 (1 μM) for 1 h prior. Protein expression of HIF-1α (E) was assessed by western blot (n = 3 experiments) and normalized to β-actin followed by fold change vs $CoCl_2$ treatment alone. (F, G) DHE was dissolved in dimethyl sulfoxide and added to wells (10 μM final concentration) followed by 30 min incubation (37°C and 5% CO2). Cells were washed in warm PBS and phenol red-free starvation medium supplemented with NucBlue™ (2 drop/mL) was added. Fluorescence was read at the following: 530/620 (DHE; O2−) and 360/460 (Hoechst 33342 with NucBlue™). Fluorometric values for DHE were normalized to Hoechst 33342 then normalized to control (n = 6-8 replicates). Cell data are expressed as means ± SD. *P ≤ 0.05, **P ≤ 0.01, ***P ≤ 0.001, ****P ≤ 0.0001. Significance (P ≤ 0.05) is denoted (E, F) by # vs control and † vs $CoCl_2$ alone.*

5.4 Raspberry consumption reduces apoptosis in HF.

Excessive inflammation and oxidative stress can lead to an apoptotic environment; thus, apoptotic pathways were assessed. The expression of the transcription factor, p53, was significantly increased (Figure 5.9A, B) in CHF animals (22.8 ± 12.4-fold) compared to RB-CHF (2.4 ± 1.3-fold, $P = 0.001$) and Sham ($P = 0.001$). The transcriptional activity of p53 can lead to BAX synthesis which was also significantly increased (Figure 5.9A, C) in CHF animals (16.5 ± 2.4-fold) compared to both RB-CHF (1.5 ± 1.0-fold, $P < 0.0001$) and Sham ($P < 0.0001$). Inverse results were observed for BCL-xL which was significantly reduced (Figure 5.9A, D) in CHF animals (0.21 ± 0.27-fold) compared to both RB-CHF (1.0 ± 0.1-fold, $P < 0.0001$) and Sham ($P < 0.0001$). Cleavage of caspase-9 and caspase-3 were significantly increased (Figure 5.9A, E, F) in CHF animals (cleaved caspase-9: 135.7 ± 79.8-fold; cleaved capsase-3: 3.5 ± 0.9-fold) compared to both RB-CHF animals (cleaved caspase-9: 5.9 ± 6.0-fold, $P = 0.002$; cleaved caspase-3: 1.3 ± 0.3-fold, $P = 0.0004$) and Sham ($P \leq 0.001$). To visualize apoptosis in the LV, TUNEL staining was performed with BrdU red fluorescent dye (Figure 5.9G). Qualitatively, there was greater apoptotic staining in CHF compared with RB-CHF and Sham; however, RB-CHF appeared to also have greater apoptosis than Sham.

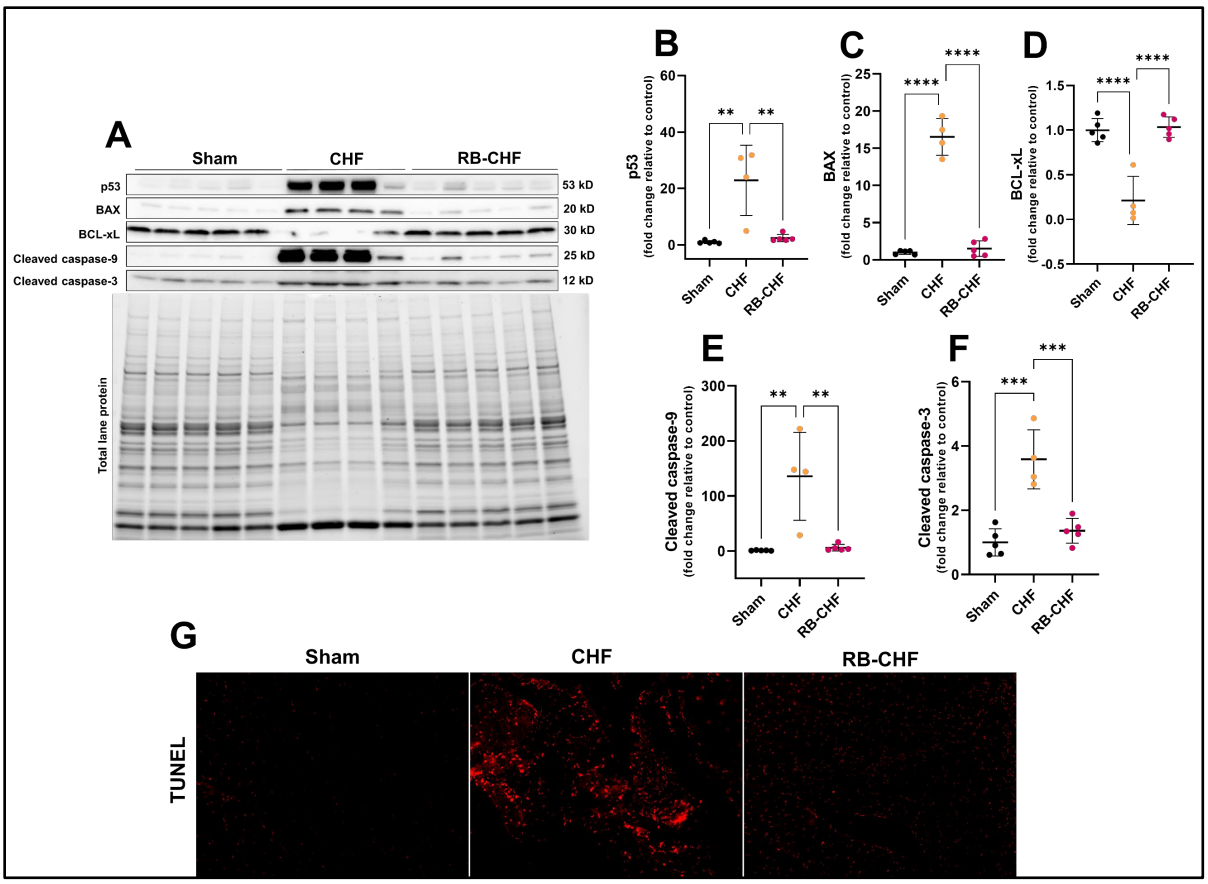

*Figure 5.9 Effects of raspberry consumption on apoptotic signaling in HF. Animals consumed a control diet (AIN-93M) or a raspberry supplemented diet for three weeks. Animals consuming the control diet underwent either a sham procedure or underwent coronary artery ligation (CHF), while animals consuming the raspberry supplemented diet only underwent coronary artery ligation (RB-CHF). After four additional weeks, animals were sacrificed. Hearts were excised and either immediately frozen in -80°C for protein analysis or 10% formalin for immunohistological analysis. Protein expression of p53 (A, B), BAX (A, C), BCL-xL (A, D), cleaved caspase-9 (A, E) and cleaved caspase-3 (A, F) were assessed by western blot and normalized to total lane protein followed by fold change vs sham for each respective protein. (G) Tissue sections were stained with TUNEL staining using BrdU red fluorescent probe from a commercially available kit. Histological images were taken at 20x magnification. Red labeling is indicative of apoptosis. Data are expressed as means ± SD. *P ≤ 0.05, **P ≤ 0.01, ***P ≤ 0.001, ****P ≤ 0.0001.*

In vitro in human cardiomyocytes, $CoCl_2$ treatment increased cleaved caspase-3 protein expression in a dose-dependent manner (0-600 µM) (Figure 5.10A) and significantly reduced cell viability by approximately 85-90% irrespective of $CoCl_2$ concentration utilized (Figure 5.10B). Upon visualization with light microscopy (Figure 5.10C), cells had a normal spindle structure

under control conditions; however, hypertrophy became evident with 24 h treatment of 200-400 μM of $CoCl_2$, while cells at 600 μM appeared fully apoptotic with complete loss of normal morphological characteristics featuring substantial rounding. RBE and TAK242 pretreatment significantly reduced cleaved caspase-3 protein expression ($P \leq 0.04$) following 24 h with 400 μM $CoCl_2$ (Figure 5.10D). Annexin FIT-C fluorescent probe revealed significantly increased apoptosis (Figure 5.10E) in cells treated with $CoCl_2$ alone compared to control, RBE pretreatment and TAK242 pretreatment ($P \leq 0.008$).

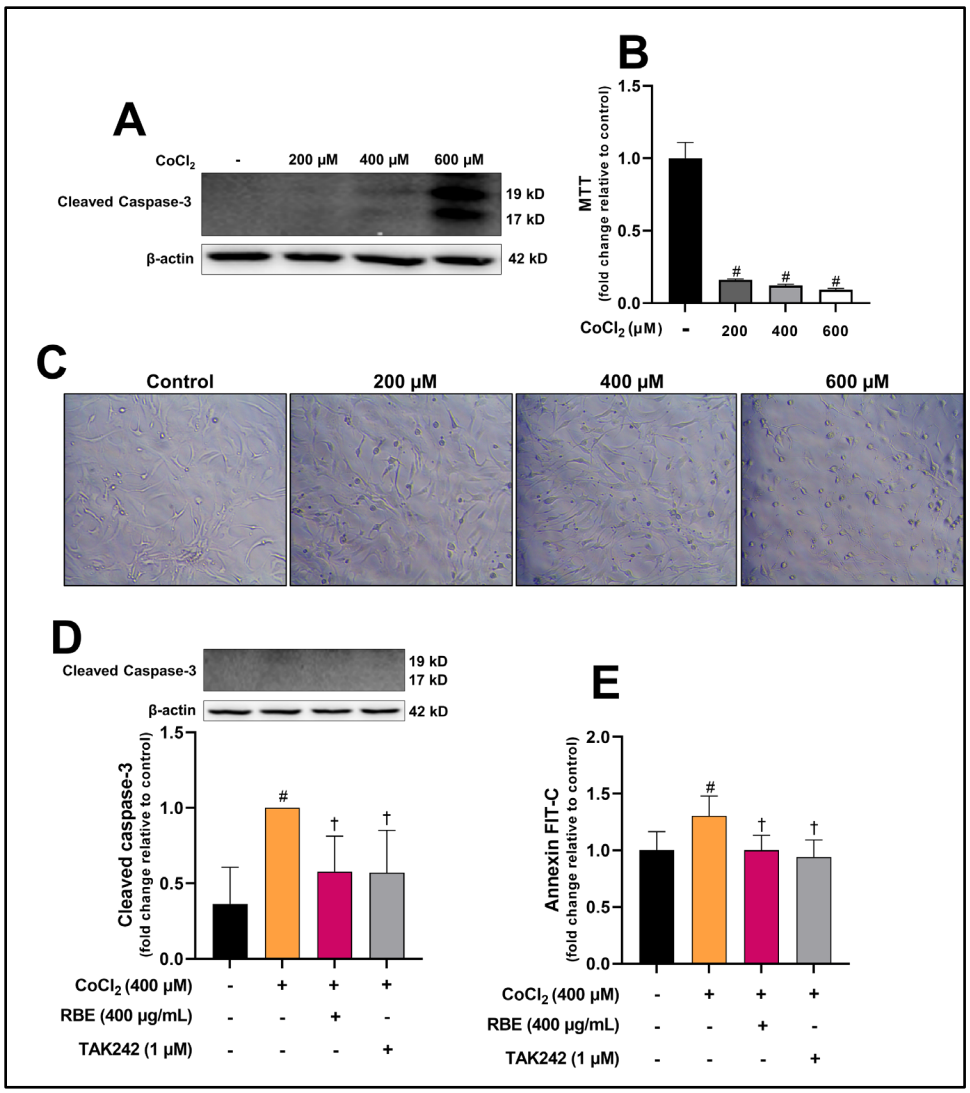

Figure 5.10 Effects of raspberry polyphenols in $CoCl_2$-induced apoptosis in human cardiomyocytes. (A, B) Human cardiomyocytes of the left ventricle were cultured in starvation medium at ~80% confluency for 24 h with $CoCl_2$ (0-600 µM). (A) Protein expression of cleaved caspase-3 and β-actin were qualitatively assessed by western blot. (B) MTT assay was conducted to determine cell viability (n = 8 replicates). Data was normalized to control. (C) Cell morphology and structure was assessed qualitatively by light microscopy at 20x magnification. (D) Cells were treated with or without $CoCl_2$ (400 µM) for 24 h with RBE (400 µg/mL) or TAK242 (1 µM) for 1 h prior. Protein expression of cleaved caspase-3 was assessed by western blot and normalized to β-actin followed by fold change vs $CoCl_2$ treatment alone (n = 3 experiments). (E) Annexin FIT-C staining was also conducted in black 96-well plates following treatments (n = 6 replicates), and data were read in a microplate reader (Ex/Em: 494/535). Data are expressed as mean ± SD. Significance ($P \leq 0.05$) is denoted (B, D & E) by # vs control and † vs $CoCl_2$ alone.

Considering the involvement of mitochondria in apoptotic signaling and energetics in the heart, these variables were assessed. Proteins involved in mitochondrial fission and fusion, DRP1 (Figure 5.11A, B) and OPA1 (Figure 5.11A, C), respectively, were quantified in the LV. Both DRP1 and OPA1 were significantly decreased in CHF animals (DRP1: 0.6 ± 0.1-fold; OPA1: 0.4 ± 0.2-fold) compared to RB-CHF animals (DRP1: 1.0 ± 0.1-fold, $P = 0.004$; OPA1: 1.0 ± 0.1-fold, $P = 0.001$) and Sham animals ($P \leq 0.01$) suggesting reduced mitochondria count/surface area in CHF animals. However, when total ATP content of tissue was quantified (Figure 5.11D), RB-CHF (0.44 ± 0.15) had significantly reduced ATP content compared to control ($P \leq 0.01$) while CHF trended towards being significantly different from control (0.54 ± 0.05-fold, $P = 0.052$). Mitochondrial depolarization was then qualitatively evaluated *in vitro* in human cardiomyocytes utilizing JC-10 fluorescent probe (Figure 5.11E). $CoCl_2$ treatment reduced mitochondrial aggregation of JC-10 irrespective of treatment compared to control. However, there was a visual increase in JC-10 aggregation in mitochondria in RBE and TAK242-pretreated cells compared to $CoCl_2$ alone.

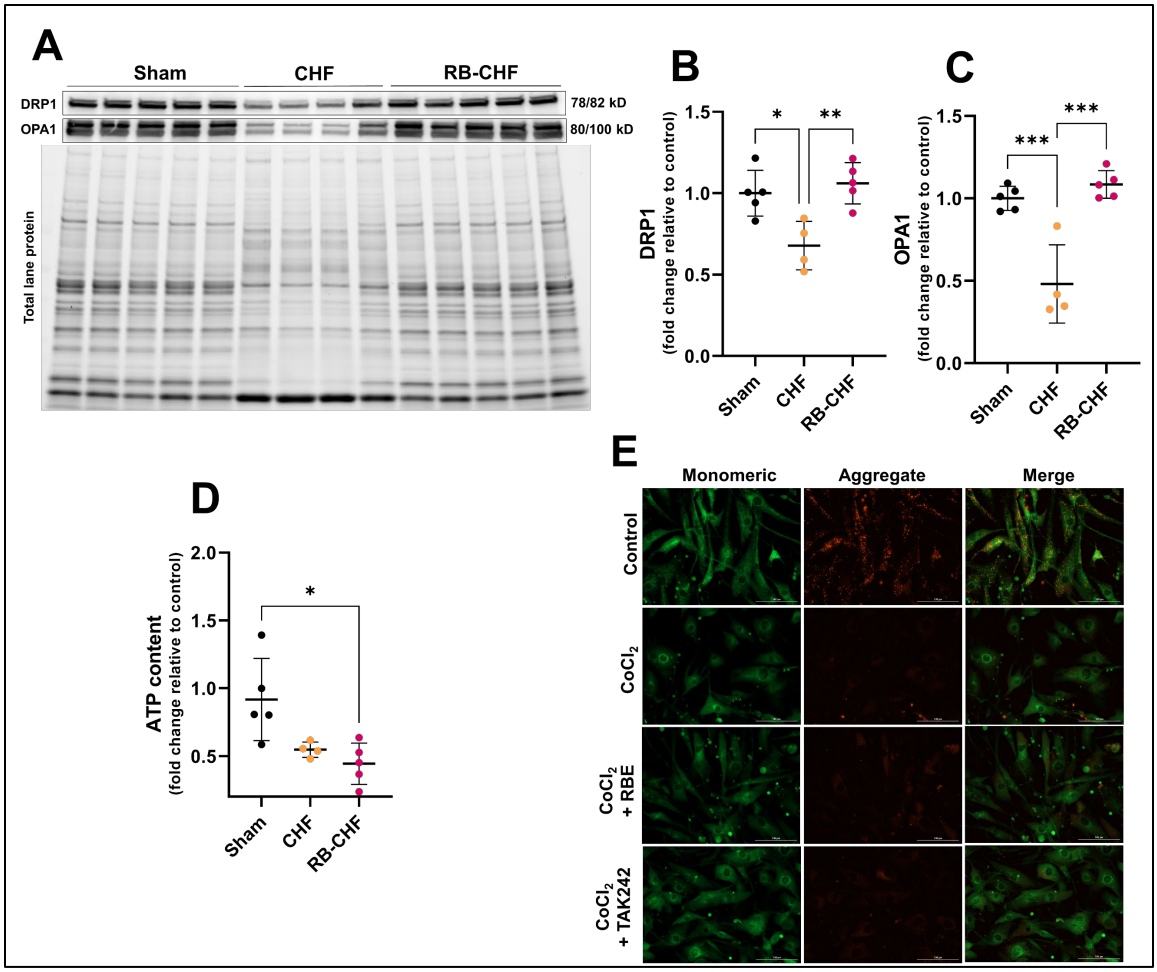

*Figure 5.11 Effects of raspberry consumption in HF in vivo and raspberry polyphenol treatment under hypoxia in vitro on mitochondria-related variables. Animals consumed a control diet (AIN-93M) or a raspberry supplemented diet for three weeks. Animals consuming the control diet underwent either a sham procedure or underwent coronary artery ligation (CHF), while animals consuming the raspberry supplemented diet only underwent coronary artery ligation (RB-CHF). After four additional weeks, animals were sacrificed. Hearts were excised and immediately frozen in -80°C for protein analysis. Protein expression of DRP1 (A, B) and OPA1 (A, C) were assessed by western blot and normalized to total lane protein followed by fold change vs sham for each respective protein. (D) Total ATP content of the LV was quantified with luminescent detection from a commercially available kit. (E) Cells were treated with or without $CoCl_2$ (400 µM) for 24 h with RBE (400 µg/mL) or TAK242 (1 µM) for 1 h prior followed by JC-10 fluorometric probe introduction via a commercially available kit. Cells were qualitatively evaluated for JC-10 aggregation in the mitochondria as indicated by red fluorescence. Data are expressed as means ± SD. *P ≤ 0.05, **P ≤ 0.01, ***P ≤ 0.001, ****P ≤ 0.0001.*

6 DISCUSSION

These data demonstrate that raspberries attenuate reductions in EF and FS induced by cardiac ischemia and attenuate pro-fibrotic signaling, improving cardiac morphology, via 1) reduction in inflammation and oxidative stress, and 2) reduction in pro-apoptotic signaling, both of which are likely mediated in a TLR4-dependant manner due to reduced DAMP signaling (Figure 6.1). These molecular effects drive poor functional capacity mainly due to increased scarring and cardiomyocyte apoptosis which impede uniform and organized contraction of the heart.

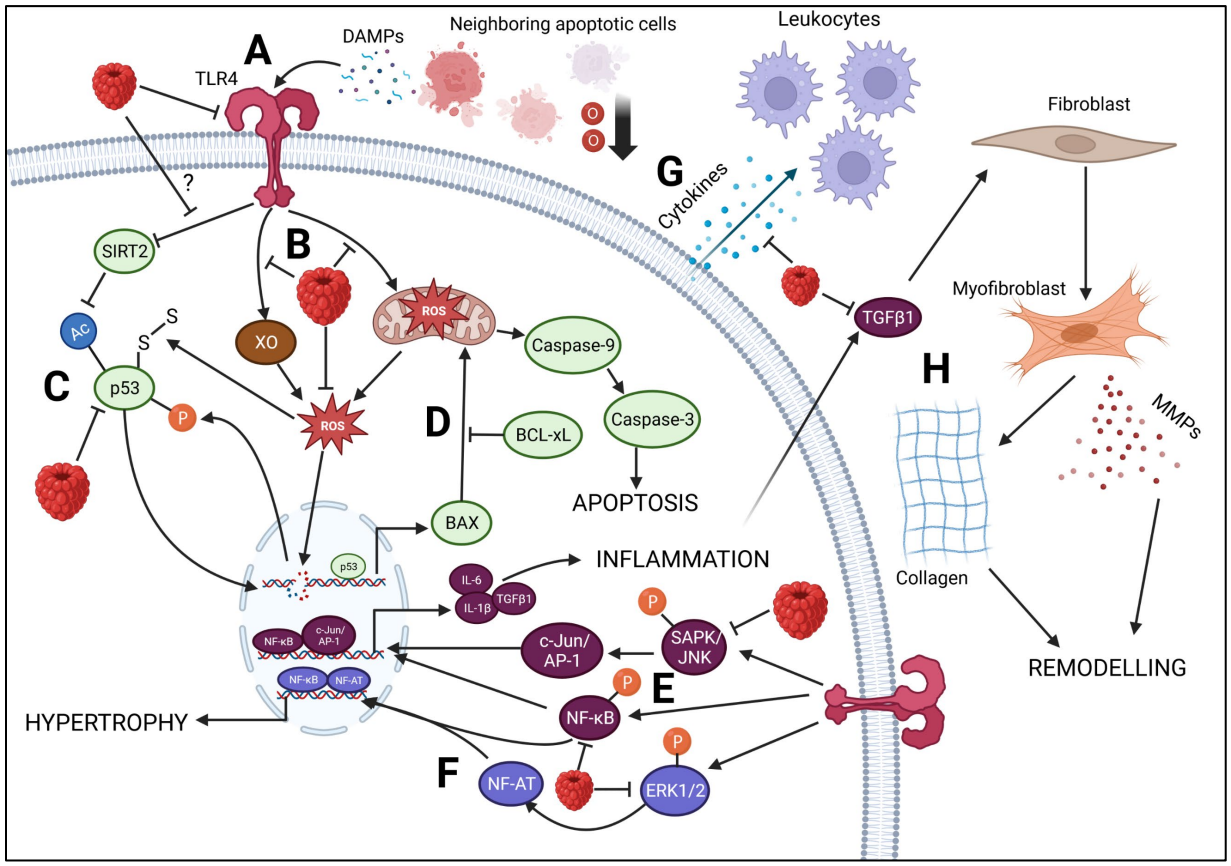

*Figure 6.1 Molecular mechanisms by which raspberry polyphenols attenuate HF. **A**) under ischemic conditions, apoptosis occurs, and apoptotic cells release a variety of damage associated molecular patterns (DAMPs) which bind to toll-like receptor (TLR)4 of neighboring cells triggering an inflammatory response. Raspberry polyphenols reduce TLR4 protein expression. **B**)*

TLR4 signaling results in reactive oxygen species (ROS) production from xanthine oxidase (XO) and mitochondria which raspberries reduce. ***C****) excessive ROS can cause DNA breaks which triggers p53 phosphorylation. Additionally, ROS can modify reactive cysteine residues on p53 creating disulfide bonds. TLR4 also acts on p53 indirectly by inhibiting sirtuin (SIRT)2, a deacetylase, resulting in accumulation of acetylated p53. These post-translational modifications all result in p53 cytosolic accumulation and eventual nuclear translocation binding to the region of DNA encoding B-cell lymphoma (BCL)-2-associated X protein (BAX) synthesis. However, raspberry polyphenols reduce p53 cytosolic accumulation likely due to a combination of these mechanisms.* ***D****) BCL-extra-large (BCL-xL) can inhibit BAX activity and prevent mitochondrial pore opening, which raspberries appeared to preserve the expression of. Mitochondrial depolarization and pore opening results in the downstream cleavage of caspase-9 followed by capase-3 leading to cellular apoptosis, all of which was attenuated by raspberry polyphenols.* ***E****) TLR4 signaling leads to the downstream phosphorylation of stress-activated protein kinases (SAPK)/Jun amino-terminal kinases (JNK) and activation of transcription factor c-Jun and activator protein (AP)-1 in parallel to the phosphorylation of the transcription factor nuclear factor-κB (NF-κB). This leads to nuclear translocation, DNA transcriptional activity and an inflammatory response. Raspberry polyphenols reduced activity of SAPK/JNK and NF-κB, likely due to initial reduction of TLR4, overall reducing the inflammatory response.* ***F****) TLR4 activation also leads to the phosphorylation of extracellular signal-regulated kinase (ERK)1/2, which activates nuclear factor of activated T-cells (NF-AT) which then forms a complex with NF-κB to bind to the region of DNA encoding fetal gene protein synthesis resulting in hypertrophy. Raspberry polyphenols inhibited the phosphorylation of ERK1/2 attenuating the hypertrophic response.* ***G****) inflammatory signaling results in the synthesis of cytokines and chemokines which attract leukocytes to infiltrate cardiac tissue, raspberry polyphenols attenuated this infiltration due to reduction of inflammatory cytokines.* ***H****) the inflammatory cytokine transforming growth factor (TGF)β1 released by both infiltrating leukocytes as well as native cardiac tissue bind to resident cardiac fibroblasts causing their differentiation into myofibroblasts. Myofibroblasts facilitate cardiac remodeling by breaking down the extracellular matrix with matrix metalloproteinases (MMPs) and by synthesizing collagen, disturbing the organized architecture of cardiomyocytes and reducing the elasticity of the heart as a whole, contributing to reduced cardiac function. Raspberry polyphenols reduced (TGF)β1 protein expression and reduced MMP2 & MMP9, all of which reduced cardiac fibrosis and attenuated remodeling.*

TLR4 is involved in the activation of NOX enzymes (191, 192), XO (193), and mitochondrial ROS (194), either via direct protein-protein interaction or indirectly through downstream activators. However, the direct source of oxidative stress in this model is unclear. Contrary to expectations, a significant decline in NOX1 and NOX4 was observed in CHF animals with no changes observed in the expression of NOX2 (Figure 5.6A-D). The role of NOX1 in mediating cardiac dysfunction in diabetes appears pathological (195, 196); however, in ischemia in isolated perfused hearts, NOX1 genetic knockout was detrimental and resulted in more

pronounced arrythmias (197). This dysfunction was ameliorated with coronary vasodilators suggesting that NOX1 may regulate the vascular tone of the heart in a protective manner. However, NOX1 may have a pathological effect in the large vessels, as NOX1-deficiency blunted the increase in blood pressure induced by Ang II infusion in mice and reduced aortic oxidative stress (198). Considering the complexity of the differing insults between these two models, it is difficult to make direct comparisons. Further, it is unclear why NOX1 protein expression was significantly decreased in CHF animals ~5-fold compared to Sham (Figure 5.6A, B); this decrease is a novel finding based on the existing literature.

With respect to NOX4, it appears to be highly localized to mitochondria in cardiomyocytes (68) which may explain why a decrease in NOX4 protein was observed in CHF animals since mitochondrial-specific proteins, DRP1 and OPA1, were also significantly reduced (Figure 5.11A-C) suggesting overall reduced mitochondria. However, in a model of CAL in mice, NOX4 protein was significantly increased in wildtype animals while NOX4 genetic knockout was found to reduce infarct size compared to wildtype (199). It is important to note that the measurement of NOX4 protein was performed only three days post-CAL and infarct size was measured two weeks post-CAL compared to four weeks in the present study; thus, these results are not directly comparable. This lack of comparison is also evident by the utilization of tubulin, specifically β-tubulin, as a loading control. We found that α-tubulin was not an appropriate loading control (Figure 5.2A, C) and other investigators have found that β-tubulin was not either (200); however, considering the short duration post-CAL, it is likely that the derangements in cytoskeletal proteins were not fully apparent. Regardless, NOX4 was also found to be pathological in a model of TAC (87). Thus, reduction in NOX4 observed in the present investigation may simply be a result of reduced mitochondria and may not be of substantial relevance with respect to overall oxidative stress status.

Regarding NOX2, investigations have identified that cardiac NOX2 protein is increased post-CAL (78, 201), even after four weeks as in the present investigation, and that its deletion is protective (77, 202) . However, it should be noted that inappropriate loading controls were used to assess NOX2 protein expression in the aforementioned investigations, as GAPDH or β-actin were used (78, 201) compromising the reliability of these findings. Nonetheless, the fact that NOX2 deletion was protective is of relevance; however, in this model, CHF animals did not have increased NOX2 protein and NOX2 was therefore not a likely source of ROS. The major sources of ROS in this model were likely derived from both XO and mitochondria which raspberries appeared to attenuate. While mitochondrial ROS was not directly measured, membrane depolarization as observed *in vitro* was increased with $CoCl_2$ treatment alone which was partially attenuated by RBE and TAK242 (Figure 5.11E). Further, while antioxidant enzymes were mostly upregulated as a compensatory mechanism in CHF animals (Figure 5.7), SOD2 was significantly reduced in CHF animals compared to RB-CHF animals (Figure 5.7A, C). Since SOD2 is specifically a mitochondrial protein, mitochondrial antioxidant defense was likely compromised, although this simply may be a result of reduced mitochondria overall.

With respect to the role of TLR4 in mediating apoptosis, it has been previously identified that TLR4 can induce apoptosis in a p53-dependant manner, as TLR4 agonism *in vivo* reduced sirtuin 2, a deacetylase, which results in increased p53 acetylation at lysine 381 (194), a post-translational modification which increases p53 binding affinity towards DNA (203). Further, p53 is regularly synthesized and ubiquitinated for proteasomal degradation unless post-translational modifications interrupt this process (204). Indeed, excessive ROS can result in these necessary post-translational modifications, stabilizing p53, by 1) directly oxidizing cysteine residues on p53 or 2) damaging DNA resulting in p53 phosphorylation (205). This then leads to p53 accumulation

and nuclear activity, and both of these ROS-mediated factors likely contributed to the observed increase in p53 protein in the present investigation (Figure 5.9A, B). Thus, by reducing TLR4 and subsequently reducing oxidative stress likely reduced p53 protein accumulation thereby reducing BAX and mitochondrial-mediated cell death through caspase-9 and caspase-3. Due to the central role of mitochondria in mediating cell death, it is interesting to note that cardiac ATP at the site of infarct was reduced in both CHF and RB-CHF animals despite an attenuation of cell death in RB-CHF animals. This reduction in ATP is not entirely unexpected considering the lack of O_2 to facilitate oxidative phosphorylation. However, raspberry polyphenol extract appeared to improve mitochondrial membrane potential *in vitro* which was similar to the effects of TAK242. Thus, raspberries likely reduced apoptosis by reducing mitochondrial ROS and partially attenuating mitochondrial depolarization in a TLR4-dependant manner.

We have previously shown that raspberry polyphenols were efficacious in reducing cardiac TLR4 signaling in a MYD88-dependant manner in obese mice fed a high-fat, high-sucrose diet (206). Indeed, single polyphenols found in raspberry were able to reduce TLR4 protein expression induced by direct antagonism with LPS (207) or indirectly with inflammatory cytokines *in vitro* (208). It is also possible that raspberry targeted cardiac fibroblasts and reduced their differentiation to myofibroblasts. For example, in primary rat cardiac fibroblasts, the raspberry polyphenol, gallic acid, reduced TGFβ1-mediated differentiation and collagen synthesis *in vitro* (178). Additionally, ROS produced from NOX4 played a key role in mediating differentiation of fibroblasts to myofibroblasts (209). Firm conclusions are difficult to draw since fibroblasts were not isolated and directly analyzed in the present investigation; however, considering the attenuation in fibrosis observed in RB-CHF animals compared to CHF animals, raspberry polyphenols likely played a protective role in these cells.

It is interesting to note that NRF2 transcriptional activity declined in all animals that underwent MI irrespective of dietary treatment (Figure 5.7J). While HO-1 is known to be transcriptionally regulated by NRF2 (210), HO-1 protein expression was unexpectedly increased despite reduced NRF2 activity (Figure 5.7I). However, this increase in HO-1 is consistent with the literature (211). In addition to NRF2, HO-1 is also regulated by HIF-1α, NF-κB and JNK which would explain this discrepancy, as these transcriptional activators were increased in this model (211). In contrast, other investigations have found that raspberry polyphenols regulate NRF2 in HF. For example, in an MI model induced by CAL, urolithin A, a microbial metabolite of ellagic acid metabolism, was provided for seven days following CAL surgery at a dose of 2.5 mg/kg/day (212). While investigators found NRF2 and NQO1 protein to be reduced which was consistent with our findings, SOD1 and HO-1 were significantly reduced which were rescued by urolithin A. It is important to comment however that β-actin was utilized as a loading control which is not an appropriate loading control in this model (185).

In an I/R model of HF in rats, urolithin B injected 0, 24 and 48 h prior to surgery in rats (0.7 mg/kg) significantly reduced cleaved caspase-3 protein expression, apoptotic TUNEL staining as well as O_2^- release in cardiac tissue (170) which were consistent with our findings. Interestingly, investigators also found that urolithin B significantly increased nuclear NRF2 compared to both Sham and I/R animals. These differences between the present study and investigators are likely due to differences in HF induction (CAL vs I/R). In humans, for example, urolithin B-glucuronide was found at a concentration of 1,894 ± 57 μg/mL and 2,985 ± 2,145 μg/mL in urine 24 h following the consumption of 200 g and 400 g, respectively, of red raspberry (213). This coincided with improvements in artery function; thus, urolithin B among other urolithins are likely major polyphenols involved in the protective molecular effects observed in the present study.

The primary pathway attenuated in HF in the present study from raspberry consumption was likely the TLR4 pathway. While the effects of urolithins on TLR4 have not been investigated in HF, anthocyanins extracted from purple rice did reduce TLR4 signaling in a model of streptozotocin-induced cardiomyopathy (154). Cardiac hypertrophy, hypertrophic signaling, and fibrosis and fibrotic signaling were also dramatically reduced to a degree comparable to the present investigation. Purple rice is a rich source of cyanidin-3-O-glucoside (214) which is a polyphenol found in abundance in red raspberries (Table 3.1); thus, it is likely that anthocyanins are also of significant relevance in mediating the protective molecular effects observed. Indeed, cyanidin-3-0-glucoside (10-20 mg/kg/d) provided for one week prior to I/R injury significantly reduced the infarct size and reduced cardiac oxidative stress compared to I/R animals without cyanidin-3-0-glucoside injection. Overall, the diverse array of polyphenols found in red raspberry mediate the protective molecular effects observed in the present investigation.

6.1 Limitations

Several limitations exist in the present investigation. First, permanent ligation of the left anterior descending coronary artery, while a common animal model of HF, is not fully representative of human HF in which the obstruction would be dealt with medically, either by a stent or otherwise. This would reintroduce oxygen and nutrient supply. Therefore, a model of I/R may be more applicable and representative of human HF and may also shed additional molecular insights. Secondly, it is not known whether this treatment would be efficacious in pressure-overload-induced HF. For example, in hypertension or with TAC which have differing, non-hypoxic mechanisms. Investigation into the efficacy of raspberry polyphenols in these models are needed. Lastly, sex differences were not evaluated; thus, these data may not be fully applicable to half the population. Indeed, HF incidence between males and females are similar (215).

Considering likely differences in vascular protein expression between sexes (216) and differences in polyphenol efficacy between sexes (217), this is an important variable which future studies should address.

7 Conclusion

In conclusion, raspberry polyphenols protect the heart from the detrimental effects of HF induced by permanent coronary artery ligation in rats in a TLR4-mediated manner. Raspberry polyphenols physiologically attenuated the decline in heart function, reduced fibrosis, attenuated hypertrophy, and at the cellular level, reduced inflammation, oxidative stress, apoptosis and pro-remodeling signaling. Thus, raspberry consumption may be a protective adjunct therapeutic in the clinical setting of HF with the equivalent consumption of ~2.5 cups of fresh red raspberry per day. However, future studies should investigate whether this efficacy remains in alternative HF models and investigate whether differences in the efficacy of treatment exist between sexes prior to clinical application.

REFERENCES

1. Malik A, Brito D, Chhabra L. Congestive Heart Failure (CHF). StatPearls. Treasure Island (FL)2020.
2. Heidenreich PA, Albert NM, Allen LA, Bluemke DA, Butler J, Fonarow GC, Ikonomidis JS, Khavjou O, Konstam MA, Maddox TM, Nichol G, Pham M, Pina IL, Trogdon JG, American Heart Association Advocacy Coordinating C, Council on Arteriosclerosis T, Vascular B, Council on Cardiovascular R, Intervention, Council on Clinical C, Council on E, Prevention, Stroke C. Forecasting the impact of heart failure in the United States: a policy statement from the American Heart Association. Circ Heart Fail. 2013;6(3):606-19. doi: 10.1161/HHF.0b013e318291329a. PubMed PMID: 23616602; PMCID: PMC3908895.
3. Inamdar AA, Inamdar AC. Heart Failure: Diagnosis, Management and Utilization. J Clin Med. 2016;5(7). Epub 2016/07/02. doi: 10.3390/jcm5070062. PubMed PMID: 27367736; PMCID: PMC4961993.
4. Dick SA, Epelman S. Chronic Heart Failure and Inflammation: What Do We Really Know? Circ Res. 2016;119(1):159-76. doi: 10.1161/CIRCRESAHA.116.308030. PubMed PMID: 27340274.
5. Ikeda M, Ide T, Tadokoro T, Miyamoto HD, Ikeda S, Okabe K, Ishikita A, Sato M, Abe K, Furusawa S, Ishimaru K, Matsushima S, Tsutsui H. Excessive Hypoxia-Inducible Factor-1alpha Expression Induces Cardiac Rupture via p53-Dependent Apoptosis After Myocardial Infarction. J Am Heart Assoc. 2021;10(17):e020895. Epub 2021/09/03. doi: 10.1161/JAHA.121.020895. PubMed PMID: 34472375; PMCID: PMC8649270.
6. Liu L, Wang Y, Cao ZY, Wang MM, Liu XM, Gao T, Hu QK, Yuan WJ, Lin L. Up-regulated TLR4 in cardiomyocytes exacerbates heart failure after long-term myocardial infarction. J Cell Mol Med. 2015;19(12):2728-40. Epub 2015/08/21. doi: 10.1111/jcmm.12659. PubMed PMID: 26290459; PMCID: PMC4687701.
7. Bedard K, Krause KH. The NOX family of ROS-generating NADPH oxidases: physiology and pathophysiology. Physiol Rev. 2007;87(1):245-313. Epub 2007/01/24. doi: 10.1152/physrev.00044.2005. PubMed PMID: 17237347.
8. Battelli MG, Polito L, Bortolotti M, Bolognesi A. Xanthine Oxidoreductase-Derived Reactive Species: Physiological and Pathological Effects. Oxid Med Cell Longev. 2016;2016:3527579. Epub 2016/01/30. doi: 10.1155/2016/3527579. PubMed PMID: 26823950; PMCID: PMC4707389.
9. Peoples JN, Saraf A, Ghazal N, Pham TT, Kwong JQ. Mitochondrial dysfunction and oxidative stress in heart disease. Exp Mol Med. 2019;51(12):1-13. Epub 2019/12/21. doi: 10.1038/s12276-019-0355-7. PubMed PMID: 31857574; PMCID: PMC6923355.
10. Tsutsui H, Kinugawa S, Matsushima S. Oxidative stress and heart failure. Am J Physiol Heart Circ Physiol. 2011;301(6):H2181-90. doi: 10.1152/ajpheart.00554.2011. PubMed PMID: 21949114.
11. Nabeebaccus A, Zhang M, Shah AM. NADPH oxidases and cardiac remodelling. Heart Fail Rev. 2011;16(1):5-12. doi: 10.1007/s10741-010-9186-2. PubMed PMID: 20658317.
12. Moe KT, Khairunnisa K, Yin NO, Chin-Dusting J, Wong P, Wong MC. Tumor necrosis factor-alpha-induced nuclear factor-kappaB activation in human cardiomyocytes is mediated by NADPH oxidase. J Physiol Biochem. 2014;70(3):769-79. doi: 10.1007/s13105-014-0345-0. PubMed PMID: 25059721.

13. Zhao H, Zhang M, Zhou F, Cao W, Bi L, Xie Y, Yang Q, Wang S. Cinnamaldehyde ameliorates LPS-induced cardiac dysfunction via TLR4-NOX4 pathway: The regulation of autophagy and ROS production. J Mol Cell Cardiol. 2016;101:11-24. doi: 10.1016/j.yjmcc.2016.10.017. PubMed PMID: 27838370.
14. Droge W. Free radicals in the physiological control of cell function. Physiol Rev. 2002;82(1):47-95. doi: 10.1152/physrev.00018.2001. PubMed PMID: 11773609.
15. Zhang X, Yang J, Yu X, Cheng S, Gan H, Xia Y. Angiotensin II-Induced Early and Late Inflammatory Responses Through NOXs and MAPK Pathways. Inflammation. 2017;40(1):154-65. doi: 10.1007/s10753-016-0464-6. PubMed PMID: 27807688.
16. Yu L, Feng Z. The Role of Toll-Like Receptor Signaling in the Progression of Heart Failure. Mediators Inflamm. 2018;2018:9874109. doi: 10.1155/2018/9874109. PubMed PMID: 29576748; PMCID: PMC5822798.
17. Yang Y, Lv J, Jiang S, Ma Z, Wang D, Hu W, Deng C, Fan C, Di S, Sun Y, Yi W. The emerging role of Toll-like receptor 4 in myocardial inflammation. Cell Death Dis. 2016;7:e2234. doi: 10.1038/cddis.2016.140. PubMed PMID: 27228349; PMCID: PMC4917669.
18. Butts B, Gary RA, Dunbar SB, Butler J. The Importance of NLRP3 Inflammasome in Heart Failure. J Card Fail. 2015;21(7):586-93. doi: 10.1016/j.cardfail.2015.04.014. PubMed PMID: 25982825; PMCID: PMC4516025.
19. Hohensinner PJ, Kaun C, Rychli K, Ben-Tal Cohen E, Kastl SP, Demyanets S, Pfaffenberger S, Speidl WS, Rega G, Ullrich R, Maurer G, Huber K, Wojta J. Monocyte chemoattractant protein (MCP-1) is expressed in human cardiac cells and is differentially regulated by inflammatory mediators and hypoxia. FEBS Lett. 2006;580(14):3532-8. doi: 10.1016/j.febslet.2006.05.043. PubMed PMID: 16730716.
20. Najjar RS, Montgomery BD. A defined, plant-based diet as a potential therapeutic approach in the treatment of heart failure: A clinical case series. Complement Ther Med. 2019;45:211-4. Epub 2019/07/25. doi: 10.1016/j.ctim.2019.06.010. PubMed PMID: 31331563.
21. Kerley CP. A Review of Plant-based Diets to Prevent and Treat Heart Failure. Card Fail Rev. 2018;4(1):54-61. doi: 10.15420/cfr.2018:1:1. PubMed PMID: 29892479; PMCID: PMC5971679.
22. Najjar RS, Feresin RG. Protective Role of Polyphenols in Heart Failure: Molecular Targets and Cellular Mechanisms Underlying Their Therapeutic Potential. Int J Mol Sci. 2021;22(4). Epub 2021/02/11. doi: 10.3390/ijms22041668. PubMed PMID: 33562294; PMCID: PMC7914665.
23. Redfield MM, Jacobsen SJ, Burnett JC, Jr., Mahoney DW, Bailey KR, Rodeheffer RJ. Burden of systolic and diastolic ventricular dysfunction in the community: appreciating the scope of the heart failure epidemic. JAMA. 2003;289(2):194-202. doi: 10.1001/jama.289.2.194. PubMed PMID: 12517230.
24. Henning RJ. Diagnosis and treatment of heart failure with preserved left ventricular ejection fraction. World J Cardiol. 2020;12(1):7-25. doi: 10.4330/wjc.v12.i1.7. PubMed PMID: 31984124; PMCID: PMC6952725.
25. Hajouli S, Ludhwani D. Heart Failure And Ejection Fraction. StatPearls. Treasure Island (FL)2020.
26. Hartupee J, Mann DL. Neurohormonal activation in heart failure with reduced ejection fraction. Nat Rev Cardiol. 2017;14(1):30-8. doi: 10.1038/nrcardio.2016.163. PubMed PMID: 27708278; PMCID: PMC5286912.

27. Pinilla-Vera M, Hahn VS, Kass DA. Leveraging Signaling Pathways to Treat Heart Failure With Reduced Ejection Fraction. Circ Res. 2019;124(11):1618-32. doi: 10.1161/CIRCRESAHA.119.313682. PubMed PMID: 31120818; PMCID: PMC6534150.
28. Engelhardt S, Hein L, Wiesmann F, Lohse MJ. Progressive hypertrophy and heart failure in beta1-adrenergic receptor transgenic mice. Proc Natl Acad Sci U S A. 1999;96(12):7059-64. doi: 10.1073/pnas.96.12.7059. PubMed PMID: 10359838; PMCID: PMC22055.
29. Ferrario CM, Strawn WB. Role of the renin-angiotensin-aldosterone system and proinflammatory mediators in cardiovascular disease. Am J Cardiol. 2006;98(1):121-8. doi: 10.1016/j.amjcard.2006.01.059. PubMed PMID: 16784934.
30. Carey RM, Wang ZQ, Siragy HM. Role of the angiotensin type 2 receptor in the regulation of blood pressure and renal function. Hypertension. 2000;35(1 Pt 2):155-63. doi: 10.1161/01.hyp.35.1.155. PubMed PMID: 10642292.
31. Nakashima H, Suzuki H, Ohtsu H, Chao JY, Utsunomiya H, Frank GD, Eguchi S. Angiotensin II regulates vascular and endothelial dysfunction: recent topics of Angiotensin II type-1 receptor signaling in the vasculature. Curr Vasc Pharmacol. 2006;4(1):67-78. doi: 10.2174/157016106775203126. PubMed PMID: 16472178.
32. Satou R, Penrose H, Navar LG. Inflammation as a Regulator of the Renin-Angiotensin System and Blood Pressure. Curr Hypertens Rep. 2018;20(12):100. doi: 10.1007/s11906-018-0900-0. PubMed PMID: 30291560; PMCID: PMC6203444.
33. Re RN. Mechanisms of disease: local renin-angiotensin-aldosterone systems and the pathogenesis and treatment of cardiovascular disease. Nat Clin Pract Cardiovasc Med. 2004;1(1):42-7. doi: 10.1038/ncpcardio0012. PubMed PMID: 16265259.
34. Scott JH, Dunn RJ. Physiology, Aldosterone. StatPearls. Treasure Island (FL)2020.
35. Yoshida M, Ma J, Tomita T, Morikawa N, Tanaka N, Masamura K, Kawai Y, Miyamori I. Mineralocorticoid receptor is overexpressed in cardiomyocytes of patients with congestive heart failure. Congest Heart Fail. 2005;11(1):12-6. doi: 10.1111/j.1527-5299.2005.03722.x. PubMed PMID: 15722665.
36. Paradis P, Dali-Youcef N, Paradis FW, Thibault G, Nemer M. Overexpression of angiotensin II type I receptor in cardiomyocytes induces cardiac hypertrophy and remodeling. Proc Natl Acad Sci U S A. 2000;97(2):931-6. doi: 10.1073/pnas.97.2.931. PubMed PMID: 10639182; PMCID: PMC15433.
37. Shah KS, Xu H, Matsouaka RA, Bhatt DL, Heidenreich PA, Hernandez AF, Devore AD, Yancy CW, Fonarow GC. Heart Failure With Preserved, Borderline, and Reduced Ejection Fraction: 5-Year Outcomes. J Am Coll Cardiol. 2017;70(20):2476-86. doi: 10.1016/j.jacc.2017.08.074. PubMed PMID: 29141781.
38. Patten RD, Hall-Porter MR. Small animal models of heart failure: development of novel therapies, past and present. Circ Heart Fail. 2009;2(2):138-44. doi: 10.1161/CIRCHEARTFAILURE.108.839761. PubMed PMID: 19808329.
39. Pfeffer JM, Pfeffer MA, Braunwald E. Influence of chronic captopril therapy on the infarcted left ventricle of the rat. Circ Res. 1985;57(1):84-95. doi: 10.1161/01.res.57.1.84. PubMed PMID: 3891127.
40. Yellon DM, Hausenloy DJ. Myocardial reperfusion injury. N Engl J Med. 2007;357(11):1121-35. doi: 10.1056/NEJMra071667. PubMed PMID: 17855673.
41. Michael LH, Entman ML, Hartley CJ, Youker KA, Zhu J, Hall SR, Hawkins HK, Berens K, Ballantyne CM. Myocardial ischemia and reperfusion: a murine model. Am J Physiol. 1995;269(6 Pt 2):H2147-54. doi: 10.1152/ajpheart.1995.269.6.H2147. PubMed PMID: 8594926.

42. Riehle C, Bauersachs J. Small animal models of heart failure. Cardiovasc Res. 2019;115(13):1838-49. doi: 10.1093/cvr/cvz161. PubMed PMID: 31243437; PMCID: PMC6803815.
43. Haase VH. Regulation of erythropoiesis by hypoxia-inducible factors. Blood Rev. 2013;27(1):41-53. Epub 2013/01/08. doi: 10.1016/j.blre.2012.12.003. PubMed PMID: 23291219; PMCID: PMC3731139.
44. Semenza GL. Hypoxia-inducible factor 1: regulator of mitochondrial metabolism and mediator of ischemic preconditioning. Biochim Biophys Acta. 2011;1813(7):1263-8. Epub 2010/08/25. doi: 10.1016/j.bbamcr.2010.08.006. PubMed PMID: 20732359; PMCID: PMC3010308.
45. Wang GL, Jiang BH, Rue EA, Semenza GL. Hypoxia-inducible factor 1 is a basic-helix-loop-helix-PAS heterodimer regulated by cellular O2 tension. Proc Natl Acad Sci U S A. 1995;92(12):5510-4. Epub 1995/06/06. doi: 10.1073/pnas.92.12.5510. PubMed PMID: 7539918; PMCID: PMC41725.
46. Sousa Fialho MDL, Abd Jamil AH, Stannard GA, Heather LC. Hypoxia-inducible factor 1 signalling, metabolism and its therapeutic potential in cardiovascular disease. Biochim Biophys Acta Mol Basis Dis. 2019;1865(4):831-43. Epub 2018/09/30. doi: 10.1016/j.bbadis.2018.09.024. PubMed PMID: 30266651.
47. Essop MF. Cardiac metabolic adaptations in response to chronic hypoxia. J Physiol. 2007;584(Pt 3):715-26. Epub 2007/09/01. doi: 10.1113/jphysiol.2007.143511. PubMed PMID: 17761770; PMCID: PMC2276994.
48. Wei H, Bedja D, Koitabashi N, Xing D, Chen J, Fox-Talbot K, Rouf R, Chen S, Steenbergen C, Harmon JW, Dietz HC, Gabrielson KL, Kass DA, Semenza GL. Endothelial expression of hypoxia-inducible factor 1 protects the murine heart and aorta from pressure overload by suppression of TGF-beta signaling. Proc Natl Acad Sci U S A. 2012;109(14):E841-50. Epub 2012/03/10. doi: 10.1073/pnas.1202081109. PubMed PMID: 22403061; PMCID: PMC3325701.
49. Bohuslavova R, Kolar F, Sedmera D, Skvorova L, Papousek F, Neckar J, Pavlinkova G. Partial deficiency of HIF-1alpha stimulates pathological cardiac changes in streptozotocin-induced diabetic mice. BMC Endocr Disord. 2014;14:11. Epub 2014/02/08. doi: 10.1186/1472-6823-14-11. PubMed PMID: 24502509; PMCID: PMC3922431.
50. Holscher M, Schafer K, Krull S, Farhat K, Hesse A, Silter M, Lin Y, Pichler BJ, Thistlethwaite P, El-Armouche A, Maier LS, Katschinski DM, Zieseniss A. Unfavourable consequences of chronic cardiac HIF-1alpha stabilization. Cardiovasc Res. 2012;94(1):77-86. Epub 2012/01/20. doi: 10.1093/cvr/cvs014. PubMed PMID: 22258630.
51. Strowitzki MJ, Cummins EP, Taylor CT. Protein Hydroxylation by Hypoxia-Inducible Factor (HIF) Hydroxylases: Unique or Ubiquitous? Cells. 2019;8(5). Epub 2019/05/01. doi: 10.3390/cells8050384. PubMed PMID: 31035491; PMCID: PMC6562979.
52. Epstein AC, Gleadle JM, McNeill LA, Hewitson KS, O'Rourke J, Mole DR, Mukherji M, Metzen E, Wilson MI, Dhanda A, Tian YM, Masson N, Hamilton DL, Jaakkola P, Barstead R, Hodgkin J, Maxwell PH, Pugh CW, Schofield CJ, Ratcliffe PJ. C. elegans EGL-9 and mammalian homologs define a family of dioxygenases that regulate HIF by prolyl hydroxylation. Cell. 2001;107(1):43-54. Epub 2001/10/12. doi: 10.1016/s0092-8674(01)00507-4. PubMed PMID: 11595184.
53. Yuan Y, Hilliard G, Ferguson T, Millhorn DE. Cobalt inhibits the interaction between hypoxia-inducible factor-alpha and von Hippel-Lindau protein by direct binding to hypoxia-

inducible factor-alpha. J Biol Chem. 2003;278(18):15911-6. Epub 2003/02/28. doi: 10.1074/jbc.M300463200. PubMed PMID: 12606543.
54. Pang Z, Wang T, Li Y, Wang L, Yang J, Dong H, Li S. Liraglutide ameliorates COCl2-induced oxidative stress and apoptosis in H9C2 cells via regulating cell autophagy. Exp Ther Med. 2020;19(6):3716-22. Epub 2020/04/30. doi: 10.3892/etm.2020.8630. PubMed PMID: 32346436; PMCID: PMC7185156.
55. Fang Z, Luo W, Luo Y. Protective effect of alpha-mangostin against CoCl2-induced apoptosis by suppressing oxidative stress in H9C2 rat cardiomyoblasts. Mol Med Rep. 2018;17(5):6697-704. Epub 2018/03/08. doi: 10.3892/mmr.2018.8680. PubMed PMID: 29512772.
56. Xi L, Taher M, Yin C, Salloum F, Kukreja RC. Cobalt chloride induces delayed cardiac preconditioning in mice through selective activation of HIF-1alpha and AP-1 and iNOS signaling. Am J Physiol Heart Circ Physiol. 2004;287(6):H2369-75. Epub 2004/07/31. doi: 10.1152/ajpheart.00422.2004. PubMed PMID: 15284066.
57. Yu L, Wang L, Chen S. Endogenous toll-like receptor ligands and their biological significance. J Cell Mol Med. 2010;14(11):2592-603. Epub 2010/07/16. doi: 10.1111/j.1582-4934.2010.01127.x. PubMed PMID: 20629986; PMCID: PMC4373479.
58. Yang Y, Lv J, Jiang S, Ma Z, Wang D, Hu W, Deng C, Fan C, Di S, Sun Y, Yi W. The emerging role of Toll-like receptor 4 in myocardial inflammation. Cell Death Dis. 2016;7(5):e2234. Epub 2016/05/27. doi: 10.1038/cddis.2016.140. PubMed PMID: 27228349; PMCID: PMC4917669.
59. Avlas O, Bragg A, Fuks A, Nicholson JD, Farkash A, Porat E, Aravot D, Levy-Drummer RS, Cohen C, Shainberg A, Arad M, Hochhauser E. TLR4 Expression Is Associated with Left Ventricular Dysfunction in Patients Undergoing Coronary Artery Bypass Surgery. PLoS One. 2015;10(6):e0120175. Epub 2015/06/02. doi: 10.1371/journal.pone.0120175. PubMed PMID: 26030867; PMCID: PMC4451004.
60. Katare PB, Bagul PK, Dinda AK, Banerjee SK. Toll-Like Receptor 4 Inhibition Improves Oxidative Stress and Mitochondrial Health in Isoproterenol-Induced Cardiac Hypertrophy in Rats. Front Immunol. 2017;8:719. Epub 2017/07/12. doi: 10.3389/fimmu.2017.00719. PubMed PMID: 28690610; PMCID: PMC5479928.
61. Timmers L, Sluijter JP, van Keulen JK, Hoefer IE, Nederhoff MG, Goumans MJ, Doevendans PA, van Echteld CJ, Joles JA, Quax PH, Piek JJ, Pasterkamp G, de Kleijn DP. Toll-like receptor 4 mediates maladaptive left ventricular remodeling and impairs cardiac function after myocardial infarction. Circ Res. 2008;102(2):257-64. Epub 2007/11/17. doi: 10.1161/CIRCRESAHA.107.158220. PubMed PMID: 18007026.
62. Cremers CM, Jakob U. Oxidant sensing by reversible disulfide bond formation. J Biol Chem. 2013;288(37):26489-96. doi: 10.1074/jbc.R113.462929. PubMed PMID: 23861395; PMCID: PMC3772196.
63. Hill MF, Singal PK. Right and left myocardial antioxidant responses during heart failure subsequent to myocardial infarction. Circulation. 1997;96(7):2414-20. doi: 10.1161/01.cir.96.7.2414. PubMed PMID: 9337218.
64. Bendall JK, Cave AC, Heymes C, Gall N, Shah AM. Pivotal role of a gp91(phox)-containing NADPH oxidase in angiotensin II-induced cardiac hypertrophy in mice. Circulation. 2002;105(3):293-6. doi: 10.1161/hc0302.103712. PubMed PMID: 11804982.

65. von Harsdorf R, Li PF, Dietz R. Signaling pathways in reactive oxygen species-induced cardiomyocyte apoptosis. Circulation. 1999;99(22):2934-41. doi: 10.1161/01.cir.99.22.2934. PubMed PMID: 10359739.
66. Tsutsui H, Ide T, Hayashidani S, Suematsu N, Utsumi H, Nakamura R, Egashira K, Takeshita A. Greater susceptibility of failing cardiac myocytes to oxygen free radical-mediated injury. Cardiovasc Res. 2001;49(1):103-9. doi: 10.1016/s0008-6363(00)00197-8. PubMed PMID: 11121801.
67. Krijnen PA, Meischl C, Hack CE, Meijer CJ, Visser CA, Roos D, Niessen HW. Increased Nox2 expression in human cardiomyocytes after acute myocardial infarction. J Clin Pathol. 2003;56(3):194-9. doi: 10.1136/jcp.56.3.194. PubMed PMID: 12610097; PMCID: PMC1769897.
68. Ago T, Kuroda J, Pain J, Fu C, Li H, Sadoshima J. Upregulation of Nox4 by hypertrophic stimuli promotes apoptosis and mitochondrial dysfunction in cardiac myocytes. Circ Res. 2010;106(7):1253-64. Epub 2010/02/27. doi: 10.1161/CIRCRESAHA.109.213116. PubMed PMID: 20185797; PMCID: PMC2855780.
69. Hwang J, Ing MH, Salazar A, Lassegue B, Griendling K, Navab M, Sevanian A, Hsiai TK. Pulsatile versus oscillatory shear stress regulates NADPH oxidase subunit expression: implication for native LDL oxidation. Circ Res. 2003;93(12):1225-32. doi: 10.1161/01.RES.0000104087.29395.66. PubMed PMID: 14593003; PMCID: PMC4433384.
70. Li JM, Shah AM. Mechanism of endothelial cell NADPH oxidase activation by angiotensin II. Role of the p47phox subunit. J Biol Chem. 2003;278(14):12094-100. doi: 10.1074/jbc.M209793200. PubMed PMID: 12560337.
71. Duerrschmidt N, Wippich N, Goettsch W, Broemme HJ, Morawietz H. Endothelin-1 induces NAD(P)H oxidase in human endothelial cells. Biochem Biophys Res Commun. 2000;269(3):713-7. doi: 10.1006/bbrc.2000.2354. PubMed PMID: 10720482.
72. Frey RS, Rahman A, Kefer JC, Minshall RD, Malik AB. PKCzeta regulates TNF-alpha-induced activation of NADPH oxidase in endothelial cells. Circ Res. 2002;90(9):1012-9. doi: 10.1161/01.res.0000017631.28815.8e. PubMed PMID: 12016268.
73. Xiao L, Pimentel DR, Wang J, Singh K, Colucci WS, Sawyer DB. Role of reactive oxygen species and NAD(P)H oxidase in alpha(1)-adrenoceptor signaling in adult rat cardiac myocytes. Am J Physiol Cell Physiol. 2002;282(4):C926-34. doi: 10.1152/ajpcell.00254.2001. PubMed PMID: 11880281.
74. Cordeiro RM. Reactive oxygen species at phospholipid bilayers: distribution, mobility and permeation. Biochim Biophys Acta. 2014;1838(1 Pt B):438-44. doi: 10.1016/j.bbamem.2013.09.016. PubMed PMID: 24095673.
75. Santillo M, Colantuoni A, Mondola P, Guida B, Damiano S. NOX signaling in molecular cardiovascular mechanisms involved in the blood pressure homeostasis. Front Physiol. 2015;6:194. doi: 10.3389/fphys.2015.00194. PubMed PMID: 26217233; PMCID: PMC4493385.
76. Groemping Y, Rittinger K. Activation and assembly of the NADPH oxidase: a structural perspective. Biochem J. 2005;386(Pt 3):401-16. doi: 10.1042/BJ20041835. PubMed PMID: 15588255; PMCID: PMC1134858.
77. Looi YH, Grieve DJ, Siva A, Walker SJ, Anilkumar N, Cave AC, Marber M, Monaghan MJ, Shah AM. Involvement of Nox2 NADPH oxidase in adverse cardiac remodeling after myocardial infarction. Hypertension. 2008;51(2):319-25. Epub 2008/01/09. doi: 10.1161/HYPERTENSIONAHA.107.101980. PubMed PMID: 18180403.
78. Doerries C, Grote K, Hilfiker-Kleiner D, Luchtefeld M, Schaefer A, Holland SM, Sorrentino S, Manes C, Schieffer B, Drexler H, Landmesser U. Critical role of the NAD(P)H

oxidase subunit p47phox for left ventricular remodeling/dysfunction and survival after myocardial infarction. Circ Res. 2007;100(6):894-903. Epub 2007/03/03. doi: 10.1161/01.RES.0000261657.76299.ff. PubMed PMID: 17332431.
79. Gimenez M, Schickling BM, Lopes LR, Miller FJ, Jr. Nox1 in cardiovascular diseases: regulation and pathophysiology. Clin Sci (Lond). 2016;130(3):151-65. doi: 10.1042/CS20150404. PubMed PMID: 26678171.
80. Jiang S, Streeter J, Schickling BM, Zimmerman K, Weiss RM, Miller FJ, Jr. Nox1 NADPH oxidase is necessary for late but not early myocardial ischaemic preconditioning. Cardiovasc Res. 2014;102(1):79-87. doi: 10.1093/cvr/cvu027. PubMed PMID: 24501329; PMCID: PMC3958622.
81. Sumimoto H, Miyano K, Takeya R. Molecular composition and regulation of the Nox family NAD(P)H oxidases. Biochem Biophys Res Commun. 2005;338(1):677-86. doi: 10.1016/j.bbrc.2005.08.210. PubMed PMID: 16157295.
82. Chatterjee K, Zhang J, Honbo N, Karliner JS. Doxorubicin cardiomyopathy. Cardiology. 2010;115(2):155-62. doi: 10.1159/000265166. PubMed PMID: 20016174; PMCID: PMC2848530.
83. Iwata K, Matsuno K, Murata A, Zhu K, Fukui H, Ikuta K, Katsuyama M, Ibi M, Matsumoto M, Ohigashi M, Wen X, Zhang J, Cui W, Yabe-Nishimura C. Up-regulation of NOX1/NADPH oxidase following drug-induced myocardial injury promotes cardiac dysfunction and fibrosis. Free Radic Biol Med. 2018;120:277-88. doi: 10.1016/j.freeradbiomed.2018.03.053. PubMed PMID: 29609020.
84. Martyn KD, Frederick LM, von Loehneysen K, Dinauer MC, Knaus UG. Functional analysis of Nox4 reveals unique characteristics compared to other NADPH oxidases. Cell Signal. 2006;18(1):69-82. doi: 10.1016/j.cellsig.2005.03.023. PubMed PMID: 15927447.
85. Nisimoto Y, Diebold BA, Cosentino-Gomes D, Lambeth JD. Nox4: a hydrogen peroxide-generating oxygen sensor. Biochemistry. 2014;53(31):5111-20. doi: 10.1021/bi500331y. PubMed PMID: 25062272; PMCID: PMC4131900.
86. Nisimoto Y, Jackson HM, Ogawa H, Kawahara T, Lambeth JD. Constitutive NADPH-dependent electron transferase activity of the Nox4 dehydrogenase domain. Biochemistry. 2010;49(11):2433-42. doi: 10.1021/bi9022285. PubMed PMID: 20163138; PMCID: PMC2839512.
87. Kuroda J, Ago T, Matsushima S, Zhai P, Schneider MD, Sadoshima J. NADPH oxidase 4 (Nox4) is a major source of oxidative stress in the failing heart. Proc Natl Acad Sci U S A. 2010;107(35):15565-70. Epub 2010/08/18. doi: 10.1073/pnas.1002178107. PubMed PMID: 20713697; PMCID: PMC2932625.
88. Manea A, Tanase LI, Raicu M, Simionescu M. Transcriptional regulation of NADPH oxidase isoforms, Nox1 and Nox4, by nuclear factor-kappaB in human aortic smooth muscle cells. Biochem Biophys Res Commun. 2010;396(4):901-7. doi: 10.1016/j.bbrc.2010.05.019. PubMed PMID: 20457132.
89. Byrne JA, Grieve DJ, Bendall JK, Li JM, Gove C, Lambeth JD, Cave AC, Shah AM. Contrasting roles of NADPH oxidase isoforms in pressure-overload versus angiotensin II-induced cardiac hypertrophy. Circ Res. 2003;93(9):802-5. doi: 10.1161/01.RES.0000099504.30207.F5. PubMed PMID: 14551238.
90. Grieve DJ, Byrne JA, Siva A, Layland J, Johar S, Cave AC, Shah AM. Involvement of the nicotinamide adenosine dinucleotide phosphate oxidase isoform Nox2 in cardiac contractile dysfunction occurring in response to pressure overload. J Am Coll Cardiol. 2006;47(4):817-26. doi: 10.1016/j.jacc.2005.09.051. PubMed PMID: 16487851.

91. Banfi B, Tirone F, Durussel I, Knisz J, Moskwa P, Molnar GZ, Krause KH, Cox JA. Mechanism of Ca2+ activation of the NADPH oxidase 5 (NOX5). J Biol Chem. 2004;279(18):18583-91. doi: 10.1074/jbc.M310268200. PubMed PMID: 14982937.
92. Piacentino V, 3rd, Weber CR, Chen X, Weisser-Thomas J, Margulies KB, Bers DM, Houser SR. Cellular basis of abnormal calcium transients of failing human ventricular myocytes. Circ Res. 2003;92(6):651-8. doi: 10.1161/01.RES.0000062469.83985.9B. PubMed PMID: 12600875.
93. Hahn NE, Meischl C, Kawahara T, Musters RJ, Verhoef VM, van der Velden J, Vonk AB, Paulus WJ, van Rossum AC, Niessen HW, Krijnen PA. NOX5 expression is increased in intramyocardial blood vessels and cardiomyocytes after acute myocardial infarction in humans. Am J Pathol. 2012;180(6):2222-9. doi: 10.1016/j.ajpath.2012.02.018. PubMed PMID: 22503554.
94. Guzik TJ, Chen W, Gongora MC, Guzik B, Lob HE, Mangalat D, Hoch N, Dikalov S, Rudzinski P, Kapelak B, Sadowski J, Harrison DG. Calcium-dependent NOX5 nicotinamide adenine dinucleotide phosphate oxidase contributes to vascular oxidative stress in human coronary artery disease. J Am Coll Cardiol. 2008;52(22):1803-9. doi: 10.1016/j.jacc.2008.07.063. PubMed PMID: 19022160; PMCID: PMC2593790.
95. Montezano AC, Burger D, Paravicini TM, Chignalia AZ, Yusuf H, Almasri M, He Y, Callera GE, He G, Krause KH, Lambeth D, Quinn MT, Touyz RM. Nicotinamide adenine dinucleotide phosphate reduced oxidase 5 (Nox5) regulation by angiotensin II and endothelin-1 is mediated via calcium/calmodulin-dependent, rac-1-independent pathways in human endothelial cells. Circ Res. 2010;106(8):1363-73. doi: 10.1161/CIRCRESAHA.109.216036. PubMed PMID: 20339118; PMCID: PMC3119893.
96. Kleikers PW, Dao VT, Gob E, Hooijmans C, Debets J, van Essen H, Kleinschnitz C, Schmidt HH. SFRR-E Young Investigator AwardeeNOXing out stroke: Identification of NOX4 and 5as targets in blood-brain-barrier stabilisation and neuroprotection. Free Radic Biol Med. 2014;75 Suppl 1:S16. Epub 2015/10/16. doi: 10.1016/j.freeradbiomed.2014.10.593. PubMed PMID: 26461296.
97. Barth E, Stammler G, Speiser B, Schaper J. Ultrastructural quantitation of mitochondria and myofilaments in cardiac muscle from 10 different animal species including man. J Mol Cell Cardiol. 1992;24(7):669-81. doi: 10.1016/0022-2828(92)93381-s. PubMed PMID: 1404407.
98. Ferrari R, Censi S, Mastrorilli F, Boraso A. Prognostic benefits of heart rate reduction in cardiovascular disease. European Heart Journal Supplements. 2003;5(G):G10-G4. doi: Doi 10.1016/S1520-765x(03)90002-2. PubMed PMID: WOS:000186031100003.
99. Goncalves RL, Quinlan CL, Perevoshchikova IV, Hey-Mogensen M, Brand MD. Sites of superoxide and hydrogen peroxide production by muscle mitochondria assessed ex vivo under conditions mimicking rest and exercise. J Biol Chem. 2015;290(1):209-27. doi: 10.1074/jbc.M114.619072. PubMed PMID: 25389297; PMCID: PMC4281723.
100. Kornfeld OS, Hwang S, Disatnik MH, Chen CH, Qvit N, Mochly-Rosen D. Mitochondrial reactive oxygen species at the heart of the matter: new therapeutic approaches for cardiovascular diseases. Circ Res. 2015;116(11):1783-99. doi: 10.1161/CIRCRESAHA.116.305432. PubMed PMID: 25999419; PMCID: PMC4443500.
101. Chen L, Gong Q, Stice JP, Knowlton AA. Mitochondrial OPA1, apoptosis, and heart failure. Cardiovasc Res. 2009;84(1):91-9. doi: 10.1093/cvr/cvp181. PubMed PMID: 19493956; PMCID: PMC2741347.

102. Adlam VJ, Harrison JC, Porteous CM, James AM, Smith RA, Murphy MP, Sammut IA. Targeting an antioxidant to mitochondria decreases cardiac ischemia-reperfusion injury. FASEB J. 2005;19(9):1088-95. doi: 10.1096/fj.05-3718com. PubMed PMID: 15985532.
103. Goh KY, He L, Song J, Jinno M, Rogers AJ, Sethu P, Halade GV, Rajasekaran NS, Liu X, Prabhu SD, Darley-Usmar V, Wende AR, Zhou L. Mitoquinone ameliorates pressure overload-induced cardiac fibrosis and left ventricular dysfunction in mice. Redox Biol. 2019;21:101100. doi: 10.1016/j.redox.2019.101100. PubMed PMID: 30641298; PMCID: PMC6330374.
104. Rossman MJ, Santos-Parker JR, Steward CAC, Bispham NZ, Cuevas LM, Rosenberg HL, Woodward KA, Chonchol M, Gioscia-Ryan RA, Murphy MP, Seals DR. Chronic Supplementation With a Mitochondrial Antioxidant (MitoQ) Improves Vascular Function in Healthy Older Adults. Hypertension. 2018;71(6):1056-63. doi: 10.1161/HYPERTENSIONAHA.117.10787. PubMed PMID: 29661838; PMCID: PMC5945293.
105. Pacher P, Nivorozhkin A, Szabo C. Therapeutic effects of xanthine oxidase inhibitors: renaissance half a century after the discovery of allopurinol. Pharmacol Rev. 2006;58(1):87-114. doi: 10.1124/pr.58.1.6. PubMed PMID: 16507884; PMCID: PMC2233605.
106. Berry CE, Hare JM. Xanthine oxidoreductase and cardiovascular disease: molecular mechanisms and pathophysiological implications. J Physiol. 2004;555(Pt 3):589-606. doi: 10.1113/jphysiol.2003.055913. PubMed PMID: 14694147; PMCID: PMC1664875.
107. Bredemeier M, Lopes LM, Eisenreich MA, Hickmann S, Bongiorno GK, d'Avila R, Morsch ALB, da Silva Stein F, Campos GGD. Xanthine oxidase inhibitors for prevention of cardiovascular events: a systematic review and meta-analysis of randomized controlled trials. BMC Cardiovasc Disord. 2018;18(1):24. doi: 10.1186/s12872-018-0757-9. PubMed PMID: 29415653; PMCID: PMC5804046.
108. Yang B, Ye D, Wang Y. Caspase-3 as a therapeutic target for heart failure. Expert Opin Ther Targets. 2013;17(3):255-63. Epub 2013/01/09. doi: 10.1517/14728222.2013.745513. PubMed PMID: 23294432.
109. Chiong M, Wang ZV, Pedrozo Z, Cao DJ, Troncoso R, Ibacache M, Criollo A, Nemchenko A, Hill JA, Lavandero S. Cardiomyocyte death: mechanisms and translational implications. Cell Death Dis. 2011;2(12):e244. Epub 2011/12/23. doi: 10.1038/cddis.2011.130. PubMed PMID: 22190003; PMCID: PMC3252742.
110. Movassagh M, Foo RS. Simplified apoptotic cascades. Heart Fail Rev. 2008;13(2):111-9. Epub 2007/12/18. doi: 10.1007/s10741-007-9070-x. PubMed PMID: 18080749.
111. Miyashita T, Reed JC. Tumor suppressor p53 is a direct transcriptional activator of the human bax gene. Cell. 1995;80(2):293-9. Epub 1995/01/27. doi: 10.1016/0092-8674(95)90412-3. PubMed PMID: 7834749.
112. Son Y, Cheong YK, Kim NH, Chung HT, Kang DG, Pae HO. Mitogen-Activated Protein Kinases and Reactive Oxygen Species: How Can ROS Activate MAPK Pathways? J Signal Transduct. 2011;2011:792639. doi: 10.1155/2011/792639. PubMed PMID: 21637379; PMCID: PMC3100083.
113. Kwon SH, Pimentel DR, Remondino A, Sawyer DB, Colucci WS. H(2)O(2) regulates cardiac myocyte phenotype via concentration-dependent activation of distinct kinase pathways. J Mol Cell Cardiol. 2003;35(6):615-21. doi: 10.1016/s0022-2828(03)00084-1. PubMed PMID: 12788379.
114. Bueno OF, De Windt LJ, Tymitz KM, Witt SA, Kimball TR, Klevitsky R, Hewett TE, Jones SP, Lefer DJ, Peng CF, Kitsis RN, Molkentin JD. The MEK1-ERK1/2 signaling pathway

promotes compensated cardiac hypertrophy in transgenic mice. EMBO J. 2000;19(23):6341-50. doi: 10.1093/emboj/19.23.6341. PubMed PMID: 11101507; PMCID: PMC305855.
115. van Rooij E, Doevendans PA, de Theije CC, Babiker FA, Molkentin JD, de Windt LJ. Requirement of nuclear factor of activated T-cells in calcineurin-mediated cardiomyocyte hypertrophy. J Biol Chem. 2002;277(50):48617-26. doi: 10.1074/jbc.M206532200. PubMed PMID: 12226086.
116. Liu Q, Chen Y, Auger-Messier M, Molkentin JD. Interaction between NFkappaB and NFAT coordinates cardiac hypertrophy and pathological remodeling. Circ Res. 2012;110(8):1077-86. doi: 10.1161/CIRCRESAHA.111.260729. PubMed PMID: 22403241; PMCID: PMC3341669.
117. Schaub MC, Hefti MA, Harder BA, Eppenberger HM. Various hypertrophic stimuli induce distinct phenotypes in cardiomyocytes. J Mol Med (Berl). 1997;75(11-12):901-20. doi: 10.1007/s001090050182. PubMed PMID: 9428623.
118. Liao P, Georgakopoulos D, Kovacs A, Zheng M, Lerner D, Pu H, Saffitz J, Chien K, Xiao RP, Kass DA, Wang Y. The in vivo role of p38 MAP kinases in cardiac remodeling and restrictive cardiomyopathy. Proc Natl Acad Sci U S A. 2001;98(21):12283-8. doi: 10.1073/pnas.211086598. PubMed PMID: 11593045; PMCID: PMC59806.
119. Zhang D, Gaussin V, Taffet GE, Belaguli NS, Yamada M, Schwartz RJ, Michael LH, Overbeek PA, Schneider MD. TAK1 is activated in the myocardium after pressure overload and is sufficient to provoke heart failure in transgenic mice. Nat Med. 2000;6(5):556-63. doi: 10.1038/75037. PubMed PMID: 10802712.
120. Petrich BG, Molkentin JD, Wang Y. Temporal activation of c-Jun N-terminal kinase in adult transgenic heart via cre-loxP-mediated DNA recombination. FASEB J. 2003;17(6):749-51. doi: 10.1096/fj.02-0438fje. PubMed PMID: 12594183.
121. Gloire G, Legrand-Poels S, Piette J. NF-kappaB activation by reactive oxygen species: fifteen years later. Biochem Pharmacol. 2006;72(11):1493-505. doi: 10.1016/j.bcp.2006.04.011. PubMed PMID: 16723122.
122. Gordon JW, Shaw JA, Kirshenbaum LA. Multiple facets of NF-kappaB in the heart: to be or not to NF-kappaB. Circ Res. 2011;108(9):1122-32. doi: 10.1161/CIRCRESAHA.110.226928. PubMed PMID: 21527742.
123. Bujak M, Dobaczewski M, Chatila K, Mendoza LH, Li N, Reddy A, Frangogiannis NG. Interleukin-1 receptor type I signaling critically regulates infarct healing and cardiac remodeling. Am J Pathol. 2008;173(1):57-67. doi: 10.2353/ajpath.2008.070974. PubMed PMID: 18535174; PMCID: PMC2438285.
124. Huynh ML, Fadok VA, Henson PM. Phosphatidylserine-dependent ingestion of apoptotic cells promotes TGF-beta1 secretion and the resolution of inflammation. J Clin Invest. 2002;109(1):41-50. doi: 10.1172/JCI11638. PubMed PMID: 11781349; PMCID: PMC150814.
125. Thompson NL, Flanders KC, Smith JM, Ellingsworth LR, Roberts AB, Sporn MB. Expression of transforming growth factor-beta 1 in specific cells and tissues of adult and neonatal mice. J Cell Biol. 1989;108(2):661-9. doi: 10.1083/jcb.108.2.661. PubMed PMID: 2645303; PMCID: PMC2115426.
126. Barcellos-Hoff MH, Dix TA. Redox-mediated activation of latent transforming growth factor-beta 1. Mol Endocrinol. 1996;10(9):1077-83. doi: 10.1210/mend.10.9.8885242. PubMed PMID: 8885242.
127. Frangogiannis NG. Cardiac fibrosis: Cell biological mechanisms, molecular pathways and therapeutic opportunities. Mol Aspects Med. 2019;65:70-99. doi: 10.1016/j.mam.2018.07.001. PubMed PMID: 30056242.

128. Iwanaga Y, Aoyama T, Kihara Y, Onozawa Y, Yoneda T, Sasayama S. Excessive activation of matrix metalloproteinases coincides with left ventricular remodeling during transition from hypertrophy to heart failure in hypertensive rats. J Am Coll Cardiol. 2002;39(8):1384-91. doi: 10.1016/s0735-1097(02)01756-4. PubMed PMID: 11955860.
129. Fukai T, Ushio-Fukai M. Superoxide dismutases: role in redox signaling, vascular function, and diseases. Antioxid Redox Signal. 2011;15(6):1583-606. doi: 10.1089/ars.2011.3999. PubMed PMID: 21473702; PMCID: PMC3151424.
130. Lubos E, Loscalzo J, Handy DE. Glutathione peroxidase-1 in health and disease: from molecular mechanisms to therapeutic opportunities. Antioxid Redox Signal. 2011;15(7):1957-97. doi: 10.1089/ars.2010.3586. PubMed PMID: 21087145; PMCID: PMC3159114.
131. Alfonso-Prieto M, Biarnes X, Vidossich P, Rovira C. The molecular mechanism of the catalase reaction. J Am Chem Soc. 2009;131(33):11751-61. doi: 10.1021/ja9018572. PubMed PMID: 19653683.
132. Morikawa K, Shimokawa H, Matoba T, Kubota H, Akaike T, Talukder MA, Hatanaka M, Fujiki T, Maeda H, Takahashi S, Takeshita A. Pivotal role of Cu,Zn-superoxide dismutase in endothelium-dependent hyperpolarization. J Clin Invest. 2003;112(12):1871-9. doi: 10.1172/JCI19351. PubMed PMID: 14679182; PMCID: PMC296996.
133. Grzenkowicz-Wydra J, Cisowski J, Nakonieczna J, Zarebski A, Udilova N, Nohl H, Jozkowicz A, Podhajska A, Dulak J. Gene transfer of CuZn superoxide dismutase enhances the synthesis of vascular endothelial growth factor. Mol Cell Biochem. 2004;264(1-2):169-81. doi: 10.1023/b:mcbi.0000044386.45054.70. PubMed PMID: 15544046.
134. Juarez JC, Manuia M, Burnett ME, Betancourt O, Boivin B, Shaw DE, Tonks NK, Mazar AP, Donate F. Superoxide dismutase 1 (SOD1) is essential for H2O2-mediated oxidation and inactivation of phosphatases in growth factor signaling. Proc Natl Acad Sci U S A. 2008;105(20):7147-52. doi: 10.1073/pnas.0709451105. PubMed PMID: 18480265; PMCID: PMC2438219.
135. Tanaka M, Mokhtari GK, Terry RD, Balsam LB, Lee KH, Kofidis T, Tsao PS, Robbins RC. Overexpression of human copper/zinc superoxide dismutase (SOD1) suppresses ischemia-reperfusion injury and subsequent development of graft coronary artery disease in murine cardiac grafts. Circulation. 2004;110(11 Suppl 1):II200-6. Epub 2004/09/15. doi: 10.1161/01.CIR.0000138390.81640.54. PubMed PMID: 15364863.
136. Kang PT, Chen CL, Ohanyan V, Luther DJ, Meszaros JG, Chilian WM, Chen YR. Overexpressing superoxide dismutase 2 induces a supernormal cardiac function by enhancing redox-dependent mitochondrial function and metabolic dilation. J Mol Cell Cardiol. 2015;88:14-28. Epub 2015/09/17. doi: 10.1016/j.yjmcc.2015.09.001. PubMed PMID: 26374996; PMCID: PMC4641048.
137. Loch T, Vakhrusheva O, Piotrowska I, Ziolkowski W, Ebelt H, Braun T, Bober E. Different extent of cardiac malfunction and resistance to oxidative stress in heterozygous and homozygous manganese-dependent superoxide dismutase-mutant mice. Cardiovasc Res. 2009;82(3):448-57. doi: 10.1093/cvr/cvp092. PubMed PMID: 19293248.
138. Shiomi T, Tsutsui H, Matsusaka H, Murakami K, Hayashidani S, Ikeuchi M, Wen J, Kubota T, Utsumi H, Takeshita A. Overexpression of glutathione peroxidase prevents left ventricular remodeling and failure after myocardial infarction in mice. Circulation. 2004;109(4):544-9. doi: 10.1161/01.CIR.0000109701.77059.E9. PubMed PMID: 14744974.
139. Pendergrass KD, Varghese ST, Maiellaro-Rafferty K, Brown ME, Taylor WR, Davis ME. Temporal effects of catalase overexpression on healing after myocardial infarction. Circ Heart

Fail. 2011;4(1):98-106. doi: 10.1161/CIRCHEARTFAILURE.110.957712. PubMed PMID: 20971939; PMCID: PMC3076122.
140. Chen QM, Maltagliati AJ. Nrf2 at the heart of oxidative stress and cardiac protection. Physiol Genomics. 2018;50(2):77-97. doi: 10.1152/physiolgenomics.00041.2017. PubMed PMID: 29187515; PMCID: PMC5867612.
141. Dinkova-Kostova AT, Kostov RV, Canning P. Keap1, the cysteine-based mammalian intracellular sensor for electrophiles and oxidants. Arch Biochem Biophys. 2017;617:84-93. doi: 10.1016/j.abb.2016.08.005. PubMed PMID: 27497696; PMCID: PMC5339396.
142. Katoh Y, Itoh K, Yoshida E, Miyagishi M, Fukamizu A, Yamamoto M. Two domains of Nrf2 cooperatively bind CBP, a CREB binding protein, and synergistically activate transcription. Genes Cells. 2001;6(10):857-68. doi: 10.1046/j.1365-2443.2001.00469.x. PubMed PMID: 11683914.
143. Wardyn JD, Ponsford AH, Sanderson CM. Dissecting molecular cross-talk between Nrf2 and NF-kappaB response pathways. Biochem Soc Trans. 2015;43(4):621-6. doi: 10.1042/BST20150014. PubMed PMID: 26551702; PMCID: PMC4613495.
144. Liu GH, Qu J, Shen X. NF-kappaB/p65 antagonizes Nrf2-ARE pathway by depriving CBP from Nrf2 and facilitating recruitment of HDAC3 to MafK. Biochim Biophys Acta. 2008;1783(5):713-27. doi: 10.1016/j.bbamcr.2008.01.002. PubMed PMID: 18241676.
145. Wang W, Li S, Wang H, Li B, Shao L, Lai Y, Horvath G, Wang Q, Yamamoto M, Janicki JS, Wang XL, Tang D, Cui T. Nrf2 enhances myocardial clearance of toxic ubiquitinated proteins. J Mol Cell Cardiol. 2014;72:305-15. doi: 10.1016/j.yjmcc.2014.04.006. PubMed PMID: 24747945; PMCID: PMC4418517.
146. Li J, Ichikawa T, Villacorta L, Janicki JS, Brower GL, Yamamoto M, Cui T. Nrf2 protects against maladaptive cardiac responses to hemodynamic stress. Arterioscler Thromb Vasc Biol. 2009;29(11):1843-50. doi: 10.1161/ATVBAHA.109.189480. PubMed PMID: 19592468.
147. Magyar K, Halmosi R, Palfi A, Feher G, Czopf L, Fulop A, Battyany I, Sumegi B, Toth K, Szabados E. Cardioprotection by resveratrol: A human clinical trial in patients with stable coronary artery disease. Clin Hemorheol Microcirc. 2012;50(3):179-87. doi: 10.3233/CH-2011-1424. PubMed PMID: 22240353.
148. Johnson SA, Figueroa A, Navaei N, Wong A, Kalfon R, Ormsbee LT, Feresin RG, Elam ML, Hooshmand S, Payton ME, Arjmandi BH. Daily blueberry consumption improves blood pressure and arterial stiffness in postmenopausal women with pre- and stage 1-hypertension: a randomized, double-blind, placebo-controlled clinical trial. J Acad Nutr Diet. 2015;115(3):369-77. doi: 10.1016/j.jand.2014.11.001. PubMed PMID: 25578927.
149. Manach C, Scalbert A, Morand C, Remesy C, Jimenez L. Polyphenols: food sources and bioavailability. Am J Clin Nutr. 2004;79(5):727-47. doi: 10.1093/ajcn/79.5.727. PubMed PMID: 15113710.
150. Surajit Pathak PK, Anushka Banerjee, Antara Banerjee, Gulcin Sagdicoglu Celep, Laura Bissi, Francesco Marotta. Metabolism of Dietary Polyphenols by Human Gut Microbiota and Their Health Benefits: Academic Press; 2018.
151. Panche AN, Diwan AD, Chandra SR. Flavonoids: an overview. J Nutr Sci. 2016;5:e47. doi: 10.1017/jns.2016.41. PubMed PMID: 28620474; PMCID: PMC5465813.
152. Nakayama A, Morita H, Nakao T, Yamaguchi T, Sumida T, Ikeda Y, Kumagai H, Motozawa Y, Takahashi T, Imaizumi A, Hashimoto T, Nagai R, Komuro I. A Food-Derived Flavonoid Luteolin Protects against Angiotensin II-Induced Cardiac Remodeling. PLoS One.

2015;10(9):e0137106. doi: 10.1371/journal.pone.0137106. PubMed PMID: 26327560; PMCID: PMC4556625.
153. Sung MM, Das SK, Levasseur J, Byrne NJ, Fung D, Kim TT, Masson G, Boisvenue J, Soltys CL, Oudit GY, Dyck JR. Resveratrol treatment of mice with pressure-overload-induced heart failure improves diastolic function and cardiac energy metabolism. Circ Heart Fail. 2015;8(1):128-37. Epub 2014/11/15. doi: 10.1161/CIRCHEARTFAILURE.114.001677. PubMed PMID: 25394648.
154. Chen YF, Shibu MA, Fan MJ, Chen MC, Viswanadha VP, Lin YL, Lai CH, Lin KH, Ho TJ, Kuo WW, Huang CY. Purple rice anthocyanin extract protects cardiac function in STZ-induced diabetes rat hearts by inhibiting cardiac hypertrophy and fibrosis. J Nutr Biochem. 2016;31:98-105. Epub 2016/05/03. doi: 10.1016/j.jnutbio.2015.12.020. PubMed PMID: 27133428.
155. Ahmet I, Spangler E, Shukitt-Hale B, Juhaszova M, Sollott SJ, Joseph JA, Ingram DK, Talan M. Blueberry-enriched diet protects rat heart from ischemic damage. PLoS One. 2009;4(6):e5954. doi: 10.1371/journal.pone.0005954. PubMed PMID: 19536295; PMCID: PMC2693933.
156. Ahmet I, Spangler E, Shukitt-Hale B, Joseph JA, Ingram DK, Talan M. Survival and cardioprotective benefits of long-term blueberry enriched diet in dilated cardiomyopathy following myocardial infarction in rats. PLoS One. 2009;4(11):e7975. doi: 10.1371/journal.pone.0007975. PubMed PMID: 19936253; PMCID: PMC2775918.
157. Zhang L, Guo Z, Wang Y, Geng J, Han S. The protective effect of kaempferol on heart via the regulation of Nrf2, NF-kappabeta, and PI3K/Akt/GSK-3beta signaling pathways in isoproterenol-induced heart failure in diabetic rats. Drug Dev Res. 2019;80(3):294-309. doi: 10.1002/ddr.21495. PubMed PMID: 30864233.
158. Lipinska L, Klewicka E, Sojka M. The structure, occurrence and biological activity of ellagitannins: a general review. Acta Sci Pol Technol Aliment. 2014;13(3):289-99. doi: 10.17306/j.afs.2014.3.7. PubMed PMID: 24887944.
159. Burton-Freeman BM, Sandhu AK, Edirisinghe I. Red Raspberries and Their Bioactive Polyphenols: Cardiometabolic and Neuronal Health Links. Adv Nutr. 2016;7(1):44-65. doi: 10.3945/an.115.009639. PubMed PMID: 26773014; PMCID: PMC4717884.
160. Nielsen SE, Breinholt V, Justesen U, Cornett C, Dragsted LO. In vitro biotransformation of flavonoids by rat liver microsomes. Xenobiotica. 1998;28(4):389-401. doi: 10.1080/004982598239498. PubMed PMID: 9604302.
161. Neveu V, Perez-Jimenez J, Vos F, Crespy V, du Chaffaut L, Mennen L, Knox C, Eisner R, Cruz J, Wishart D, Scalbert A. Phenol-Explorer: an online comprehensive database on polyphenol contents in foods. Database (Oxford). 2010;2010:bap024. Epub 2010/04/30. doi: 10.1093/database/bap024. PubMed PMID: 20428313; PMCID: PMC2860900.
162. de Ferrars RM, Czank C, Zhang Q, Botting NP, Kroon PA, Cassidy A, Kay CD. The pharmacokinetics of anthocyanins and their metabolites in humans. Br J Pharmacol. 2014;171(13):3268-82. doi: 10.1111/bph.12676. PubMed PMID: 24602005; PMCID: PMC4080980.
163. Olivas-Aguirre FJ, Rodrigo-Garcia J, Martinez-Ruiz ND, Cardenas-Robles AI, Mendoza-Diaz SO, Alvarez-Parrilla E, Gonzalez-Aguilar GA, de la Rosa LA, Ramos-Jimenez A, Wall-Medrano A. Cyanidin-3-O-glucoside: Physical-Chemistry, Foodomics and Health Effects. Molecules. 2016;21(9). doi: 10.3390/molecules21091264. PubMed PMID: 27657039; PMCID: PMC6273591.

164. Sandhu AK, Miller MG, Thangthaeng N, Scott TM, Shukitt-Hale B, Edirisinghe I, Burton-Freeman B. Metabolic fate of strawberry polyphenols after chronic intake in healthy older adults. Food Funct. 2018;9(1):96-106. doi: 10.1039/c7fo01843f. PubMed PMID: 29318244.
165. Zhang X, Sandhu A, Edirisinghe I, Burton-Freeman B. An exploratory study of red raspberry (Rubus idaeus L.) (poly)phenols/metabolites in human biological samples. Food Funct. 2018;9(2):806-18. doi: 10.1039/c7fo00893g. PubMed PMID: 29344587.
166. Kensler TW, Egner PA, Agyeman AS, Visvanathan K, Groopman JD, Chen JG, Chen TY, Fahey JW, Talalay P. Keap1-nrf2 signaling: a target for cancer prevention by sulforaphane. Top Curr Chem. 2013;329:163-77. doi: 10.1007/128_2012_339. PubMed PMID: 22752583; PMCID: PMC3553557.
167. Bello M, Morales-Gonzalez JA. Molecular recognition between potential natural inhibitors of the Keap1-Nrf2 complex. Int J Biol Macromol. 2017;105(Pt 1):981-92. doi: 10.1016/j.ijbiomac.2017.07.117. PubMed PMID: 28746889.
168. Hayes JD, Dinkova-Kostova AT. The Nrf2 regulatory network provides an interface between redox and intermediary metabolism. Trends Biochem Sci. 2014;39(4):199-218. doi: 10.1016/j.tibs.2014.02.002. PubMed PMID: 24647116.
169. Silva-Islas CA, Maldonado PD. Canonical and non-canonical mechanisms of Nrf2 activation. Pharmacol Res. 2018;134:92-9. doi: 10.1016/j.phrs.2018.06.013. PubMed PMID: 29913224.
170. Zheng D, Liu Z, Zhou Y, Hou N, Yan W, Qin Y, Ye Q, Cheng X, Xiao Q, Bao Y, Luo J, Wu X. Urolithin B, a gut microbiota metabolite, protects against myocardial ischemia/reperfusion injury via p62/Keap1/Nrf2 signaling pathway. Pharmacol Res. 2020;153:104655. doi: 10.1016/j.phrs.2020.104655. PubMed PMID: 31996327.
171. Ding Y, Zhang B, Zhou K, Chen M, Wang M, Jia Y, Song Y, Li Y, Wen A. Dietary ellagic acid improves oxidant-induced endothelial dysfunction and atherosclerosis: role of Nrf2 activation. Int J Cardiol. 2014;175(3):508-14. doi: 10.1016/j.ijcard.2014.06.045. PubMed PMID: 25017906.
172. Jin L, Piao ZH, Sun S, Liu B, Kim GR, Seok YM, Lin MQ, Ryu Y, Choi SY, Kee HJ, Jeong MH. Gallic Acid Reduces Blood Pressure and Attenuates Oxidative Stress and Cardiac Hypertrophy in Spontaneously Hypertensive Rats. Sci Rep. 2017;7(1):15607. doi: 10.1038/s41598-017-15925-1. PubMed PMID: 29142252; PMCID: PMC5688141.
173. Rozentsvit A, Vinokur K, Samuel S, Li Y, Gerdes AM, Carrillo-Sepulveda MA. Ellagic Acid Reduces High Glucose-Induced Vascular Oxidative Stress Through ERK1/2/NOX4 Signaling Pathway. Cell Physiol Biochem. 2017;44(3):1174-87. doi: 10.1159/000485448. PubMed PMID: 29179217.
174. Lin MC, Yin MC. Preventive effects of ellagic acid against doxorubicin-induced cardio-toxicity in mice. Cardiovasc Toxicol. 2013;13(3):185-93. doi: 10.1007/s12012-013-9197-z. PubMed PMID: 23322372.
175. Panchal SK, Ward L, Brown L. Ellagic acid attenuates high-carbohydrate, high-fat diet-induced metabolic syndrome in rats. Eur J Nutr. 2013;52(2):559-68. doi: 10.1007/s00394-012-0358-9. PubMed PMID: 22538930.
176. Kannan MM, Quine SD. Ellagic acid ameliorates isoproterenol induced oxidative stress: Evidence from electrocardiological, biochemical and histological study. Eur J Pharmacol. 2011;659(1):45-52. doi: 10.1016/j.ejphar.2011.02.037. PubMed PMID: 21385579.
177. Yan X, Zhang YL, Zhang L, Zou LX, Chen C, Liu Y, Xia YL, Li HH. Gallic Acid Suppresses Cardiac Hypertrophic Remodeling and Heart Failure. Mol Nutr Food Res.

2019;63(5):e1800807. Epub 2018/12/07. doi: 10.1002/mnfr.201800807. PubMed PMID: 30521107.
178. Jin L, Sun S, Ryu Y, Piao ZH, Liu B, Choi SY, Kim GR, Kim HS, Kee HJ, Jeong MH. Gallic acid improves cardiac dysfunction and fibrosis in pressure overload-induced heart failure. Sci Rep. 2018;8(1):9302. Epub 2018/06/20. doi: 10.1038/s41598-018-27599-4. PubMed PMID: 29915390; PMCID: PMC6006337.
179. Yamazaki KG, Romero-Perez D, Barraza-Hidalgo M, Cruz M, Rivas M, Cortez-Gomez B, Ceballos G, Villarreal F. Short- and long-term effects of (-)-epicatechin on myocardial ischemia-reperfusion injury. Am J Physiol Heart Circ Physiol. 2008;295(2):H761-7. Epub 2008/06/24. doi: 10.1152/ajpheart.00413.2008. PubMed PMID: 18567705; PMCID: PMC2519218.
180. Kurin E, Atanasov AG, Donath O, Heiss EH, Dirsch VM, Nagy M. Synergy study of the inhibitory potential of red wine polyphenols on vascular smooth muscle cell proliferation. Planta Med. 2012;78(8):772-8. doi: 10.1055/s-0031-1298440. PubMed PMID: 22499559.
181. Park CM, Jin KS, Lee YW, Song YS. Luteolin and chicoric acid synergistically inhibited inflammatory responses via inactivation of PI3K-Akt pathway and impairment of NF-kappaB translocation in LPS stimulated RAW 264.7 cells. Eur J Pharmacol. 2011;660(2-3):454-9. doi: 10.1016/j.ejphar.2011.04.007. PubMed PMID: 21513709.
182. Feresin RG, Huang J, Klarich DS, Zhao Y, Pourafshar S, Arjmandi BH, Salazar G. Blackberry, raspberry and black raspberry polyphenol extracts attenuate angiotensin II-induced senescence in vascular smooth muscle cells. Food Funct. 2016;7(10):4175-87. doi: 10.1039/c6fo00743k. PubMed PMID: 27506987.
183. Nair AB, Jacob S. A simple practice guide for dose conversion between animals and human. J Basic Clin Pharm. 2016;7(2):27-31. Epub 2016/04/09. doi: 10.4103/0976-0105.177703. PubMed PMID: 27057123; PMCID: PMC4804402.
184. Ye J, Yang L, Sethi R, Copps J, Ramjiawan B, Summers R, Deslauriers R. A new technique of coronary artery ligation: experimental myocardial infarction in rats in vivo with reduced mortality. Mol Cell Biochem. 1997;176(1-2):227-33. PubMed PMID: 9406166.
185. Nie X, Li C, Hu S, Xue F, Kang YJ, Zhang W. An appropriate loading control for western blot analysis in animal models of myocardial ischemic infarction. Biochem Biophys Rep. 2017;12:108-13. Epub 2017/09/29. doi: 10.1016/j.bbrep.2017.09.001. PubMed PMID: 28955798; PMCID: PMC5613232.
186. Colombe AS, Gerbaud P, Benitah JP, Pidoux G. Housekeeping Proteins Exhibit a High Level of Expression Variability Within Control Group and Between Ischemic Human Heart Biopsies. J Am Heart Assoc. 2022;11(18):e026292. Epub 2022/09/09. doi: 10.1161/JAHA.122.026292. PubMed PMID: 36073642; PMCID: PMC9683656.
187. Benzie IFF, Devaki M. The ferric reducing/antioxidant power (FRAP) assay for non-enzymatic antioxidant capacity: concepts, procedures, limitations and applications. Measurement of Antioxidant Activity & Capacity2018. p. 77-106.
188. Santos CMM, Silva AMS. The Antioxidant Activity of Prenylflavonoids. Molecules. 2020;25(3). Epub 2020/02/12. doi: 10.3390/molecules25030696. PubMed PMID: 32041233; PMCID: PMC7037609.
189. Feresin RG, Pourafshar S, Huang J, Zhao Y, Arjmandi BH, Salazar G. Extraction and Purification of Polyphenols from Freeze-dried Berry Powder for the Treatment of Vascular Smooth Muscle Cells In Vitro. J Vis Exp. 2017(125). Epub 2017/07/18. doi: 10.3791/55605. PubMed PMID: 28715389; PMCID: PMC5608541.

190. Matsunaga N, Tsuchimori N, Matsumoto T, Ii M. TAK-242 (resatorvid), a small-molecule inhibitor of Toll-like receptor (TLR) 4 signaling, binds selectively to TLR4 and interferes with interactions between TLR4 and its adaptor molecules. Mol Pharmacol. 2011;79(1):34-41. Epub 2010/10/01. doi: 10.1124/mol.110.068064. PubMed PMID: 20881006.
191. Singh A, Singh V, Tiwari RL, Chandra T, Kumar A, Dikshit M, Barthwal MK. The IRAK-ERK-p67phox-Nox-2 axis mediates TLR4, 2-induced ROS production for IL-1beta transcription and processing in monocytes. Cell Mol Immunol. 2016;13(6):745-63. Epub 2015/09/01. doi: 10.1038/cmi.2015.62. PubMed PMID: 26320741; PMCID: PMC5101443.
192. Park HS, Jung HY, Park EY, Kim J, Lee WJ, Bae YS. Cutting edge: direct interaction of TLR4 with NAD(P)H oxidase 4 isozyme is essential for lipopolysaccharide-induced production of reactive oxygen species and activation of NF-kappa B. J Immunol. 2004;173(6):3589-93. Epub 2004/09/10. doi: 10.4049/jimmunol.173.6.3589. PubMed PMID: 15356101.
193. Lorne E, Zmijewski JW, Zhao X, Liu G, Tsuruta Y, Park YJ, Dupont H, Abraham E. Role of extracellular superoxide in neutrophil activation: interactions between xanthine oxidase and TLR4 induce proinflammatory cytokine production. Am J Physiol Cell Physiol. 2008;294(4):C985-93. Epub 2008/02/22. doi: 10.1152/ajpcell.00454.2007. PubMed PMID: 18287332.
194. Katare PB, Nizami HL, Paramesha B, Dinda AK, Banerjee SK. Activation of toll like receptor 4 (TLR4) promotes cardiomyocyte apoptosis through SIRT2 dependent p53 deacetylation. Sci Rep. 2020;10(1):19232. Epub 2020/11/08. doi: 10.1038/s41598-020-75301-4. PubMed PMID: 33159115; PMCID: PMC7648754.
195. Zhang D, Li Y, Wang W, Lang X, Zhang Y, Zhao Q, Yan J, Zhang Y. NOX1 promotes myocardial fibrosis and cardiac dysfunction via activating the TLR2/NF-kappaB pathway in diabetic cardiomyopathy. Front Pharmacol. 2022;13:928762. Epub 2022/10/14. doi: 10.3389/fphar.2022.928762. PubMed PMID: 36225554; PMCID: PMC9549956.
196. Xu L, Balzarolo M, Robinson EL, Lorenz V, Della Verde G, Joray L, Mochizuki M, Kaufmann BA, Valstar G, de Jager SCA, den Ruijter HM, Heymans S, Pfister O, Kuster GM. NOX1 mediates metabolic heart disease in mice and is upregulated in monocytes of humans with diastolic dysfunction. Cardiovasc Res. 2022;118(14):2973-84. Epub 2021/12/02. doi: 10.1093/cvr/cvab349. PubMed PMID: 34849611; PMCID: PMC9648822.
197. Kojima A, Matsumoto A, Nishida H, Reien Y, Iwata K, Shirayama T, Yabe-Nishimura C, Nakaya H. A protective role of Nox1/NADPH oxidase in a mouse model with hypoxia-induced bradycardia. J Pharmacol Sci. 2015;127(3):370-6. Epub 2015/04/04. doi: 10.1016/j.jphs.2015.02.007. PubMed PMID: 25837936.
198. Matsuno K, Yamada H, Iwata K, Jin D, Katsuyama M, Matsuki M, Takai S, Yamanishi K, Miyazaki M, Matsubara H, Yabe-Nishimura C. Nox1 is involved in angiotensin II-mediated hypertension: a study in Nox1-deficient mice. Circulation. 2005;112(17):2677-85. Epub 2005/10/26. doi: 10.1161/CIRCULATIONAHA.105.573709. PubMed PMID: 16246966.
199. Stevenson MD, Canugovi C, Vendrov AE, Hayami T, Bowles DE, Krause KH, Madamanchi NR, Runge MS. NADPH Oxidase 4 Regulates Inflammation in Ischemic Heart Failure: Role of Soluble Epoxide Hydrolase. Antioxid Redox Signal. 2019;31(1):39-58. Epub 2018/11/20. doi: 10.1089/ars.2018.7548. PubMed PMID: 30450923; PMCID: PMC6552006.
200. Aquila-Pastir LA, DiPaola NR, Matteo RG, Smedira NG, McCarthy PM, Moravec CS. Quantitation and distribution of beta-tubulin in human cardiac myocytes. J Mol Cell Cardiol. 2002;34(11):1513-23. Epub 2002/11/15. doi: 10.1006/jmcc.2002.2105. PubMed PMID: 12431450.

201. Li B, Tian J, Sun Y, Xu TR, Chi RF, Zhang XL, Hu XL, Zhang YA, Qin FZ, Zhang WF. Activation of NADPH oxidase mediates increased endoplasmic reticulum stress and left ventricular remodeling after myocardial infarction in rabbits. Biochim Biophys Acta. 2015;1852(5):805-15. Epub 2015/01/24. doi: 10.1016/j.bbadis.2015.01.010. PubMed PMID: 25615792.
202. Sirker A, Murdoch CE, Protti A, Sawyer GJ, Santos CX, Martin D, Zhang X, Brewer AC, Zhang M, Shah AM. Cell-specific effects of Nox2 on the acute and chronic response to myocardial infarction. J Mol Cell Cardiol. 2016;98:11-7. Epub 2016/07/12. doi: 10.1016/j.yjmcc.2016.07.003. PubMed PMID: 27397876; PMCID: PMC5029266.
203. Reed SM, Quelle DE. p53 Acetylation: Regulation and Consequences. Cancers (Basel). 2014;7(1):30-69. Epub 2014/12/30. doi: 10.3390/cancers7010030. PubMed PMID: 25545885; PMCID: PMC4381250.
204. Xu Y. Regulation of p53 responses by post-translational modifications. Cell Death Differ. 2003;10(4):400-3. Epub 2003/04/30. doi: 10.1038/sj.cdd.4401182. PubMed PMID: 12719715.
205. Shi T, Dansen TB. Reactive Oxygen Species Induced p53 Activation: DNA Damage, Redox Signaling, or Both? Antioxid Redox Signal. 2020;33(12):839-59. Epub 2020/03/11. doi: 10.1089/ars.2020.8074. PubMed PMID: 32151151.
206. Najjar RS, Knapp D, Wanders D, Feresin RG. Raspberry and blackberry act in a synergistic manner to improve cardiac redox proteins and reduce NF-kappaB and SAPK/JNK in mice fed a high-fat, high-sucrose diet. Nutr Metab Cardiovasc Dis. 2022;32(7):1784-96. Epub 2022/04/30. doi: 10.1016/j.numecd.2022.03.015. PubMed PMID: 35487829.
207. Abdelazeem KNM, Kalo MZ, Beer-Hammer S, Lang F. The gut microbiota metabolite urolithin A inhibits NF-kappaB activation in LPS stimulated BMDMs. Sci Rep. 2021;11(1):7117. Epub 2021/03/31. doi: 10.1038/s41598-021-86514-6. PubMed PMID: 33782464; PMCID: PMC8007722.
208. Granica S, Piwowarski JP, Kiss AK. Ellagitannins modulate the inflammatory response of human neutrophils ex vivo. Phytomedicine. 2015;22(14):1215-22. Epub 2015/12/15. doi: 10.1016/j.phymed.2015.10.004. PubMed PMID: 26655403.
209. Cucoranu I, Clempus R, Dikalova A, Phelan PJ, Ariyan S, Dikalov S, Sorescu D. NAD(P)H oxidase 4 mediates transforming growth factor-beta1-induced differentiation of cardiac fibroblasts into myofibroblasts. Circ Res. 2005;97(9):900-7. Epub 2005/09/24. doi: 10.1161/01.RES.0000187457.24338.3D. PubMed PMID: 16179589.
210. Alam J, Stewart D, Touchard C, Boinapally S, Choi AM, Cook JL. Nrf2, a Cap'n'Collar transcription factor, regulates induction of the heme oxygenase-1 gene. J Biol Chem. 1999;274(37):26071-8. Epub 1999/09/03. doi: 10.1074/jbc.274.37.26071. PubMed PMID: 10473555.
211. Lakkisto P, Palojoki E, Backlund T, Saraste A, Tikkanen I, Voipio-Pulkki LM, Pulkki K. Expression of heme oxygenase-1 in response to myocardial infarction in rats. J Mol Cell Cardiol. 2002;34(10):1357-65. Epub 2002/10/24. doi: 10.1006/jmcc.2002.2094. PubMed PMID: 12392996.
212. Chen P, Pei J, Wang X, Tai S, Tang L, Hu X. Gut bacterial metabolite Urolithin A inhibits myocardial fibrosis through activation of Nrf2 pathway in vitro and in vivo. Mol Med. 2022;28(1):19. Epub 2022/02/10. doi: 10.1186/s10020-022-00444-1. PubMed PMID: 35135471; PMCID: PMC8822684.
213. Istas G, Feliciano RP, Weber T, Garcia-Villalba R, Tomas-Barberan F, Heiss C, Rodriguez-Mateos A. Plasma urolithin metabolites correlate with improvements in endothelial

function after red raspberry consumption: A double-blind randomized controlled trial. Arch Biochem Biophys. 2018;651:43-51. Epub 2018/05/29. doi: 10.1016/j.abb.2018.05.016. PubMed PMID: 29802820.
214. Pattananandecha T, Apichai S, Sirilun S, Julsrigival J, Sawangrat K, Ogata F, Kawasaki N, Sirithunyalug B, Saenjum C. Anthocyanin Profile, Antioxidant, Anti-Inflammatory, and Antimicrobial against Foodborne Pathogens Activities of Purple Rice Cultivars in Northern Thailand. Molecules. 2021;26(17). Epub 2021/09/11. doi: 10.3390/molecules26175234. PubMed PMID: 34500669; PMCID: PMC8433650.
215. Lloyd-Jones DM, Larson MG, Leip EP, Beiser A, D'Agostino RB, Kannel WB, Murabito JM, Vasan RS, Benjamin EJ, Levy D, Framingham Heart S. Lifetime risk for developing congestive heart failure: the Framingham Heart Study. Circulation. 2002;106(24):3068-72. Epub 2002/12/11. doi: 10.1161/01.cir.0000039105.49749.6f. PubMed PMID: 12473553.
216. Najjar RS, Wong BJ, Feresin RG. Tissue Derivation and Biological Sex Uniquely Mediate Endothelial Cell Protein Expression, Redox Status, and Nitric Oxide Synthesis. Cells. 2022;12(1). Epub 2023/01/09. doi: 10.3390/cells12010093. PubMed PMID: 36611888; PMCID: PMC9818567.
217. Najjar RS, Turner CG, Wong BJ, Feresin RG. Berry-Derived Polyphenols in Cardiovascular Pathologies: Mechanisms of Disease and the Role of Diet and Sex. Nutrients. 2021;13(2). Epub 2021/01/31. doi: 10.3390/nu13020387. PubMed PMID: 33513742; PMCID: PMC7911141.